P-04-149

# Forsmark site investigation

# Fracture mineralogy

## Results from fracture minerals and wall rock alteration in boreholes KFM01A, KFM02A, KFM03A and KFM03B

Björn Sandström, Marcus Savolainen
Department of Geology, Earth Science Centre
Göteborg University

Eva-Lena Tullborg
Terralogica AB, GRÅBO

December 2004

**Svensk Kärnbränslehantering AB**
Swedish Nuclear Fuel
and Waste Management Co
Box 5864
SE-102 40 Stockholm Sweden
Tel 08-459 84 00
+46 8 459 84 00
Fax 08-661 57 19
+46 8 661 57 19

ISSN 1651-4416
SKB P-04-149

# Forsmark site investigation

# Fracture mineralogy

## Results from fracture minerals and wall rock alteration in boreholes KFM01A, KFM02A, KFM03A and KFM03B

Björn Sandström, Marcus Savolainen
Department of Geology, Earth Science Centre
Göteborg University

Eva-Lena Tullborg
Terralogica AB, GRÅBO

December 2004

*Keywords:* AP PF 400-04-32, Fracture mineralogy, Sequence of events, Low temperature minerals, Stable isotopes.

# Abstract

Fracture mineralogical investigations have been carried out on drill cores from the boreholes KFM01A, KFM02A, KFM03A and KFM03B in Forsmark, Sweden. Both open and sealed fractures were sampled in order to identify the fracture mineralogy of the area and to sort out different fracture mineral generations and their formation conditions.

The analyses carried out, reported in this P-report, include microscopy (both trans-missive and reflected light) and electron microscopy (SEM/EDS). Fracture calcites have been paid special attention to, since they occur in many fractures and can be formed during various conditions. Stable isotope results as well as chemical composition and morphology of the calcites can provide palaeohydrogeological information.

The most common fracture minerals in the area are quartz, low-temperature K-feldspar (adularia), chlorite, laumontite, calcite, prehnite, epidote, pyrite, analcime and apo-phyllite. Among the clay minerals, the most common is corrensite, which is a mixed layer clay with alternating layers of chlorite and smectite or vermiculite. Other clay minerals, less common in the samples here studied, are illite, smectite and mixed-layer illite/smectite. It is probable that the amount of clay minerals is reduced due to the impact of flushing and other disturbances during drilling.

From the examined drill-cores, 6 different generations of fracture mineralizations have been distinguished, presented with decreasing ages; 1) quartz-epidote, 2) prehnite, 3) laumontite-calcite-adularia-chlorite/corrensite 4) idiomorphic quartz-adularia-albite-analcime, 5) calcite and pyrite 6) calcite-clay minerals-asphaltite. The present under-standing is that Generation 1 is clearly separated in time from Generations 2 and 3. The latters probably represent one prolonged and intense period of hydrothermal alteration and creation of new fractures in the area. Subsequently, Generations 4 and 5 have precipitated, probably as a result of a significantly later period of hydrothermal circulation grading into low temperatures < 100°C. It is probable that all these events are older than 600 Ma. However, precipitation of minerals in Generation 6 can have occurred during the period from Proterozoic to Quaternary, and it is possible that the continuation of the fracture mineral studies will produce a subdivision of the mineral-izations that have taken place during this long time period. The wall rock alteration is most extensive around the epidote and laumontite filled fractures. The dominant alter-ation is saussuritization of the plagioclase, chloritization of the biotite and seritization of the K-feldspar. The altered wall rock is red-coloured due to micro-grains of hematite, mainly in the plagioclase.

# Sammanfattning

Sprickmineralogiska undersökningar har utförts på prover från borrhålen KFM01A, KFM02A, KFM03A and KFM03B i Forsmark. Såväl öppna som läkta sprickor har provtagits i syfte att identifiera sprickmineral samt för att sortera ut olika mineral-parageneser och olika sekvenser av hydrotermala händelser och senare lågtemperatur-utfällningar i sprickor.

De analyser som redovisas i denna P-rapport omfattar mikroskopi (polariserat ljus) och elektronmikroskopi (SEM/EDS). Sprickfyllnadskalciter har ägnats speciellt intresse eftersom de förekommer i många sprickor och dessutom representerar flera olika generationer och därmed olika bildningsmiljöer. Stabila isotoper samt kemisk sammansättning och kristallmorfologi har utnyttjats för att särskilja olika generationer och för att där så är möjligt ge palaeohydrogeologisk information.

De vanligaste sprickmineralen i området är: kvarts, lågtemperatur K-fältspat (adularia), klorit, laumontit, kalcit, prehnit, epidot, pyrit, analcim and apophyllit. Corrensit, som är ett blandskiktsmineral med alternerande lager av klorit och smektit eller vermikulit, är det vanligaste lermineralet. Andra lermineral som också identifierats är illit, smektit och ett blandskiktsmineral bestående av smektit och illit-lager. Det är troligt att mängden lermineral är reducerad beroende på störningar vid borrningen genom spolning och i viss mån genom att olika borrkärnsbitar har roterat mot varandra.

Från de undersökta borrkärnorna har 6 olika generationer av sprickmineraliseringar urskiljts, 1) kvarts – epidot, 2) prehnit, 3) laumontit-kalcit-adularia, klorit/corrensit 4) idiomorf kvarts-adularia-albit-analcim, 5) kalcit-pyrit 6) lermineral, kalcit, asfaltit. Generation 1 är klart separerad i tid från Generationerna 2 och 3. De senare representerar sannolikt en omfattande (kanske utdragen) period av hydrotermal omvandling och nybildning av sprickor. Därefter följer ytterligare en period av hydrotermal omvandling (Generation 4 och 5) under såväl reaktivering av tidigare sprickor som nybildning av sprickor, men denna period är förmodligen signifikant yngre än Generation 2 och 3 och sträcker sig sannolikt i temperaturer ner mot lågtemperatur-området (< 100°C). Det är troligt att alla dessa generationer är äldre än 600 Ma. Generation 6 utgörs av olika mineral som kan vara utfällda under mycket skiftande betingelser med bildningsåldrar som kan variera från proterozoikum till kvartär. Det är troligt att de fortsatta sprick-mineralogiska studierna kommer att leda till en mer detaljerad uppdelning av denna grupp än vad som för närvarande är möjligt. Sidobergsomvandlingen är mest omfattande runt de epidot- och laumontit-fyllda sprickorna. Omvandlingen består mest av saussuritisation av plagioklas, kloritisering av biotit och seriticering av kalifältspat samt en rödfärgning som uppstår på grund av att mikrokorn av hematit har bildats, oftast i plagioklasen.

# Contents

# 1 Introduction

This document reports the results gained by the study of fracture minerals from boreholes KFM01A, KFM02A and KFM03A and KFM03B at the Forsmark site, Sweden. The work was carried out in accordance with activity plan SKB PF 400-04-32. In Table 1-1 controlling documents for performing this activity are listed. Both activity plan and method descriptions are SKB's internal controlling documents.

**Table 1-1. Controlling documents for the performance of the activity.**

| Activity plan | Number | Version |
|---|---|---|
| Sprickmineralogiska undersökningar | AP PF 400-04-32 | 1.0 |
| **Method descriptions** | **Number** | **Version** |
| Sprickmineralogi | SKB MD 144.000 | 1.0 |

Mapping of fractures and fracture minerals is carried out on all cored boreholes within the site investigation programme and this information serves as a basis for the fracture mineral study /1, 2, 3/. However, to identify fracture minerals macroscopically can be very difficult. After drilling of KFM01A, KFM02A, KFM03A and KFM03B, regular drill-core mapping (so called bore mapping) was performed whereby fracture minerals were mapped and identified, although a number of question marks have been noted. Several of these fractures minerals have been sampled for XRD (X-ray diffractometry) identification, of which the results are accounted for in /4/. In addition, fracture minerals have been sampled for recognition of different fracture generations. Furthermore, calcites were sampled since they provide palaeohydrogeological information.

The locations of the three boreholes studied are shown in the map, Figure 1-1.

To be able to relate the fractures in this study to other structures, information from the Borehole Imaging Processing System (BIPS) has been used. BIPS is a tool for visualization of the borehole wall. Information of the strike and dip of fractures/structures in a drill-core sample can be estimated from the comparison of the sample with the BIPS-images of the borehole wall, using a specialized computer program.

The flow logging has been used as a tool for the selection of samples of hydraulically conductive fractures.

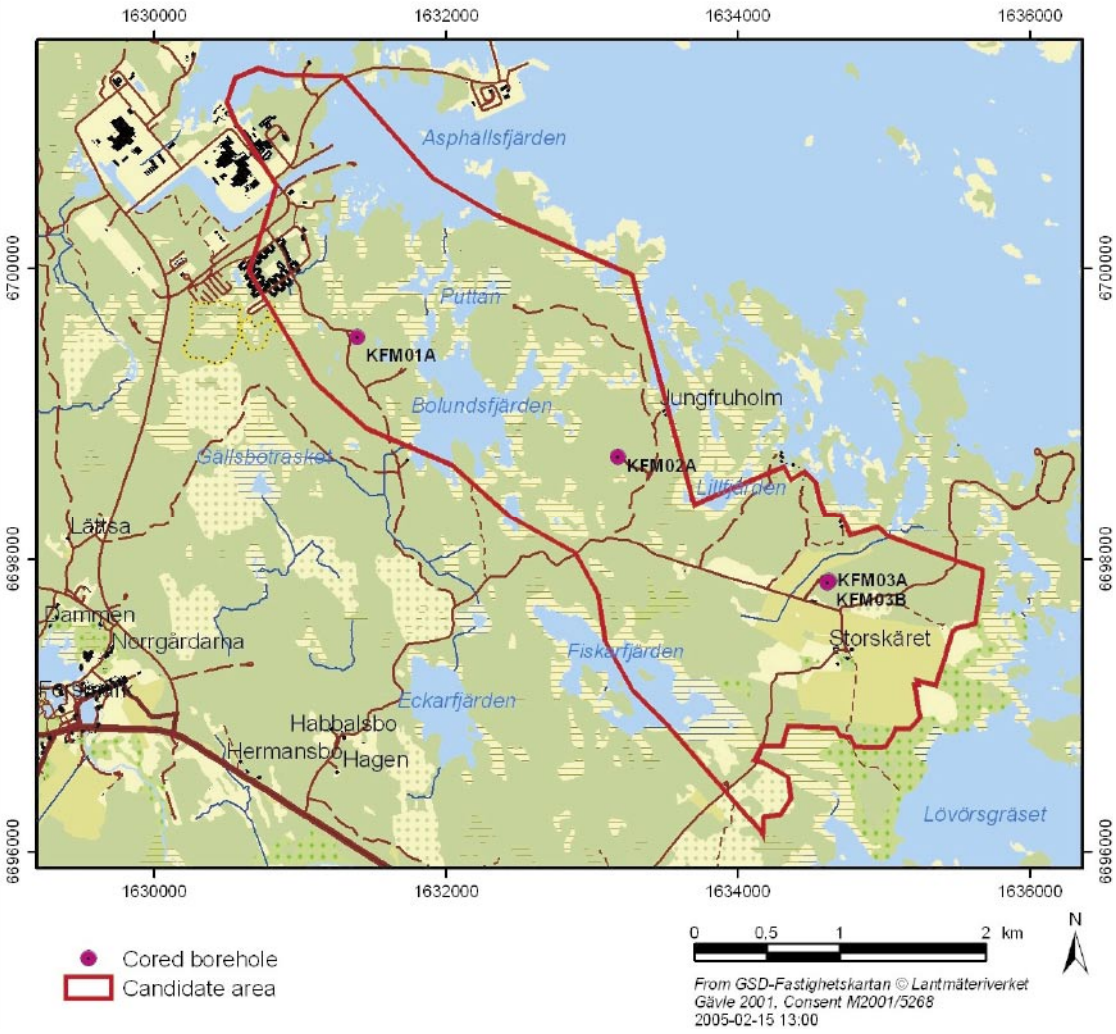


***Figure 1-1.*** *General overview of the Forsmark site investigation area, showing the boreholes dealt with in this report.*

# 2 Objective and scope

The basic idea behind the fracture mineral study is to:

- Identify fracture minerals.
- Distinguish different events of fracture mineral precipitation and to create a “sequence of events” based on this information.
- Provide mineralogical and geochemical information for the hydrogeochemical modelling.
- Give palaeohydrogeological evidences, mainly based on calcite geochemistry and stable isotope composition.
- Give background information for the selection of samples within the Transport Programme (measurements of porosity, Kd, diffusivity etc).

# 3 Equipment

## 3.1 Description of equipment/interpretation tools

The analyses carried out include microscopy by transmissive light and electron microscope (SEM). Semi-quantitative analyses was performed with Energy Dispersive Spectroscopy (EDS).

The SEM-EDS analyses were conducted on an Oxford Instruments Link EDS mounted to a Zeiss DSM 940 SEM at the Earth Sciences Centre in Gothenburg. Polished thin-sections were coated with carbon and fracture surface samples with gold for electron conductivity. The acceleration voltage was 25 kV, the working distance 24 mm (18 mm for fracture surface samples), and the specimen current was about 0.7 nA. The instrument was calibrated at least once an hour using a cobalt standard linked to simple oxide and mineral standards to confirm that the drift was acceptable. ZAF calculations were maintained by an on-line LINK ISIS computer system. The quantitative microprobe analyses supply mineral compositions but Fe(II) and Fe(III) are not distinguished, and the $H_2O$ content is not calculated. Detection limits for major elements are higher than 0.1% oxide, except for $Na_2O$ with a detection limit of 0.3%.

Fracture filling material was scraped from the fracture walls for the XRD analyses. The amount received was highly variable. The analytical technique is described in /4/.

Fracture calcites have been analysed for stable carbon and oxygen isotope composition and trace element composition by ICP-MS on leachate samples according to:

Samples, usually between 150 and 300 µg each, were roasted in vacuum for 30 minutes at 400°C to remove possible organic material and moisture. Thereafter, the samples were analysed using a VG Prism Series II mass spectrometer with a VG Isocarb preparation system on line. In the preparation system each sample was reacted with 100% phosphoric acid at 90°C for 10 minutes, whereupon the released $CO_2$ gas was analysed in the mass spectrometer. All isotope results are reported as ð per mil relative to the Vienna Pee Dee Belemnite (VPDB) standard. The analysing system is calibrated to the PDB scale via NBS-19.

For the Sr isotope analyses, about 30 to 40 mg of the carbonate samples were transferred to 2 ml centrifuge tubes, added 200 µl 0.2 M HCl, and shaken. The samples were let to react for 10 minutes while shaken in order to release the $CO_2$ gas. Then 20 µl 2 M HCl was added once or twice until most of the calcite was decomposed. The samples were centrifuged for about 4 minutes and the liquids transferred to new clean centrifuge tubes by use of a pipette. The centrifuge tubes were put on a hotplate and evaporated to dryness. To avoid disturbances in measuring the isotopic composition, strontium had to be separated from other elements present in the sample. After evaporation to dryness, the samples were dissolved in 200 µl ultrapure 3M $HNO_3$, centrifuged and loaded onto ion-exchange columns packed with a Sr-Spec crown-ether resin from EIChrom, which retained Sr and allowed most other elements to pass. After rinsing out the remaining unwanted elements from the columns, strontium was collected with ultrapure water (Millipore). The collected Sr-fractions were then evaporated to dryness and loaded on pre-gassed Re filaments on a turret holding 12 samples and 1 NIST/NBS 987 Sr standard. The isotopic composition of Sr was determined by thermal ionization mass spectrometry (TIMS) on a Finnigan MAT 261 with a precision of about 20 ppm and a Sr blank of 50–100 pg.

The $^{87}Sr/^{86}Sr$ ratio of the carbonate analysis was monitored by analysing one NIST/NBS SRM 987 Sr standard, for each turret of 12 samples, and the standard has a recommended $^{87}Sr/^{86}Sr$ value of 0.710248. The presented results are not corrected to the NBS 987 recommended value but given together with the specific measured NBS 987 value for the relevant turret.

The ICP-MS analyses on calcites leachates were carried out following the here given procedure: a 12 mg calcite sample (weight registered ± 0.01 mg) was placed in a 50 ml tube, where 47 ml 5% $HNO_3$ was added, containing 15 ppb of indium and rhenium respectively, to be used as internal standards. The sample was leached for 1 hour with stirring every 15 minutes. Thereafter, 20 ml of the solution was used for analyses carried out on a Hewlett-Packard ICP-MS, model HP 4500. Certified multielement standards from Merck (nr VI) och Agilent (nr 1) have been used.

Pyrite samples were analysed for stable sulphur isotope ratios according to the procedure given below: Approximately 1–2 mg of the samples were transferred to tin capsules with 1–2 mg of $V_2O_5$. Further preparation was done with a Carlo Erba NCS 2500 element analyser. The procedure involves flash combustion of the samples at approximately 1,700°C with $WO_3$, reduction of $SO_3$ to $SO_2$ in the presence of Cu at 1,000°C, separation of combustion products by gas chromatography using a 2 m Porak Q column and transfer of $SO_2$ to a Micromass Optima isotope mass spectrometer for determination of $\delta^{34}S$. The isotope ratio is related to sulphur in trolilite (CDT = Canyon Diablo Trolilite). The standards S-1 and S-2 from IAEA were used for calibration. The NBS127 standard was analysed as unknown. The accuracy is 0.2‰. Detection limit is approximately 5 µg, depending on the sulphur concentration and the matrix.

# 4 Execution

## 4.1 General

The aim of the study has been to identify fracture minerals and to reveal sequences of fracture minerals. Samples of fracture fillings suitable for microscopy were selected from the drill-cores of KFM01A, KFM02A and KFM03A+B. Fractures that were assumed to have been filled with minerals of different generations were preferred. Approximately 40 samples were selected from representative fractures. Most of the samples derive from KFM01A, whereas the samples from KFM02A and KFM03A are concentrated on hydraulically conductive sections in the boreholes which earlier had been subjected to groundwater sampling. The selection of the samples was more based on the information that could be expected from each of the samples than to get a statistic overview of the drill-core. Fractures with well preserved open fracture surfaces were sampled as well.

## 4.2 Selection of samples

Samples have been selected on different grounds:

- For mineralogical identification. Sampling has been initiated by the geologists carrying out the drill-core logging. These samples often result in XRD analyses but can as well be used for thin section preparation and subsequent microscopy.
- Samples selected for mineralogical studies (thin section preparation); these samples often show complex sealing and coatings and are usually chosen to represent several generations of fracture mineralization.
- Samples of open fracture surfaces (preferably with idiomorphic crystals of calcite or pyrite grown on the surface). These samples are selected for the calcite study including stable isotopes trace element composition and morphological determinations.
- Samples are preferably selected to match the groundwater sample sections.
- Poor drill-core quality due to flushing of loose material and polishing of fracture surfaces has significantly reduced the number of suitable samples, especially for drill-core KFM03A and partly for KFM03B, KFM02A and KFM01A.

## 4.3 Execution of work

Thin-sections with a thickness of 30 µm were prepared and analysed with optical microscope and scanning electron microscope (SEM) equipped with an energy dispersive spectrometer (EDS). In order to study minerals grown in the open space of some fractures, these fracture surfaces were also prepared and examined by SEM. Additional fracture surfaces were only briefly examined with stereomicroscope. Samples for XRD identification were scraped from the fracture surface and XRD analyses were executed according to the procedure in Section 3.1.

## 4.4 Data handling/post processing

The data from the microscopy and the different chemical analyses, including stable isotopes, have been compiled and are shown in appendices in this report. The XRD results and the chemical composition of a smaller set of fracture fillings are presented in the P-report /1/. For the fracture mineral studies, the main problem is the small amounts of fracture minerals present in each fracture and also the presence of fracture minerals of different generations. The latter is especially valid for calcite, which may occur as similar looking precipitates of different generations in some of the fractures. Due to the above described problems, all the fracture analyses need to be regarded as potentially contaminated with other minerals or mixed generations. The data from the present fracture mineral study will therefore only be available together with this report and data are stored in SICADA as raw data files.

## 4.5 Analyses and interpretations

- The thin-sections produced have been used to identify mineral parageneses from different fracture filling generations. The division into different generations has been based on textural and mineralogical observations, e.g. cross-cutting relations and dissolution/replacement textures. Ductile, semi-ductile and brittle deformation has been noted as well. Different chemical compositions determined by SEM/EDS-analysis have been used in order to separate different generations of e.g. chlorite and calcites.
- The stable isotope ratios on calcite and pyrite samples have been used to interpret the formation environments for the different mineral generations. Attempts have also been made to relate the calcite generations to the sequence of events.

# 5 Results

The results from the present study are shown in appendices to this report. They are:

**Appendix 1:** Results from microscopy including order of mineralizations.

**Appendix 2:** Semi-quantitative chemical analyses of different fracture mineral phases; chlorite, calcite, laumontite, prehnite, epidote, analcime, K-feldspar/adularia and albite/ plagioclase.

**Appendix 3:** Compilation of the order of fracture mineral generations.

**Appendix 4:** Stable isotope analyses of calcites including O, C and Sr isotopes.

**Appendix 5:** ICP analyses on calcite leachates.

**Appendix 6:** Stable S isotopes in pyrite samples

## 5.1 Minerals identified

A list of fracture minerals identified within the Forsmark area is presented below (the XRD information referred to is published in P-report /1/)

*Quartz* ($SiO_2$) has been identified in many of the analysed samples, often as very small and hematite stained idiomorphic crystals covering the fracture walls and often showing light brownish colour and sugary appearance.

*Albite (Na-Plagioclase)* ($NaAlSi_3O_8$) is often found in fillings together with hydrothermal K-feldspar (adularia). The fillings can be brick red due to hematite staining.

*K-feldspar* ($KAlSi_3O_8$) is in the Forsmark fracture samples usually adularia (the low-temperature form) but is also present showing typical microcline twinnings. Like in albite, the colour can be brick red.

*Epidote* ($Ca_2Al_2Fe(SiO_4)(Si_2O_7)(O,OH)_2$) is relatively rare especially in the open fractures of KFM01A, KFM02A and KFM03A+B. According to the chemical analyses (Appendix 2), the Fe content varies between 8 and 14 weight % given as FeO. In reality, however, most of the Fe in epidote is Fe(III).

*Prehnite* ($Ca_2Al_2Si_3O_{10}(OH)_2$ ). Light greyish green to grey, hydrothermal mineral, but also typical for burial metamorphism (prehnite-pumpellyite facies). In the samples from Forsmark it is often in-mixed with quartz or calcite and in some cases with analcime. The Fe content varies between 1.0 and 5 weight % given as FeO in the analysed prehnite samples. Like in epidote most of the Fe is Fe(III).

*Laumontite* ($CaAl_2Si_4O_{12}x4H_2O$) is a very common zeolite mineral in the Forsmark area. It shows a prismatic shape and is brittle. The mineral is white, but is mostly coloured red by micro-grains of hematite, although white varieties are observed as well. Zeolites have open structures suitable for ion exchange. Detectable amounts of K and Na are therefore to be expected. In the analysed minerals, both $K_2O$ and $Na_2O$ constitute less than 1 weight %.

*Analcime* ($Na(Si_2Al)O_6xH2O$) has colourless, usually trapetzohedral crystals (like garnet). This is considered as one of the highest temperature zeolites but has a large range of formation temperatures. In Forsmark, relatively big crystals have been found in some fractures (in the order of 5 to 10 mm).

*Apophyllite* ($(K,Na)Ca_4Si_8O_{20}Fx8H_2O$) is a hydrothermal sheet silicate with white to silvery surface. It is detected in some fractures at Forsmark, and based on a few SEM/EDS analyses it seems to be a relatively pure K-Ca-apophyllite.

*Pyrite* ($FeS_2$) is found in many fractures as small idiomorphic, cubic crystals grown on open fracture surfaces.

*Hematite* ($Fe_2O_3$) is common in the Forsmark fractures but the amount is relatively low (does not so often turn up in the diffractograms). However, micro-grains of hematite cause intense red-staining of many fracture coatings.

*Chlorite* ($((Mg,Fe)_6(Si,Al)_4O_{10}(OH)_8$) is a usually dark-green mineral found in several associations. XRD identifies the chlorite as clinochlore but large variations in FeO/MgO ratios are indicated from SEM/EDS analyses (from 6 down to < 1). The occurrence of K and Ca in many of the chlorite samples indicates possible ingrowths of clay minerals, mostly corrensite. The Mn and Ti contents in the chlorites are usually low but a few samples have $TiO_2$ values between 1 and 1.5 weight %.

*Calcite* ($CaCO_3$) is like chlorite very common and occurs in different assemblages and with different crystal shape. The calcite analysed generally shows low contents of both Mg, Mn and Fe.

*Fluorite* ($CaF_2$). Violet fluorite is found in a few fractures.

**Clay minerals:**

*Corrensite* ($((Mg,Fe)_9(Si,Al)_8O_{20}(OH)_{10}xH_2O$) is a chlorite-like mixed-layer clay with layers of chlorite and smectite/vermiculite, usually with a ratio of 1:1. Some of the corrensite samples identified from Forsmark show irregular ordering in the layering, indicating either that they have not reached to perfect corrensite crystallinity or that they are altered. Corrensite is the clay mineral most frequently found, and as mentioned above often found together with chlorite. This is a swelling type of clay as are also mixed-layer illite/smectite and saponite (see below).

*Illite* ($(K, H_2O)Al_2[(Al,Si)Si_3O_{10}] (OH)_2$ Occurs as micro – to cryptocrystalline, micaceous-flakes, and is in the Forsmark samples usually light grey in colour.

*Mixed-Layer clays.* Mixed-layer clay with layers of illite and smectite has been identified in some fractures. The ratio is 3:2 when determined.

*Saponite* ($Mg_3(Si_4O_{10})(OH)_2xnH_2O$). This is a variety of swelling smectite. It is identified in some fractures, most of which are in borehole KFM03A.

## 5.2 Results from microscopy

Appendix 3 shows the compilation of established sequences of mineralizations. From this compilation, it is obvious that several generations of minerals occur like quartz, K-feldspar, chlorite and calcite. It can also been seen that e.g. epidote belongs to the oldest generation only in the thin sections studied, whereas e.g. analcime and clay minerals are found in later generations. Summarising the information from the microscopy, the following six generations of fracture mineralizations can be established:

### 5.2.1 Generation 1

The oldest generation in the area mainly consists of epidote and quartz cataclasite in places with thin mylonites, cf Figure 5-1. Epidote, chlorite, quartz, K-feldspar and in some fractures fluorite have been formed during this period. The altered rock fragments in the cataclasites mostly contain quartz, K-feldspar and albite. A later cataclastic reactivation, usually accompanied by hematitisation causing red-staining, has been observed in some samples. As a last phase, larger epidote crystals have been formed along some fractures. The FeO content in the epidote varies between 7.6 to 14% and shows large variations between different samples as well as between adjacent crystals. In conclusion, it seems as the Generation 1 represents a time period during which P-T conditions gradually moved from semi-ductile to brittle at greenschist facies.

It can be concluded that Generation 1 is less represented in boreholes KFM01A, KFM02A and KFM03A, which are all situated within the central parts of the candidate area, but seems to be more common along the SE-NW striking zone constituting the western border of the site, as indicated by results from the mapping of drill-core KFM04A and the fracture mineral study in progress.

It has not been possible to make any clear correlation between the epidote generation and preferred orientation of fractures for the boreholes KFM01A, KFM02A and KFM03A.


***Figure 5-1.*** *Epidote mylonite-cataclasite. The fine-grained matrix consists of epidote. (Microphotograph KFM02A 516.60–516.65 m).*

### 5.2.2 Generations 2 and 3

Generation 2 and 3: This is a sequence of hydrothermal mineralizations of which the first phase includes prehnite (Generation 2; cf Figure 5-2), followed by a second phase of laumontite, calcite and small grains of hematite (Generation 3). It is very difficult to find samples with both prehnite and laumontite, but one sample shows prehnite in the wall rock close to the fracture which is sealed with laumontite. The core logging shows that laumontite is common in NE striking, relatively steep fractures. The abundance and orientation of fractures containing prehnite is less clear, partly due to the difficulties in the macroscopic identification of prehnite. It is evident that especially the laumontite has crystallised during a period with extensive brittle deformation; new fractures are formed, often with distinct angle to the foliation and the laumonitite has sealed brecciated parts of the wall rock (breccias in the order of centimetres to decimetre width; cf Figure 5-3). Chlorite and corrensite are also found together with prehnite and laumontite in Generations 2 and 3. Brick red fillings in thin sealed fractures of dominantly adularia with albite and quartz in various portions are common within the Forsmark area. The redstaining is caused by micrograins of hematite. These fractures are found in close relation with the laumontite fillings, cf Figure 5-4 and Figure 5-5. The exact relation between the laumontite and the red-stained feldspar mineralizations is unclear, but some observations support that the laumontite post-dates the feldspar fillings.

The reason for the few observations of coexisting prehnite and laumontite may be explained by dissolution and alteration of prehnite during zeolite phases. The abundance of laumontite indicates that the hydrothermal circulation during upper zeolite phases has been more intense than during prehnite-pumpellyite phases.

Light greyish green adularia precipitates postdating the laumontite fillings are found as coatings in open fractures, cf Figure 5-3. It is not clear whether this represents a final event within Generation 3 or a first event of Generation 4. At present, this type of mineralization has been found in too few samples to make conclusive interpretations possible.


***Figure 5-2.*** *Mylonite with epidote, chlorite and quartz (Generation 1) on which prehnite (Generation 2) has crystallized. (Microphotograph KFM03A 451.85–451.90 m).*

After the hydrothermal activity responsible for the prehnite/laumontite mineralizations, there has been a period of extensive dissolution and breakdown of earlier formed hydrothermal minerals. It is possible that this period is close in time to Generation 4 (see below).

***Figure 5-3.*** *Laumontite sealed breccia (Generation 3) cut by a fracture filled with adularia (Generation 4 or possibly a very late phase of Generation 3). The diameter of the drill-core is c 5 cm (KFM01A 124.4–124.8 m).*

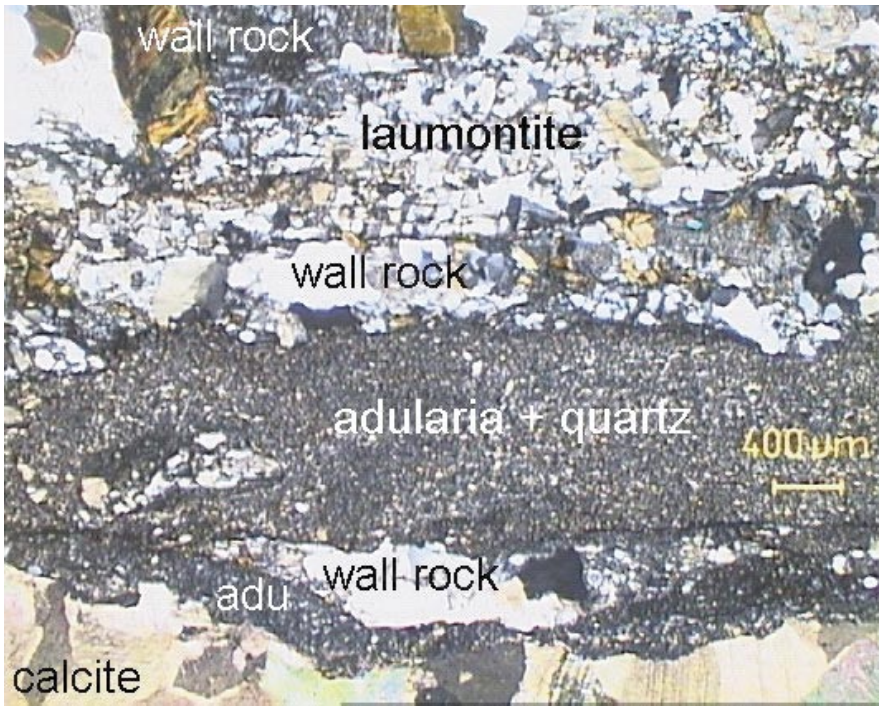


***Figure 5-4.*** *Parallel fracture fillings with laumontite, adularia + quartz, calcite and pure adularia. (Microphotograph KFM03A 334.41–334.56 m).*

***Figure 5-5.*** *Fracture filled with adularia that is brick coloured due to micro-grains of hematite. Some calcite is also present in the fracture. The diameter of the drill-core is c 5 cm. (KFM03A 184.34–184.50 m).*

### 5.2.3 Generations 4 and 5

Generation 4 follows the dissolution phase and consists mainly of quartz, analcime, adularia and often albite with or without chlorite/corrensite, the latter usually Fe-rich. Calcite may be co-precipitated with this assemblage but is usually later. This generation is very common all over the area, and quartz coatings are represented by many fractures in most directions including horizontal and sub-horizontal ones. Quartz is the overall dominant filling of this generation and thin coatings of tiny idiomorphic quartz crystals cover many fracture surfaces, cf Figure 5-6.

Apophyllite has been identified in a few samples from KFM02A and KFM03A (Figure 5-7). It is at present not clear if this mineralization is part of Generation 4 or Generation 3.

It looks like the event corresponding to Generation 4 is mainly a phase of reactivation but a generation of new fractures has probably also started. The preceding period of dissolution has made interpretations of cross-cutting relations more difficult. Many of the voids and cavities in the fractures are created during this period. Although some dissolution must have taken place, the conditions during this phase has not completely exceeded the stability for laumontite (< 250°C). Fission track studies on apatites /5/ indicate that the temperature has not exceeded 100 °C in south-central Sweden during the last 600 Ma. The abundance of the quartz coating is a sign of a hydrothermal circulation of considerable proportions, and is not likely to have developed at temperatures below 100 °C. This would give Generation 4 a minimum age of c 600 Ma.

Calcite, pyrite and rarely barite are found on top of the quartz coatings. These calcite crystals have a short C-axis or are equant. Analcime may belong to this late phase as well. These minerals have been interpreted to represent Generation 5, which probably is closely related in time to Generation 4.

***Figure 5-6.*** *Calcite and pyrite crystals (Generation 5) on top of a quartz coated fracture surface (Generation 4). Length of photograph is 2.5 cm (KFM01A 267.0 m).*

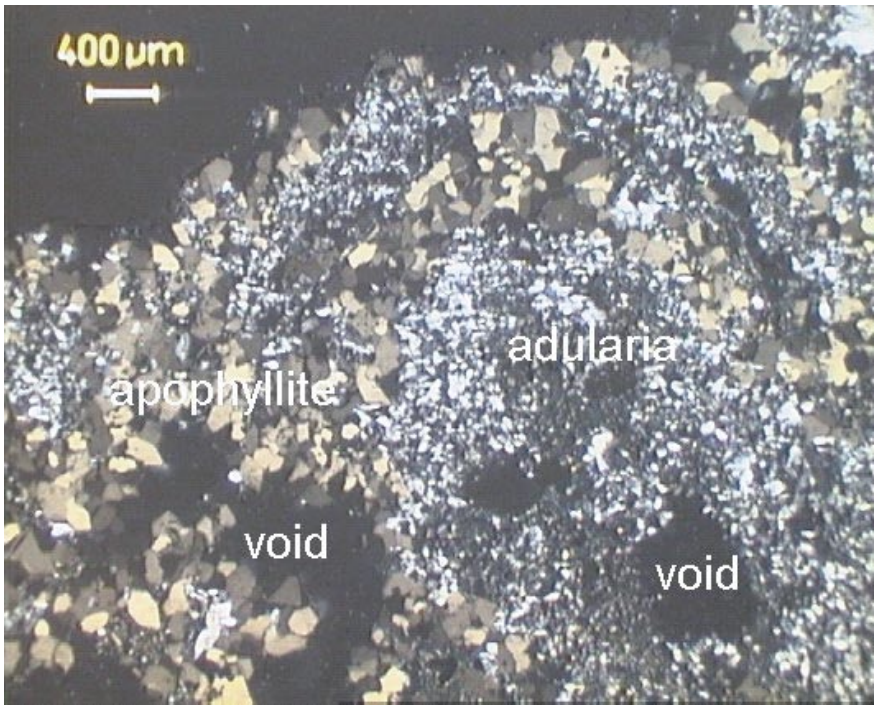


***Figure 5-7.*** *Adularia surrounded by apophyllite. Microphotograph (KFM03A 813.88–813.97 m).*

### 5.2.4 Generation 6

This generation includes the low temperature fillings of clay minerals and late calcite.

The clay minerals found in this late phase are dominantly illite, mixed-layer clays and smectite. Two prehnite fillings (KFM01A 185 m and KFM02A 111 m) show intense alteration probably during oxidizing conditions. This resulted in formation of illite and precipitation of hematite. The oxidizing conditions are supported by the presence of a small but significant positive Ce anomaly in the fracture filling from KFM01A 185 m (cf /4/).

The minerals from this generation has been the most difficult to study due to the loss and disturbances of the soft and loose minerals during drilling. It is likely that lots of these minerals have been lost when flushing the borehole during drilling, larger amounts of soft material can be seen in the BIPS-image than in the drill-core. Based on the material sampled so far and the analyses of different late calcites, it can be suggested that low temperature alteration has occurred during a long time span (or during repeated occasions).

Asphaltite has been recorded in some samples from KFM01B and KFM02A. The formation conditions for the asphaltite is yet not clear but it looks like it post-dates the quartz formation of Generation 4 (cf Figure 5-8). Analyses of the asphaltite are at present carried out and more information will be available in the next reporting state.

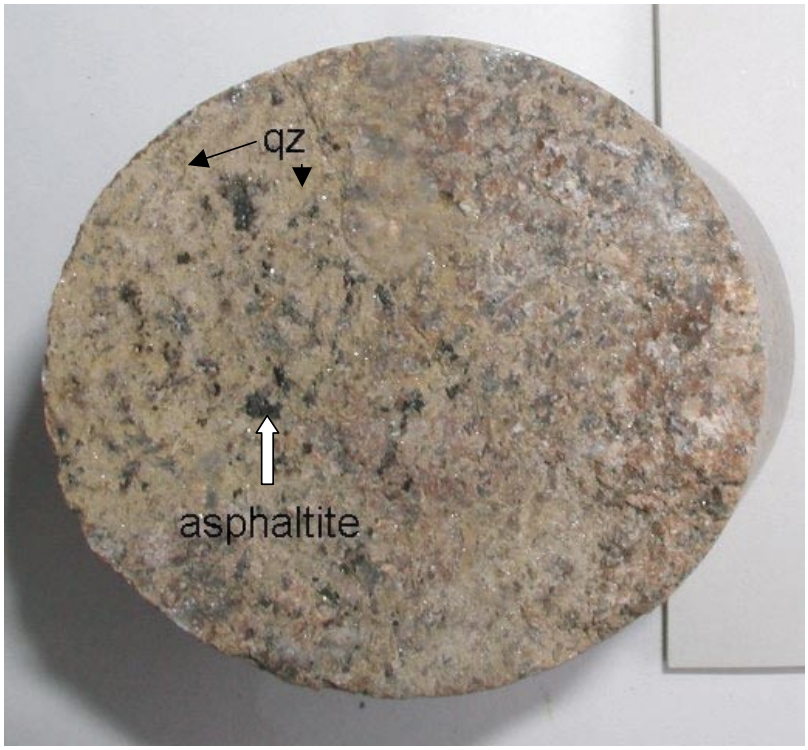


***Figure 5-8.*** *Beige coating of small idiomorphic quartz crystals (Generation 4) with small asphaltite crystals on top (Generation 6?). The diameter of the drill-core is c 5 cm. (KFM02A 179.39–179.44).*

## 5.3 Wall rock alteration.

The wall rock surrounding the hydrothermally altered fractures shows a various degree of alteration, which however is most intense adjacent to epidote- and laumontite-filled fractures (cf Figure 5-9). The dominant alteration is saussuritization of the plagioclase, chloritization of the biotite and sericitization of the K-feldspar. The altered wall rock is red-coloured due to micro-grains of hematite mainly in the plagioclase. The extent of the alteration rim is highly variable from < 1 cm to tens of centimetres. Quartz dissolution is obvious in some samples and especially in samples from borehole KFM02A 100 to 300 m. This alteration has increased the porosity along some of the fracture pathways considerably.

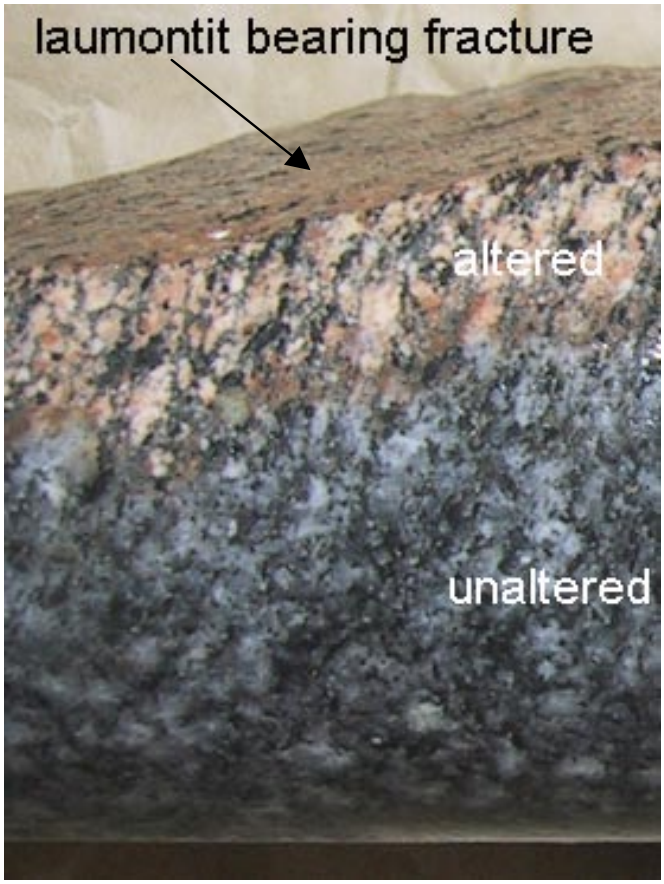


***Figure 5-9.*** *Laumontite bearing fracture in metatonalite with red-coloured altered aureole. The width of the aureole is c 1 cm on both sides of the fracture. (KFM03A 332.72–333.00 m).*

## 5.4 Redox conditions

The presence of pyrite (Fe(II)) and hematite (Fe (III)) provides indications of redox conditions during the period of mineralization. Many of the fracture coatings are red-stained due to presence of micro-grains of hematite. This is e.g. the case for the laumontite and some of the adularia/albite sealings. Oxidizing conditions are also indicated for the event that altered prehnite to illite and hematite. However, pyrite formation is indicated as a late phase (Generations 5 and 6) in many of the open fractures and the preservation of these pyrites is a strong indication of reducing conditions at present (valid at least for this set of samples representing depths larger than 100 m). Uranium series analyses on fracture filling material will be carried out during the next phase of the fracture filling studies and will add information about the redox conditions during the last 1 Ma.

## 5.5 Fracture calcites.

In order to sort out different calcite generations and to provide palaeohydrogeological information, 54 samples have been analysed for $\delta^{13}C/\delta^{18}O$, of which 16 were selected for $^{87}Sr/^{86}Sr$ and a smaller set (7 samples) analysed for chemical composition. Appendix 4 shows all calcites analysed for stable isotopes and trace element chemistry. The calcites represent both sealed and open fractures. In some of the latter it has been possible to sample calcites grown in open space, showing euhedral crystal forms. Notations have been made on crystal morphology when possible, since correspondence between calcite morphology (long and short C-axis) and groundwater salinity has been found in fracture mineral studies e.g. in Sellafield /6/. The indication from these studies is that fresh water carbonates usually show short C-axis (nailhead shaped crystals), whereas calcite precipitated from saline waters preferably show long C-axis (scaleohedral shapes). Equant crystals are common in transition zones of brackish water. Concerning the Forsmark samples (from depths between 0–500 m) most crystals show short C-axis and equant crystal forms, indicating fresh or brackish water precipitates. This is in contradiction to the post-glacial groundwater chemistry which shows saline water at depths below c100 m /7/ and supports an older origin of the calcites sampled.

The $\delta^{13}C/\delta^{18}O$ values of calcites from boreholes KFM01A, KFM02A, KFM03A and KFM03B are plotted together with previously analysed calcites from the Finnsjön area (/8/; Figure 5-10). There is a remarkable similarity between the range of the Forsmark samples and that of the Finnsjön calcites, although the more extreme $\delta^{13}C$ values were not identified in the Finnsjön samples, possibly due to mixing of different generations in this early sampling campaign. The Forsmark calcites show $\delta^{18}O$ values ranging from –7,4 to –18 o/oo and $\delta^{13}C$ values from –36 to +8 o/oo. The calcites with the lowest $\delta^{18}O$ values have $\delta^{13}C$ typical for hydrothermal calcites without signs of biogenically modified carbon (–7 to –2 o/oo). The calcites with higher $\delta^{18}O$ values (indicating possible precipitates from meteoric or brackish Baltic Sea water based on fractionation fractures by O´Neil et al. (1969) /9/ and ambient temperatures in the range of 7–15°C also show larger variation in their $\delta^{13}C$ carbon isotope values, supporting interaction with biogenic carbon. Extreme $\delta^{13}C$ values are recorded both on the low and high side (< –20 o/oo and > 0 o/oo). These are interpreted to be the result of microbial activity in situ (in the bedrock) causing locally extreme enrichment or depletion in $^{13}C$ in the $CO_2$–$HCO_3^-$ system which is then inherited by the calcites. It should be noted that the fractionation between $HCO_3^-$ and $CaCO_3$ is only a few per mille and that the $\delta^{13}C$ value in the calcite therefore largely reflects the $\delta^{13}C$ value in the bicarbonate at the time of calcite formation.

The calcites with euhedral crystals show $\delta^{18}O$ values between –9 and –12.2‰ and $\delta^{13}C$ values usually within the range of –5 to –20‰, except for the only two samples showing typical elongated scaleohedral shapes. The latter two samples are part of a population of five fracture samples displaying positive $\delta^{13}C$ values (+5 to +8‰), all of which belong to borehole KFM02A and four of them to a fracture zone at c 110–118 m depth.

There are no indications of low temperature precipitates from marine Sea water, although brackish water origins (e.g. similar to Littorina Sea composition) cannot be ruled out for a number of samples in the $\delta^{18}O$-interval –7.4‰ to – 9,5‰, for example those showing scalenohedral shapes in the KFM02 borehole at 110–118 m depth.

Figure 5-11 presents $\delta^{18}O$ versus $\delta^{13}C$ for the Forsmark samples only, with the shape of the euhedral calcites distinguished. In some cases, it has been possible to sample two generations of calcites and the arrows in Figure 5-11 tie these samples together, pointing from the oldest generation towards the youngest. A sequence of at least three different calcite generations, which can be correlated to the fracture mineralogical subdivision, has been documented. These are:

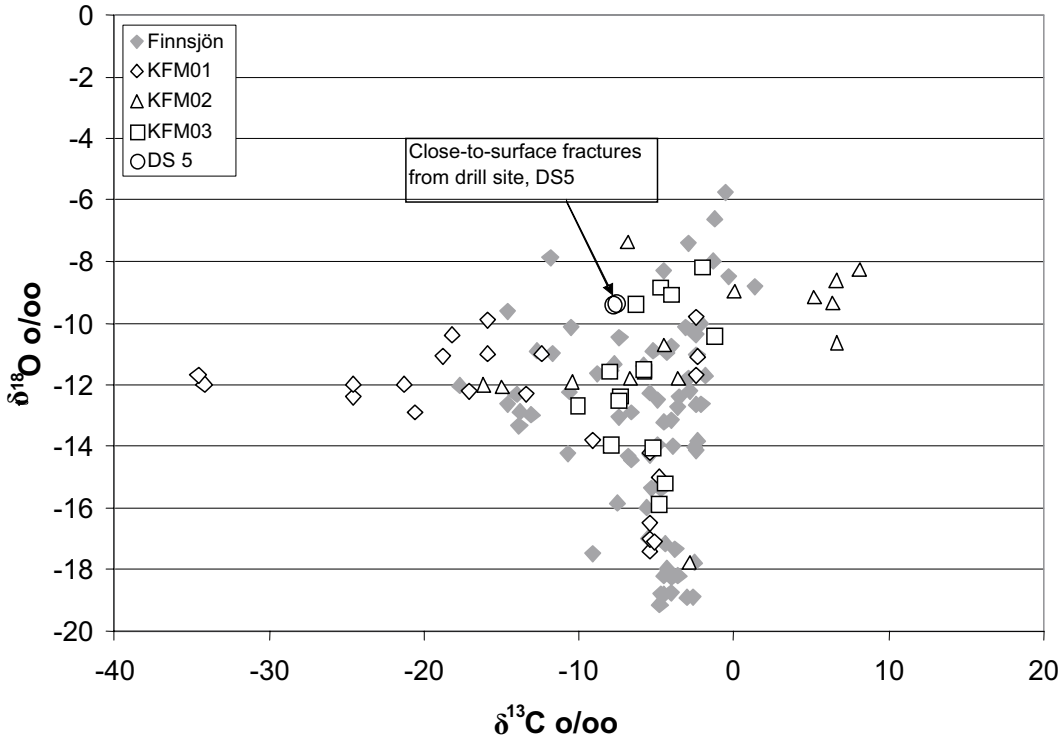


***Figure 5-10.*** *$\delta^{13}C/\delta^{18}O$ values for fracture calcites from KFM01A, KFM02A, KFM03A, KFM03B and two surface samples from the site DS5 (the drilling site for the fifth deep borehole KFM05A), plotted together with earlier analysed samples from the nearby Finnsjön site /8/.*

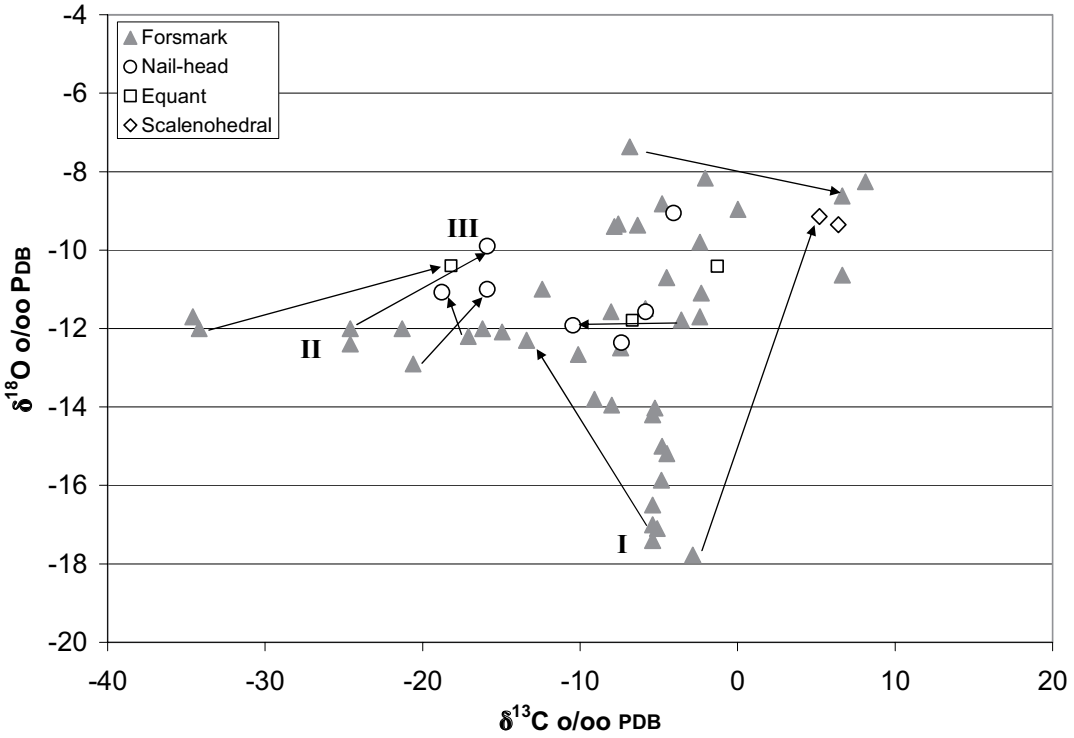


***Figure 5-11.*** *$\delta^{13}C/\delta^{18}O$ values for fracture calcites from KFM01A, KFM02A, KFM03A, KFM03B and the two surface samples from DS5. The arrows indicate samples where two calcite generations have been sampled in the same fracture. Directions are from the oldest, pointing towards the youngest. Note that crystal shapes are indicated were possible to distinguish.*

I) Hydrothermal calcites with mostly low $\delta^{18}O$-values (down to –18‰) and high $\delta^{13}C$ (–5 to –2‰). These calcites are found together with prehnite and laumontite and thus support a close relationship between these two generations (Generations 2 and 3).

II) Calcites with extremely low $\delta^{13}C$-values (down to –36‰) and $\delta^{18}O$-values around –12‰: These are found together with quartz fracture coatings (Generation 4).

III) Euhedral calcites grown possibly as a latest phase on top of the quartz adularia coatings, usually found together with pyrite (Generation 5). $\delta^{18}O$-values vary between –11 and –10 and the $\delta^{13}C$-values are in the range –18 to –20‰.

Figures 5-12 and 5-13 show $\delta^{18}O$ and $\delta^{13}C$ plotted versus depth for the analysed samples from Forsmark. These plots put the focus on the inhomogeneous distribution of the samples versus depth. The interval between 100 to 500 m is relatively well represented whereas only four samples derive from larger depths than 600 m. In the uppermost 100 m there is only a group of samples from the near-surface available yet. It can be noted that no specimens with hydrothermal signature have been found among these shallow samples, probably due to dissolution of old calcite. Concentrating on the $\delta^{13}C$ versus depth plot, it can be seen that that the biogenic signatures are common down to 300 m. The shallow samples in contrast show values between –2 and –7.8‰, typical for atmospheric values with little input of biogenic $CO_2$. The samples from 100 m to 200 m expose the largest variations in $\delta^{13}C$-values (–35 to +8‰), which may be a result of a larger input of organic material supporting higher microbial activity. At larger depths, the spread in $\delta^{13}C$ values decreases and only weak biogenic modified values are found below 450 m depth.

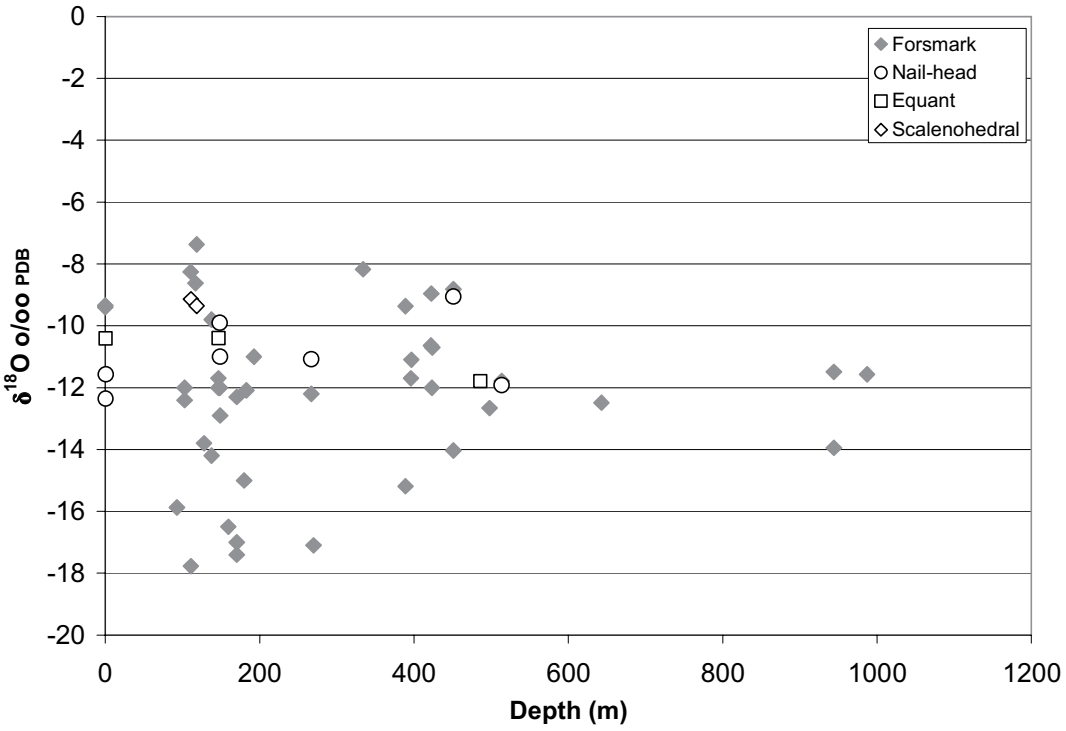


***Figure 5-12.*** *$\delta^{18}O$ values for fracture calcites from KFM0A1, KFM02A, KFM03A, KFM03B and DS5 plotted versus depth. Crystal shapes distinguished when possible.*

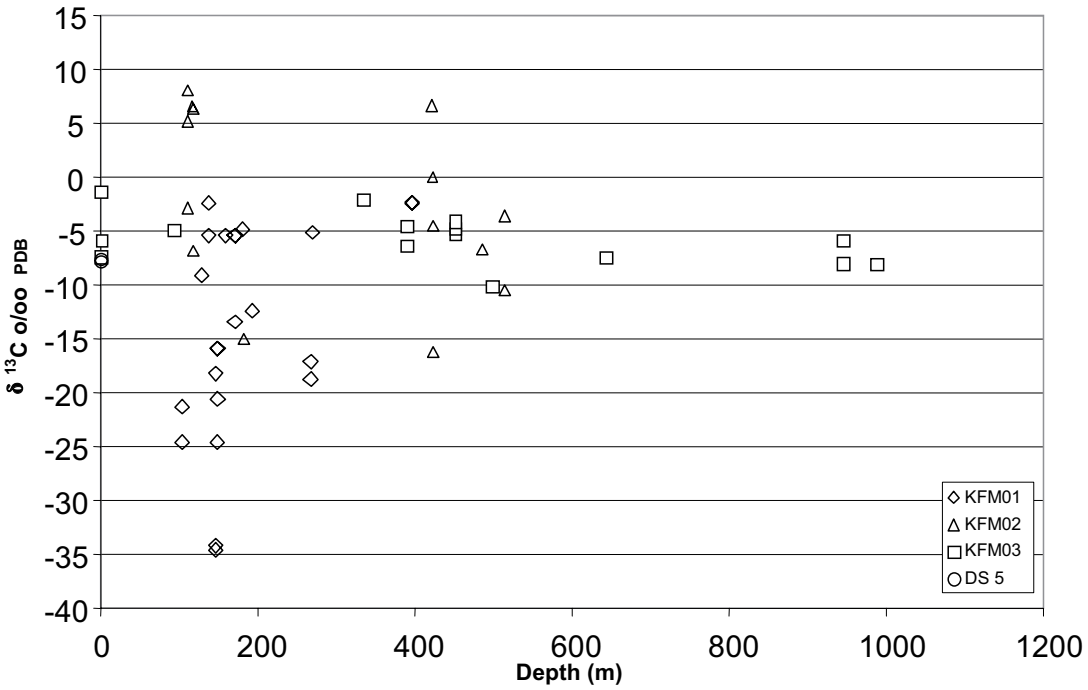


***Figure 5-13.*** *$\delta^{13}C$ values for fracture calcites from KFM0A, KFM02A, KFM03A, KFM03B and DS5 versus depth.*

The Sr isotope values ($^{87}Sr/^{86}Sr$-ratios) have been analysed for 16 of the samples from borehole KFM01A. The samples demonstrate values between 0.707377 and 0.717800 with a clear bimodal distribution; six samples showing values from 0.707377 to 0.710752 and ten samples values between 0.714936 and 0.717800. Referring to the subdivision into different generations, it can be concluded that Generations 2 and 3 (the prehnite and laumontite generations) are characterized by a close relationship in that the co-precipitated calcites of these generations do not only show similarities in O and C isotope values but also in Sr isotope ratios and in a significantly higher Sr content than Generations 4 and 5 (Figure 5-14 and 5-15). Generations 4 and 5 calcites display largely uniform $^{87}Sr/^{86}Sr$ ratios that are significantly higher than the ones measured in Generations 2 and 3 samples. This may indicate a similar relationship between Generations 4 and 5 as indicated for Generations 2 and 3. They could therefore be part of two different prolonged events. These two events are probably clearly separated in time. Another possibility is however, that the hydrothermal fluids were very different in composition and therefore their Sr-isotope ratios were distinctly different. For a more extensive evaluation, there is a need for Sr isotope data from the groundwater which are not available yet.

Trace element analyses have been carried out on seven calcite samples. The results are shown in Appendix 5. Duplicates have been made on two samples. These analyses are made on leachates from calcite samples and it can be suspected that minor amounts of contaminant minerals have dissolved as well, or that ion exchanged elements are released from clay minerals included in the calcite samples, see Figure 5-16. This is, however, still the best way to gain information about the trace element contents in the very small calcite samples.

The trace element contents are generally low, but some differences between Generation 3 calcites (Laumontite-generation) and 4 (quartz and adularia generation) can be seen; Generation 3 are higher in Sr and Mg, lower in light REE and shows mostly negative Ce-anomlies. One sample from Generation 3 shows a significantly higher Mn value than the other samples analysed. The reason for this is at present not understood.

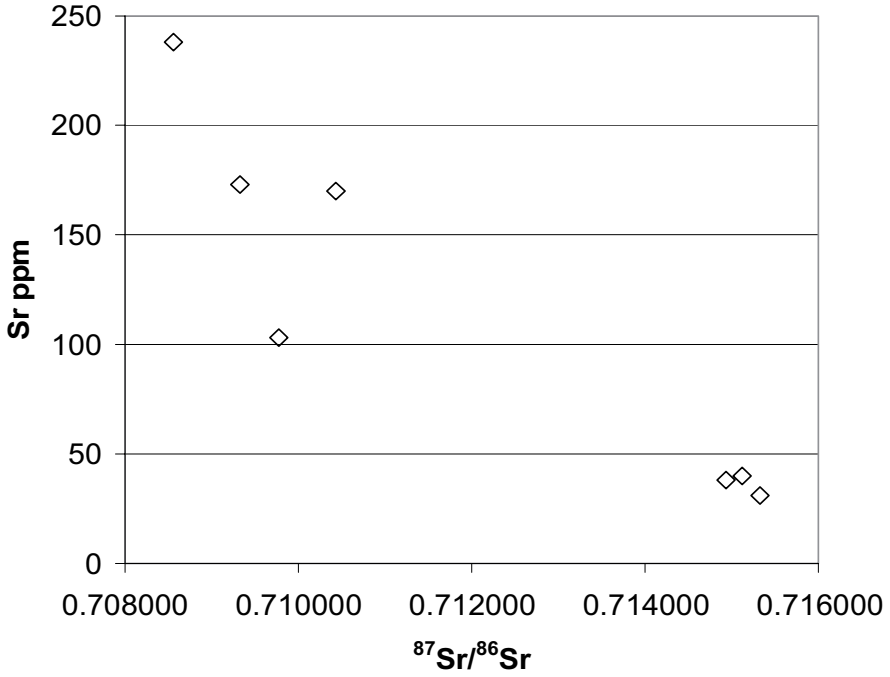


***Figure 5-14.*** *$^{87}Sr/^{86}Sr$ ratios plotted versus Sr contents in fracture calcites from KFM01A.*

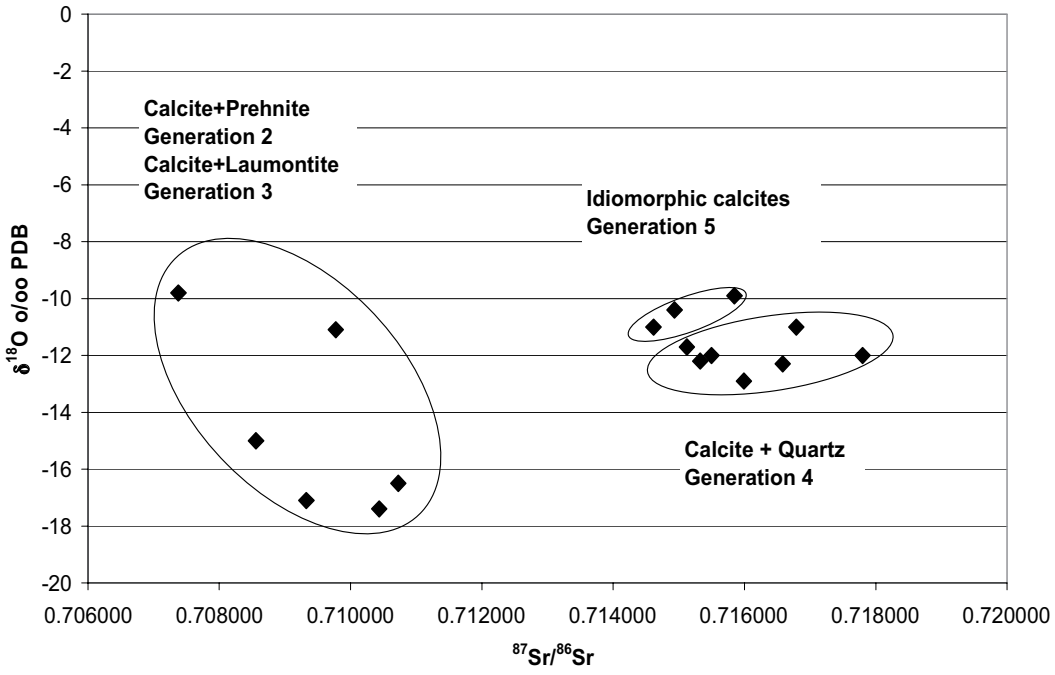


***Figure 5-15.*** *$^{87}Sr/^{86}Sr$ ratios plotted versus $\delta^{18}O$ values for fracture calcites in KFM01A.*

The negative Ce-anomalies in the Generation 3 samples may have several explanations: one is that oxidation has occurred during the hydrothermal event causing immobilisation of Ce and in turn a negative Ce-anomaly in the hydrothermal fluid responsible for the calcite precipitation.

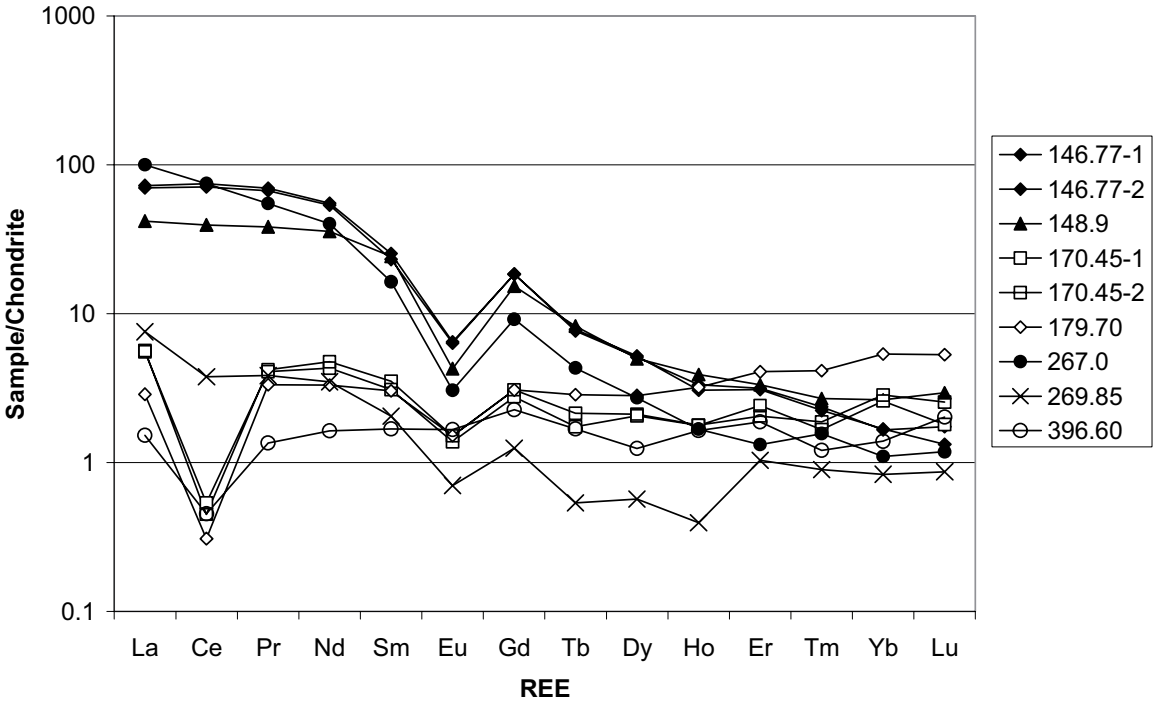


***Figure 5-16.*** *Chondrite normalised REEs patterns for fracture calcites from KFM01A. Note that these analyses are made on leacheates of calcite samples which contain small amounts of contaminant minerals.*

In conclusion: calcites have been precipitated in the fractures at several occasions, starting with the hydrothermal prehnite-laumontite generation. Taken all the stable isotope data into account there is a strong support for these two generations to be part of the same prolonged event; the tailing in $\delta^{18}O$ for this group from –18 to at least –14 o/oo may be due to precipitation from a hydrothermal fluid during decreasing temperatures. The connection between the calcite in the prehnite and laumontite generations are in accordance with earlier observations from Finnsjön /8/.

Calcite with extremely low $\delta^{13}C$ values has been produced during the event responsible for the quartz and analicime formation. These mineralizations must have been precipitated during lower temperatures than the preceding laumontite formation, although it is reasonable to assume that it was still hydrothermal (< 200°C is suggested). The very low $\delta^{13}C$ values are usually interpreted as due to microbial activity in situ which implies that the temperature was not significantly above 100°C when the carbon isotope signature was modified. However, the temperature may have increased subsequently during a period of calcite precipitation. Based on Sr isotope values this period is clearly separated from the prehnite-laumontite formation either in time (the radiogenic $^{87}Sr$ is much higher in the latter generation), or the chemistry of the hydrothermal fluid was significantly different and preferred dissolution of K-Rb minerals occurred.

The euhedral crystals (mostly equant in shape) grown on top of the quartz-calcite-adularia coatings in some of the fractures are possible the latest phase of these events.

Several calcite precipitates have not yet been possible to relate to any specific fracture mineralization event. For example, a group of calcites in KFM02A at 110 to 118 m shows significantly positive $\delta^{13}C$ values (+6 to +8‰) and $\delta^{18}O$ values of –8 to –11‰. There is also a cluster of samples that may include relatively late (Quaternary) precipitates. More analyses are, however, needed in order to better identify this group.

## 5.6 Fracture pyrites

Pyrites have been found on many fracture surfaces, especially associated with Generations 4 and 5 quartz and calcite coatings. A number of six pyrite samples have been analysed for $\delta^{34}S$ (Appendix 6). The values range from 15.7 to 5.4‰ with the exception of one value of 31.5‰. The obtained values indicate a dominantly hydrothermal origin and they do probably represent more than one single event. Additional analyses are planned for the next phase of the fracture mineralogical study.

# 6 Summary

The fracture mineral history traced by this study starts with epidote, quartz and chlorite formation during greenschist facies, semi-ductile to brittle condition (Generation 1). Only very thin mylonites are present whereas cataclasites are more frequent. No age information is available but earlier dating of epidote in altered wall rock from this area gives Rb-Sr ages older than 1,500 Ma /10/. Orientations in NW (steeply dipping) are indicated for these fractures but also a sub-horizontal set is recorded based on the core mapping /1, 2, 3/.

Next phase of fracture mineralization is the hydrothermal event responsible for prehnite (Generation 2) and laumontite (Generation 3) crystallization. In addition, calcite as well as chlorite/corrensite, adularia and quartz have been precipitated during this event. The stable isotope ratios of O, C and Sr for the calcites support a close relationship between the prehnite and laumontite formation. The results show typical hydrothermal signatures for the carbon isotopes, a narrow interval in $^{87}Sr/^{86}Sr$ supporting a common origin, and increasing trend in the oxygen isotope values, indicative of precipitation during decreasing temperatures. This information supports the interpretation of fracture mineralization during brittle conditions and P-T conditions changing from prehnite-pumpellyite phases over to upper zeolite phases. The Generations 2 and 3 represent a clearly separated stress regime as compared to Generation 1. There is a clear dominance of steep NE-oriented fractures which cut the foliation during Generation 3. Furthermore, this period seems to represent an event of new fracturing characterized by laumontite as the oldest coating in these fractures. The age of this hydrothermal event is so far unclear, but earlier datings in the area indicate Post-Jotnian formation ages. The frequent brick red thin sealed fracture (hematite stained adularia +/– albite +/– quartz) commonly found in the area belongs most probably to this generation

The following phase starts with dissolution along older laumontite/prehnite sealed fractures causing cavities in fractures and to a lesser extent in the adjacent host rock. Subsequent temperature decrease has caused precipitation of quartz covering fracture surfaces and coating voids. Adularia, chlorite/corrensite and calcite are also precipitated during this period (Generation 4) and in a later phase analcime, pyrite and calcite (Generation 5). Stable isotopes support a common origin for calcites of Generation 4 and 5. The $^{87}Sr/^{86}Sr$ ratios indicate a significantly higher input of radiogenic Sr during this period compared with that during the period for Generations 2 and 3. This can be explained either by a relatively long separation in time or by significantly different chemistry of the hydrothermal fluids involved; a preferential leaching of K-Rb rich minerals yields solutions rich in radiogenic Sr. The carbon isotopes in calcites are depleted in $^{13}C$. Such values are usually caused by microbial activity along the fractures in the bedrock. However, microbial activity is not expected above 100°C. This is in contrast to the extensive quartz and adularia formation which is not believed to have taken place at such low temperatures. This contradiction may be explained by microbiologically modified $HCO_3$ that was transported into higher temperature domains where it precipitated together with quartz and adularia at temperatures in the range of 100 to 200°C. The event during which Generation 5 was formed seems to have affected large parts of the fracture systems at Forsmark. However, it has not been possible to recognize any preferred directions of fractures in which this mineral assemblage was precipitated. Reactivation of fractures is obviously common during this period although new fractures were probably formed. No age information is available, but based on the indicated formation temperatures, a pre-Cambrian age is suggested.

Generation 6 includes the precipitates found as a top-layer on the fractures and represents calcite, clay minerals like illite, mixed-layer clays and smectites. Asphaltite may also belong to this generation, but further analyses are needed to be certain. It is probable that the continued fracture mineral studies will provide further subdivision of the formation of this mineral assemblage, which probably extends from the pre-Cambrian until the Quaternary; for example the scalenohedral calcites grown on fractures in KFM02A at depths of 111 and 118 m indicate a possibility of low temperature precipitates from saline-brackish water similar to Littorina type.

# References


/1/ **Petersson J, Wängnerud A, 2003.** Boremap mapping of telescopic drilled borehole KFM01A. Forsmark site investigation, SKB P-03-23, Svensk Kärnbränslehantering AB, 97 p.

/2/ **Petersson J, Wängnerud A, Stråhle A, 2003.** Boremap mapping of telescopic drilled borehole KFM02A. Forsmark site investigation, SKB P-03-98, Svensk Kärnbränslehantering AB, 102 p.

/3/ **Peterson J, Wängerud A, Danielsson P, Stråhle A, 2003.** Boremap mapping of telescopic drilled borehole KFM03A and KFM03B, SKB P-04-102, Svensk Kärnbränslehantering AB.

/4/ **Petersson J, Tullborg E-L, Mattsson H, Thunehed H, Isaksson H, Berglund J, Lindroos H, Danielsson P, Wängnerud A, 2004.** Petrography, geochemistry, petrophysics and fracture mineralogy of boreholes KFM01A, KFM02A and KFM03A+B. SKB P-04-103. Svensk Kärnbränslehantering AB.

/5/ **Cederbom C, Larson S Å, Tullborg E-L, Stiberg J-P, 2000.** Fission track thermo chronology applied to Phanerozoic thermotectonic events in central and southern Sweden, Tectonophysics, 136, p. 153–167.

/6/ **Milodowski A E, Gillespie M R, Pearce J M, Metcalfe R, 1998.** Collaboration with the SKB EQUIP programme; Petrographic characterisation of calcites from Äspö and Laxemar deep boreholes by scanning electron microscopy, electron microprobe and cathodoluminescence petrography, WG/98/45C, British Geological Survey, Keyworth, Nottingham, (1998).

/7/ **Laaksoharju M (ed), Gimeno M, Auqué L, Gomez J, Smellie J, Tullborg E-L, Gurban I, 2004.** Hydrogeochemical evaluation of the Forsmark site, model version 1.1. R-04-05, Svensk Kärnbränslehantering AB.

/8/ **Tullborg E-L, Larson S Å, 1982.** Fissure fillings from Finnsjön and Studsvik, Sweden. Identification, chemistry and dating. SKB Technical Report SKB TR 82-20. ISSN 0348-7504. 76 pp.

/9/ **O'Neil J R, Clayton R N, Mayeda T K, 1969.** Oxygen isotope fractionation in divalent metal carbonates, Journal of Chemistry and Physics, 51 (12), p 5547–5558.

/10/ **Wickman F E, Åberg G, Levi B, 1983.** Rb-Sr Dating of alteration events in granitoids, Contribution to Mineralogy and Petrology, 83, p 358–362.

# Appendix I

## Sample descriptions

Sample: KFM01A 103.0 m
Rock type: Metagranitoid
Fracture: A rough open fracture surface with very thin filling mineral coverings scattered over the fracture surface.
Orientation: N34E/73SE
Minerals: Pyrite, quartz

Sequence of mineralisations:

1. Pyrite + quartz

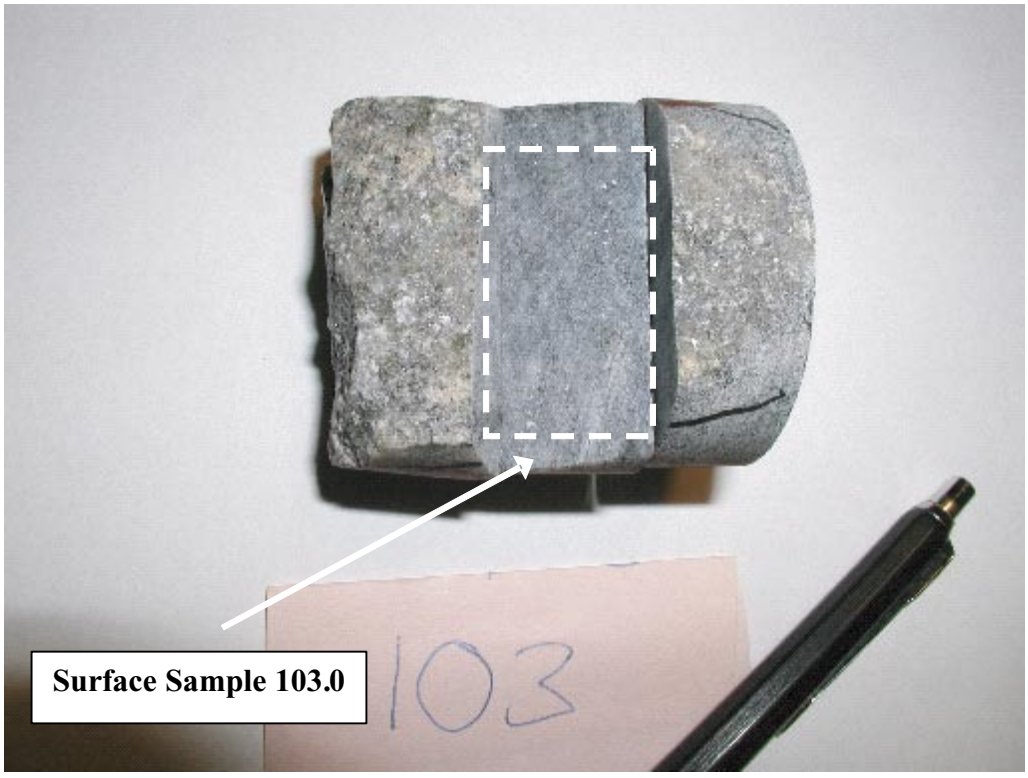


***Figure A-1.*** *Pyrite and quartz covered fracture (KFM01A 103.0 m).*

| | |
|---|---|
| Sample: | KFMA01A 110.90 m |
| Rock type: | Metagranitoid |
| Fracture: | Open fracture surface covered for most of its length with a thin, finely grained, mineral growth. Some of this growth cuts parallel with the surface into the wall rock. |
| Orientation: | N21E/12E |
| Minerals: | Quartz, K-feldspar, albite, Fe-chlorite, epidote, calcite. |

Sequence of mineralisations:

1. Intergrowth of quartz, adularia and albite. Some crystals of epidote and Fe-rich chlorite
2. Calcite

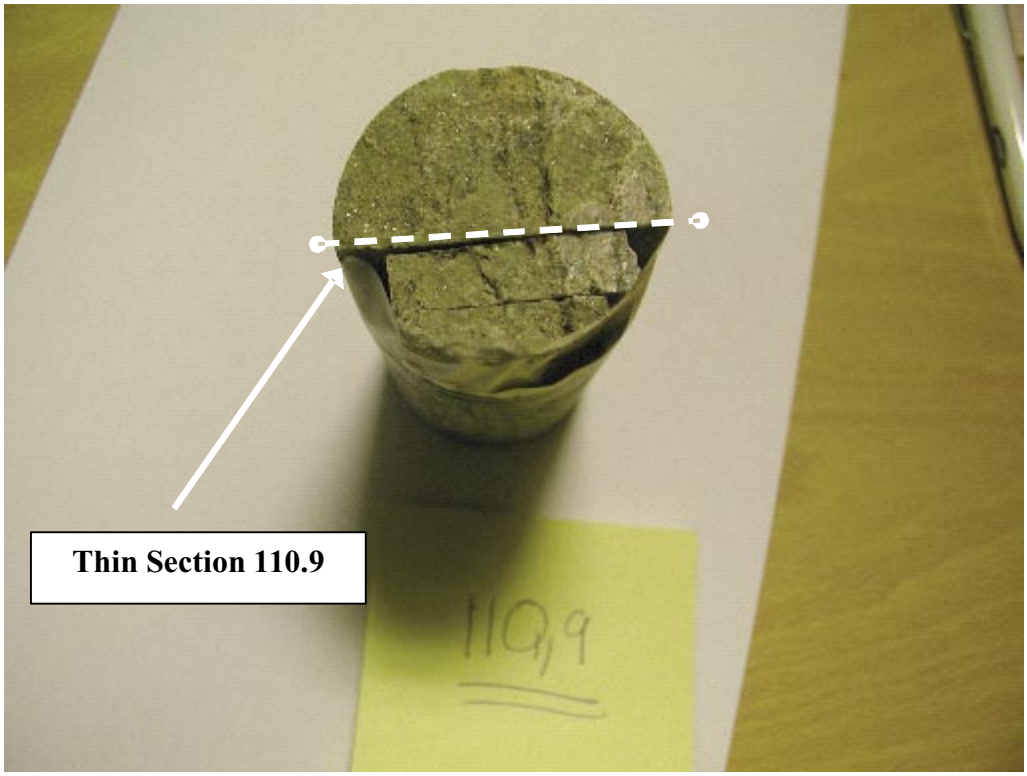


***Figure A-2.*** *Quartz, K-feldspar and albite covered fracture with later calcite. The diameter of the drill-core is c 5 cm (KFMA01A 110.90 m).*

Sample: KFM01A 112.88–112.95 m
Rock type: Metagranitoid
Fracture: This is a network of mostly sealed fissures with the dominating fissure direction being steep. Some fissures are wider and some fissures are also brecciated.
Orientation: N51E/76NW
Minerals: Laumontite, hematite, (quartz, K-feldspar, albite), Fe-chlorite.

Sequence of mineralisations:

1. Laumontite + wall rock fragments (qz+K-fsp+albite) + hematite
2. Hematite (laumontite surfaces)
3. Fe-chlorite


***Figure A-3.*** *Mainly laumontite filled fracture network. (KFM01A 112.88–112.95 m).*

Sample: KFM01A 127.4–127.45 m
Rock type: Metagranitoid
Fracture: Open fissure surface with mineral overgrowth.
Orientation: N58W/17NE
Minerals: Analcime, quartz, hematite, adularia, Fe-chlorite.

Sequence of mineralisations:

1. Adularia
2. K-feldspar + quartz + hematite
2. Analcime
3. Fe-chlorite


***Figure A-4.*** *Open fracture with mineral overgrowth. (KFM01A 127.4–127.45 m).*

Sample: KFM01A 128.0 m
Rock type: Metagranitoid
Fracture: An open wall rock surface covered at few places with very thin mineral growths, especially at irregularities of wall rock surface.
Orientation: N19W/74E
Minerals: Quartz, adularia.

Sequence of mineralisations:

1. Quartz + adularia

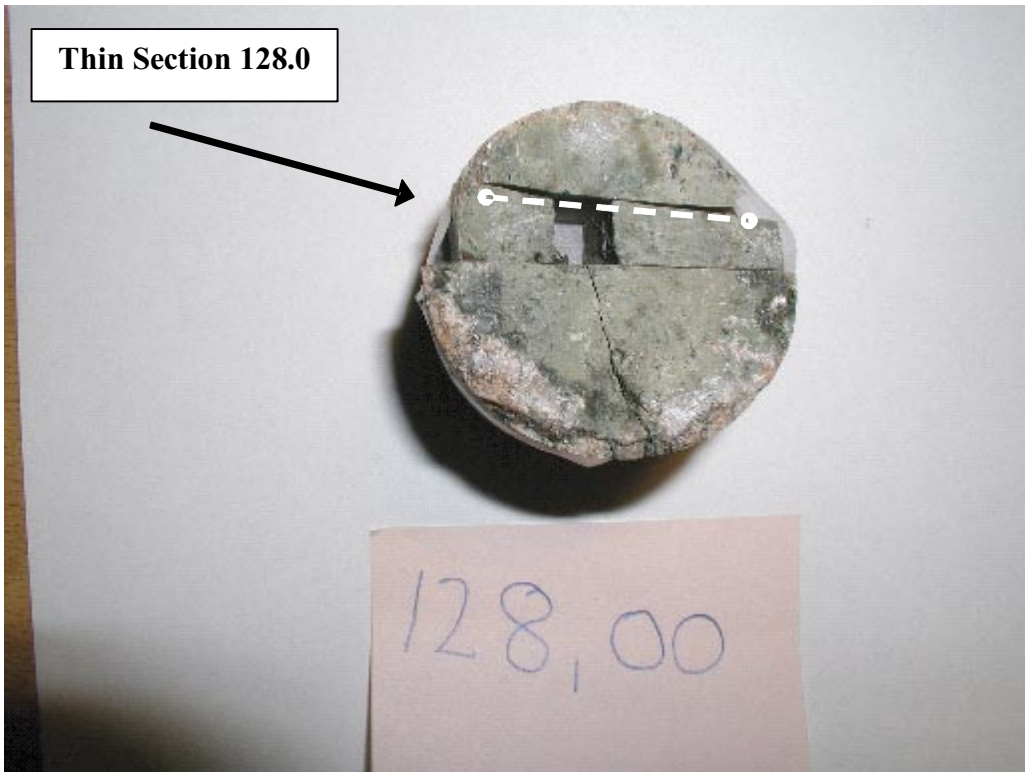


***Figure A-5.*** *Fracture surface with thin quartz and adularia coating. The diameter of the drill-core is c 5 cm (KFM01A 128.0 m).*

Sample: KFM01A 128.4–128.7 m (A)
Rock type: Metagranitoid
Fracture: Several veins mineralizations in a steep fissure with some open cavities. This sample is from a sealed and brecciated part of the fissure.
Orientation: N49E/78NW
Minerals: K-feldspar, albite, chlorite, quartz, laumontite, adularia.

Sequence of mineralisations:

1. K-feldspar + albite + chlorite + quartz
2. Laumontite + wall rock fragments (quartz + K-feldspar)
3. Adularia


***Figure A-6.*** *Laumontite sealed breccia. The diameter of the drill-core is c 5 cm (KFM01A 128.4–128.7 m (A)).*

Sample: KFM01A 128.4–128.7 m (B)
Rock type: Metagranitoid
Fracture: A sealed and steep fissure with large central cavities.
Orientation: N71E/75N
Minerals: K-feldspar, quartz, albite, prehnite, adularia, chlorite.

Sequence of mineralisations:

1. K-feldspar + quartz + chlorite + albite
2. Prehnite
3. K-feldspar
4. Adularia + chlorite

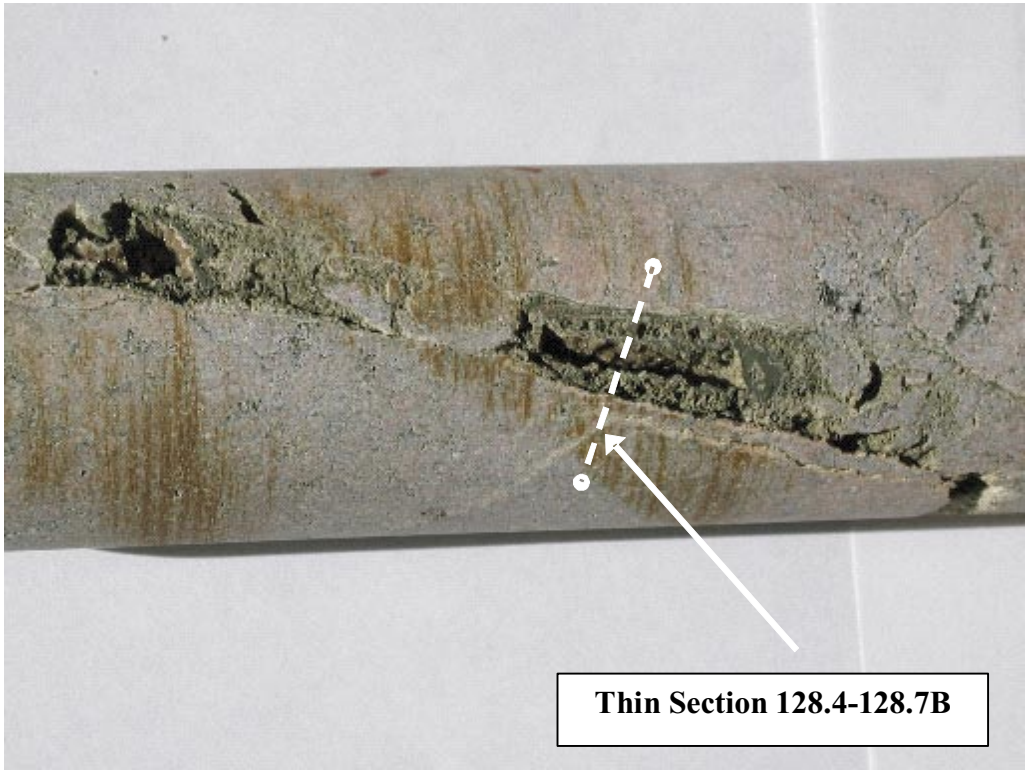


***Figure A-7.*** *Mineral filled fracture. The diameter of the drill-core is c 5 cm (KFM01A 128.4–128.7 m (B)).*

Sample: KFMA01A 137.8–137.95 m
Rock type: Amphibolite
Fracture: This is a steep, open, red-stained fracture surface with thin mineral coating. In addition a thin vein.
Orientation: N46E/59NW (uncertain)
Minerals: Epidote, calcite, laumontite, hematite.

Sequence of mineralisations:

1. Epidote
2. Mn-calcite
3. Calcite
4. Laumontite + hematite

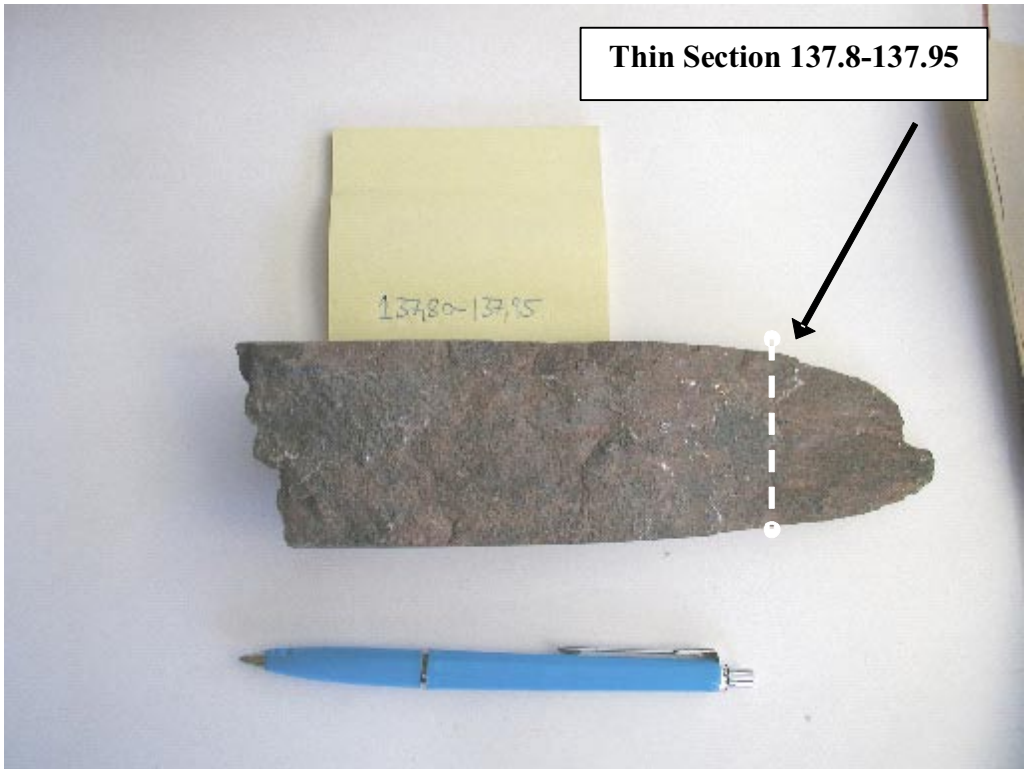


***Figure A-8.*** *Open mineral covered fracture (KFMA01A 137.8–137.95 m).*

Sample: KFMA01A 146.77–146.90 m
Rock type: Metagranitoid
Fracture: A fracture surface covered by thick mineral coating.
Orientation: N32E/77NW
Minerals: Quartz, K-feldspar, pyrite, calcite, epidote, titanite, chlorite.

Sequence of mineralisations:

1. Quartz + K-feldspar + epidote + titanite + chlorite
2. K-feldspar
3. Idiomorphic quartz
4. Calcite

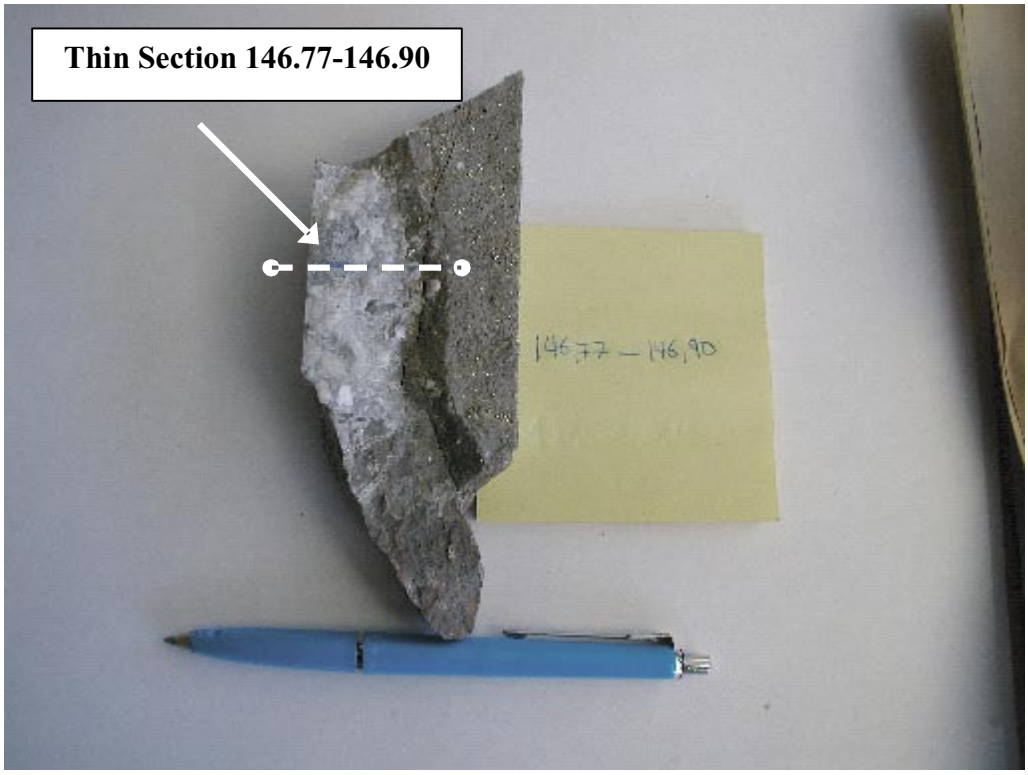


***Figure A-9.*** *Mineral coated open fracture (KFMA01A 146.77–146.90 m).*

Sample: KFM01A 148.9–149.1 m
Rock type: Meta-granitoid
Fracture: A steep and very long fracture composed of several mineralizations. Some of these mineralizations are fractured with open cavities.
Orientation: N69E/81N
Minerals: Prehnite, adularia, pyrite, analcime, quartz, chlorite, K-feldspar.

Sequence of mineralisations:

1. Prehnite
2. Pyrite
3. Adularia
4. Chlorite
5. Analcime
6. Calcite
7. K-feldspar + quartz + chlorite.

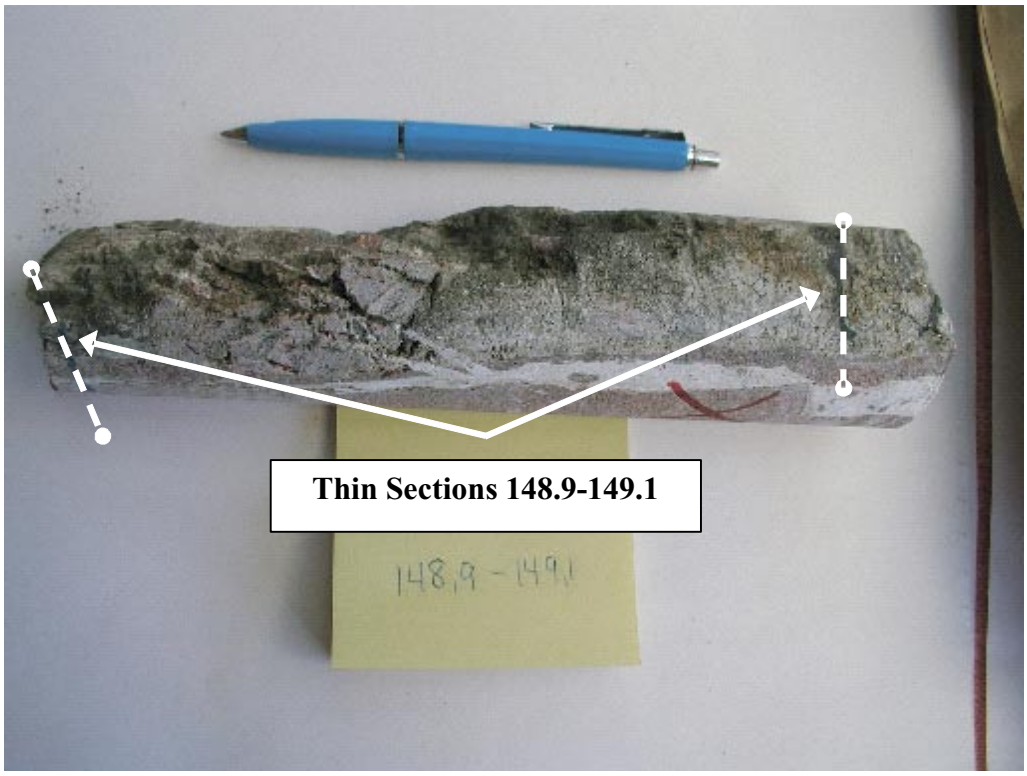


***Figure A-10.*** *Mineral filled fracture (KFM01A 148.9–149.1 m).*

Sample: KFM01A 159.4 m
Rock type: Metagranitoid
Fracture: This is an open fracture with secondary mineral growth covering most of the fracture surface although some areas lack covering. Some thinner fissures penetrate the host rock. These fissures are mostly parallel with the fracture surface and do not penetrate far into the rock type.
Orientation: N32W/61SW
Minerals: Quartz, K-feldspar, calcite, Mg-chlorite, laumontite, hematite.

Sequence of mineralisations:

1. Quartz + (K-feldspar)
2. Calcite + laumontite + hematite
3. Mg-chlorite

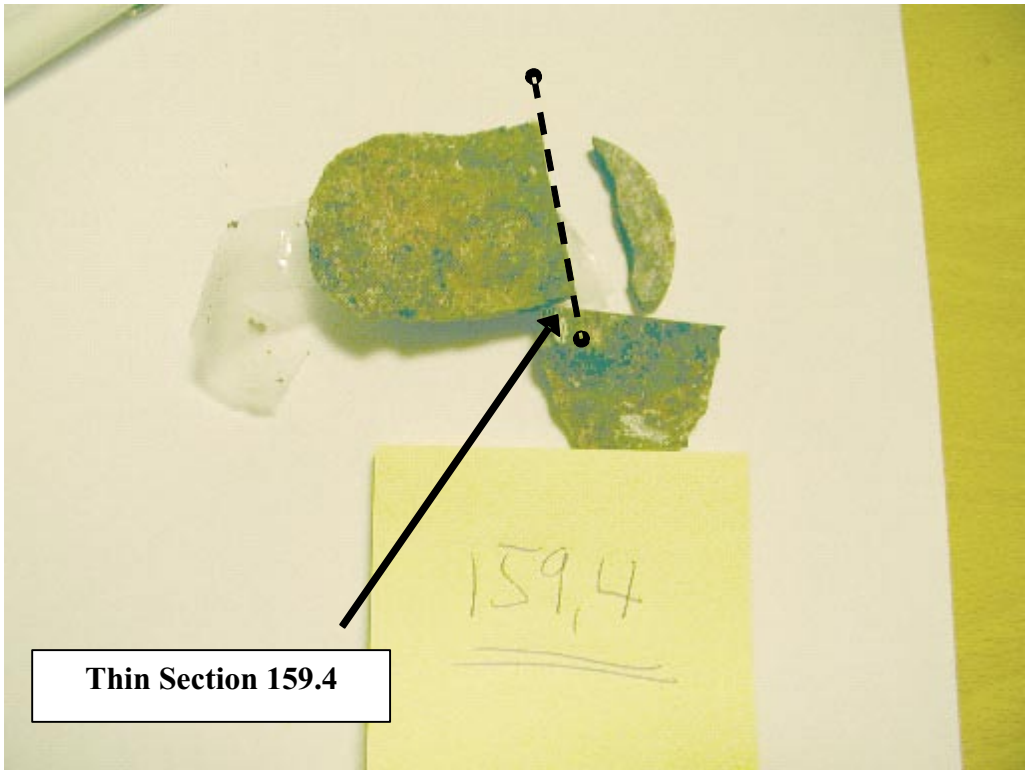


***Figure A-11.*** *Open fracture with mineral cover. The diameter of the drill-core is c 5 cm (KFM01A 159.4 m).*

Sample: KFM01A 170.45 m (A)
Rock type: Metagranitoid
Fracture: A steep and open fissure surface. The mineralization is thick and banded.
Orientation: N37W/68SW
Minerals: Epidote, chlorite, quartz, adularia, laumontite, hematite, calcite.

Sequence of mineralisations:

1. Epidote + chlorite + recrystallized quartz
2. Adularia
3. Laumontite + hematite + calcite
4. Quartz + calcite

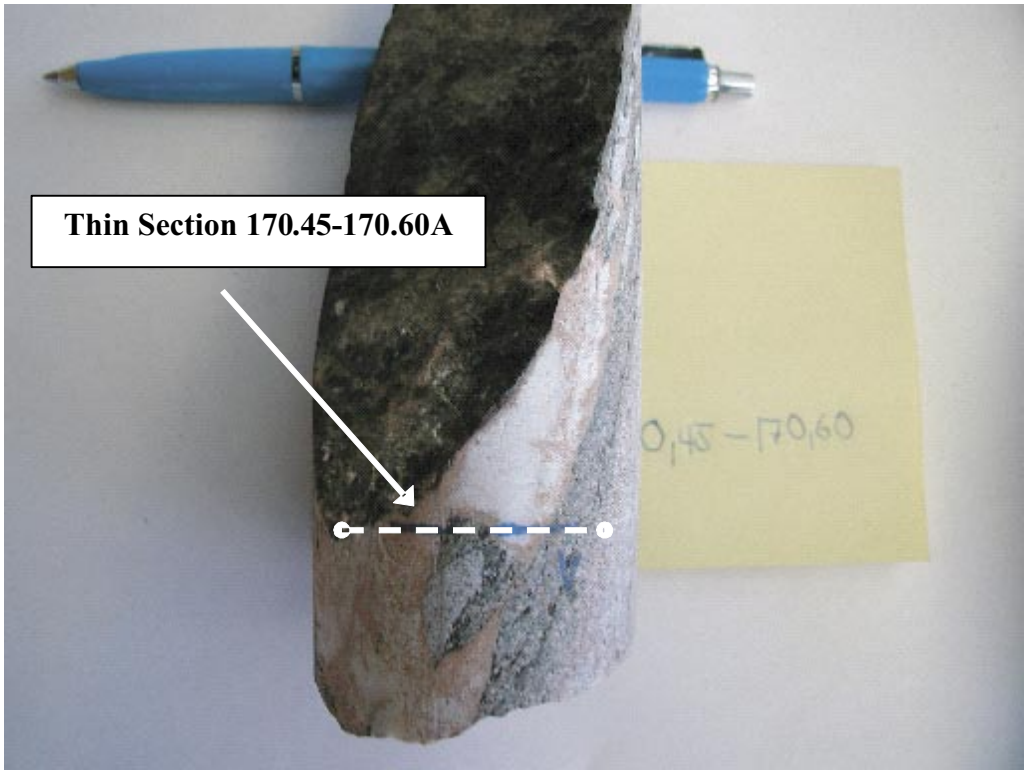


***Figure A-12.*** *Sealed fracture cut by open fracture (KFM01A 170.45 m (A)).*

Sample: KFM01A 170.45 m (B)
Rock type: Metagranitoid
Fracture: A steep and open fissure surface. The fracture is thick and banded with 2 main fractures.
Orientation: N37W/68SW
Minerals: Epidote, chlorite, quartz, adularia, laumontite, hematite, calcite.

Sequence of mineralisations:

1. Epidote + Chlorite+Req Qz
2. Adularia
3. Laumontite + Hematite
4. Calcite + Quartz

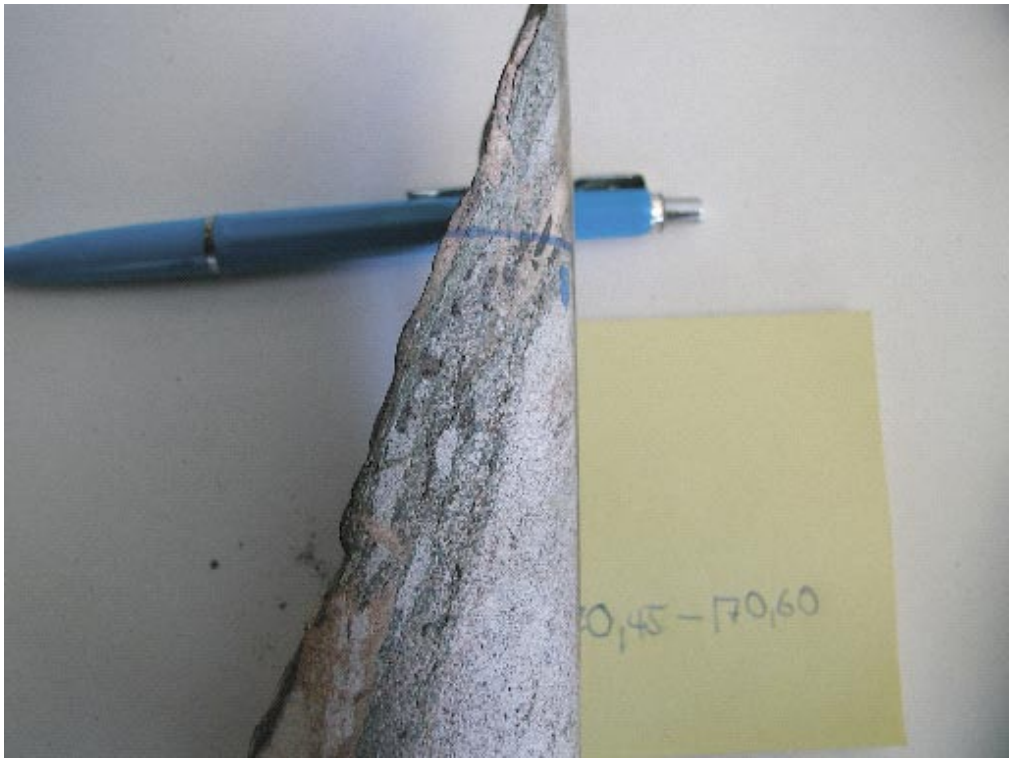

***Figure A-13.*** *Sealed fracture cut by open fracture (KFM01A 170.45 m (B)).*

Sample: KFM01A 179.7–179.85 m
Rock type: Breccia
Fracture: A large network of thin, sealed, reddish fissures.
Orientation: N70E/72N
Minerals: Laumontite, calcite, fluorite, hematite.

Sequence of mineralisations:

1. Laumontite + hematite
2. Calcite
3. Fluorite


***Figure A-14.*** *Laumontite sealed breccia (KFM01A 179.7–179.85 m).*

Sample: KFM01A 185.25–185.35 m
Rock type: Metagranitoid
Fracture: Several steep, red stained, sealed fissures with some brecciation of the rock type. The fissures are soft with some clay.
Orientation: N73E/80N
Minerals: Prehnite, K-feldspar, calcite, clay mineral, hematite.

Sequence of mineralisations:

1. Prehnite
2. K-feldspar
3. Calcite
4. Clay minerals (illite, clinochlore) + hematite

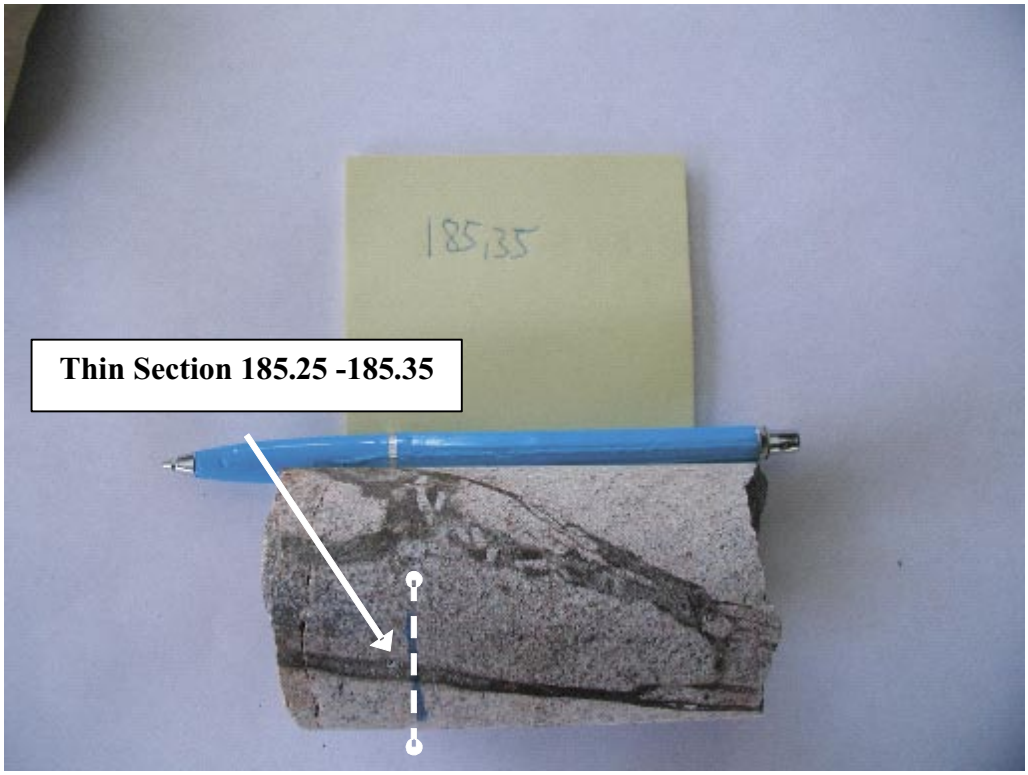


***Figure A-15.*** *Mineral filled fractures (KFM01A 185.25–185.35 m).*

Sample: KFM01A 219.0–219.1 m
Rock type: Breccia
Fracture: A very red-stained network of brecciated fissures.
Orientation: N76E/69N
Minerals: Laumontite, calcite, epidote, titanite, quartz, hematite, K-feldspar, Fe-chlorite.

Sequence of mineralisations:

1. Mylonite (K-feldspar + quartz + titanite + epidote + hematite + chlorite)
2. Calcite
3. Laumontite
4. Fe-chlorite

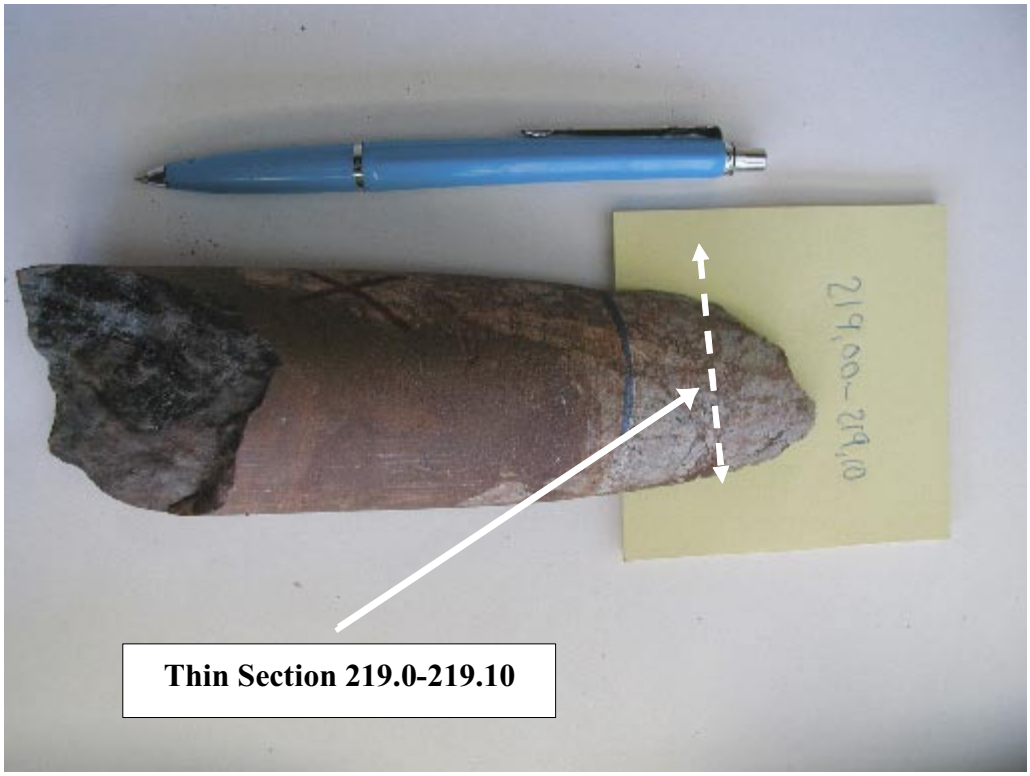


***Figure A-16.*** *Laumontite sealed breccia (KFM01A 219.0–219.1 m).*

Sample: KFM01A 221.9–222.0 m
Rock type: Metagranitoid
Fracture: A mostly sealed, steep fissure. Some smaller cavities occur along the centre of the fissure. These cavities connect into a thin, jagged looking, empty space.
Orientation: Data missing (steep fissure)
Minerals: Prehnite, epidote, fluorite, Fe-rich chlorite, K-feldspar, calcite, adularia.

Sequence of mineralisations:

1. Epidote + Fluorite
2. Prehnite
3. Calcite
4. Fe-Chlorite
5. Adularia

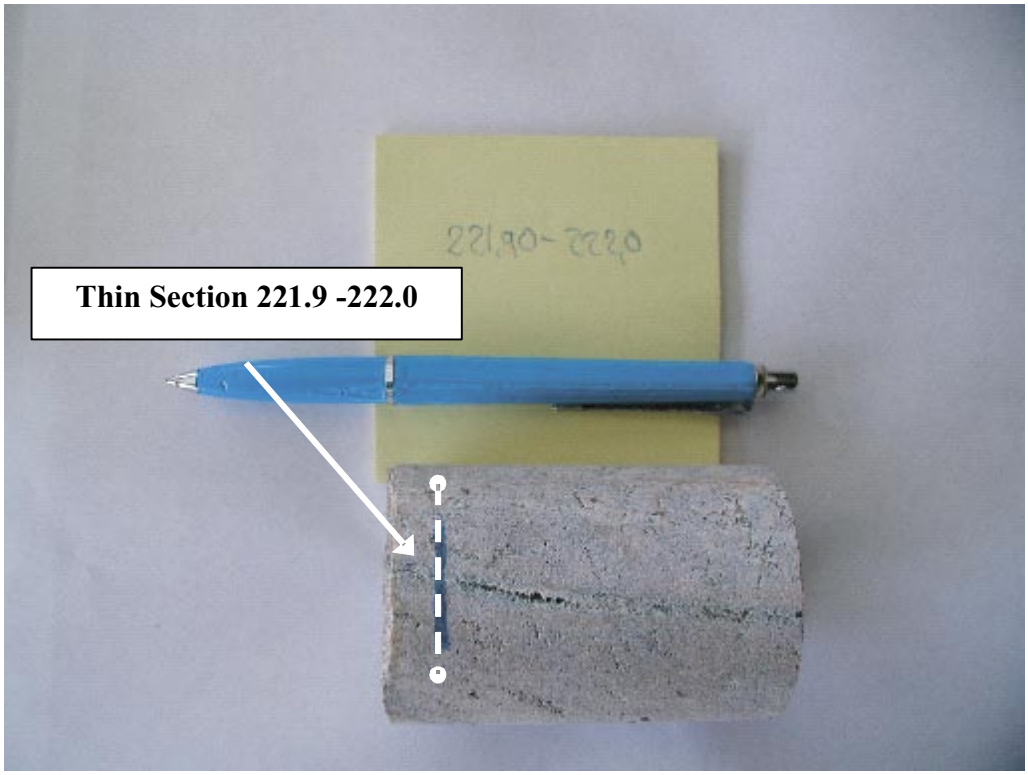


***Figure A-17.*** *Mineral filled fracture with small cavities (KFM01A 221.9–222.0 m).*

Sample: KFM01A 267.0–267.2 m
Rock type: Metagranitoid
Fracture: A mostly sealed fissure with some larger open cavities.
Orientation: N64E/82S
Minerals: Quartz, K-feldspar, epidote, titanite, laumontite, Fe-chlorite.

Sequence of mineralisations:

1. Fragments of quartz + K-feldspar + (epidote + titanite)
2. Laumontite
3. K-feldspar + quartz + (Fe-chlorite + laumontite fragments)
4. Idiomorphic quartz

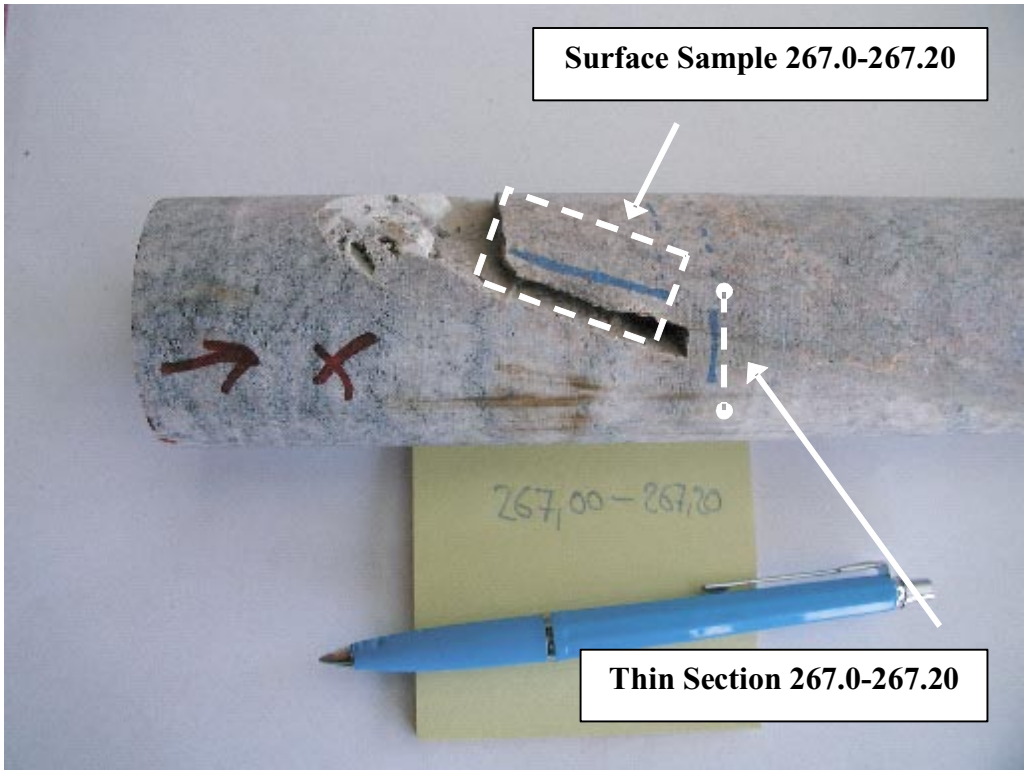


***Figure A-18.*** *Mineral filled fracture with some larger cavities (KFM01A 267.0–267.2 m).*

Sample: KFM01A 268.8 m
Rock type: Metagranitoid
Fracture: A very steep, striated and open fracture.
Orientation: N58E/85E
Minerals: Quartz, K-feldspar, Pyrite, Baryte, Mixed-layer clay.

Sequence of mineralisations:

1. Idiomorphic quartz + (some idiomorphic K-feldspar)
2. Idiomorphic pyrite
3. Baryte
3. Mixed-layer clay

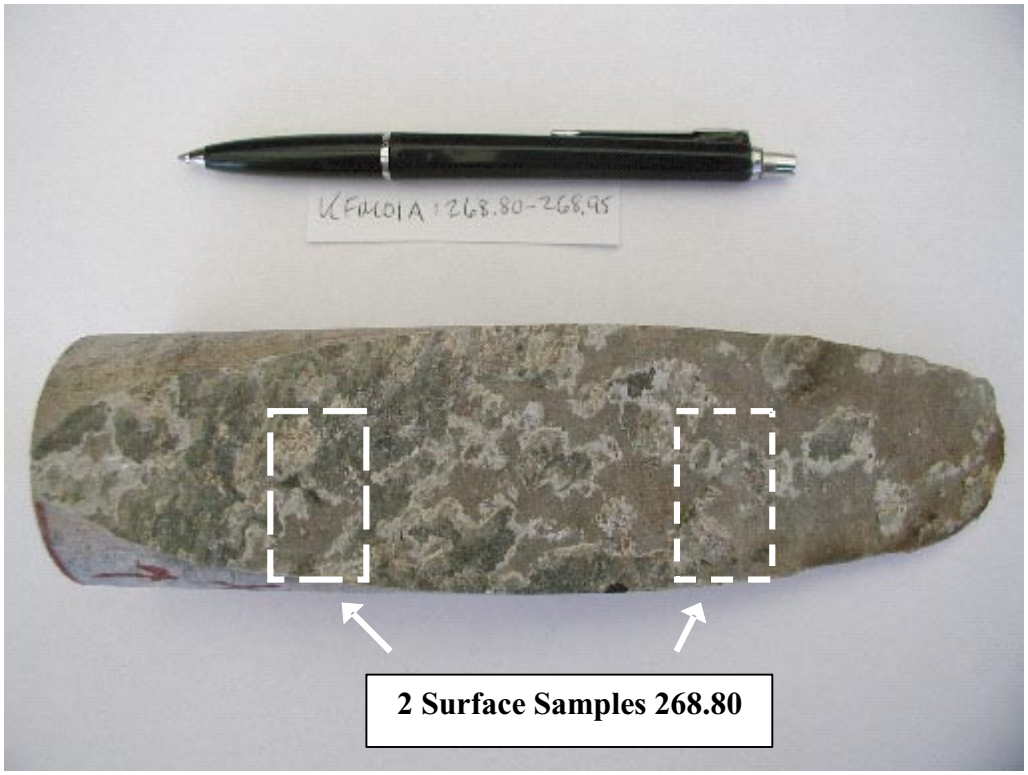


***Figure A-19.*** *Quartz covered fracture surface with pyrite, barite and mixed-layer clay (KFM01A 268.8 m).*

Sample: KFM01A 269.5–269.9 m
Rock type: Metagranitoid
Fracture: A steep and open fracture surface. The fracture filling has a banded appearance.
Orientation: N69E/79S
Minerals: Calcite, prehnite, analcime, Mg-chlorite, adularia, pyrite, quartz, calcite, Fe-chlorite.

Sequence of mineralisations:

1. Calcite and prehnite fragments
2. Analcime
3. Mg-chlorite
4. Pyrite
5. Adularia
6. Idiomorphic quartz + calcite
7. Fe-chlorite


***Figure A-20.*** *Mineral coating on an open fracture surface (KFM01A 269.5–269.9 m).*

Sample: KFM01A 270.72–270.75 m
Rock type: Metagranitoid
Fracture: Network of several, sealed, thin, red coloured fissures with a rough, wider, partly open fragmented fracture.
Orientation: N69E/79S
Minerals: Laumontite, hematite, quartz, K-feldspar, pyrite, calcite, mixed-layer clay.

Sequence of mineralisations:

1. Laumontite + hematite + rock type fragments (quartz + K-feldspar + albite)
2. Idiomorphic quartz
3. Calcite
4. Idiomorphic pyrite
5. Mixed-layer clay

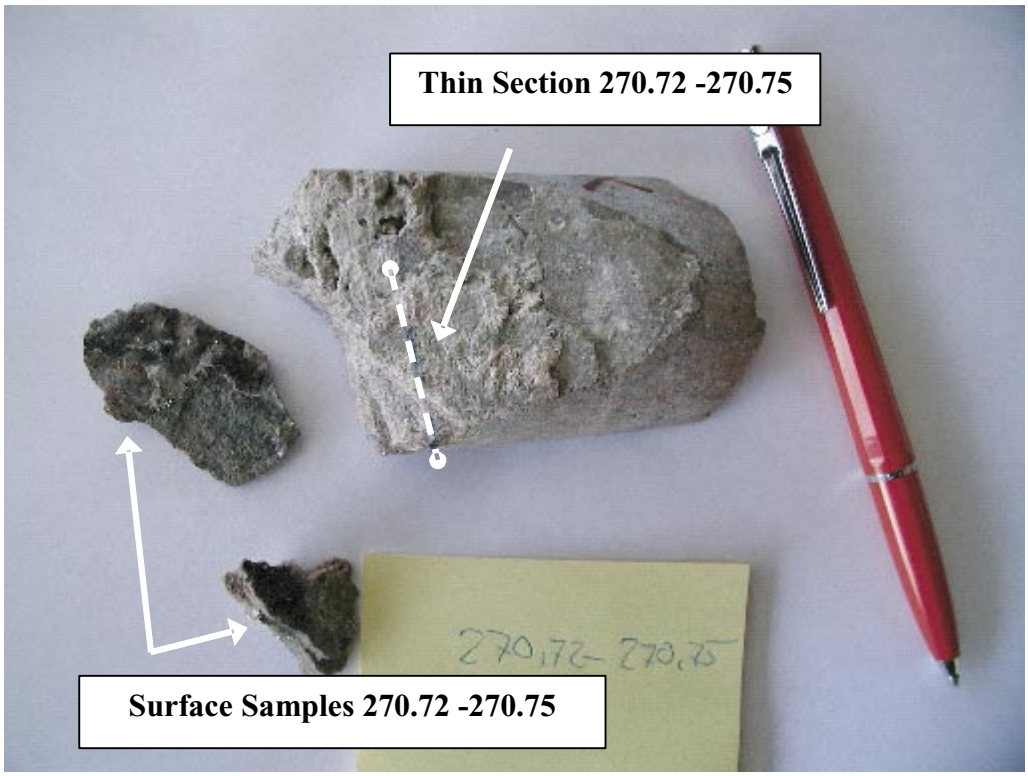


***Figure A-21.*** *Sealed and open fractures (KFM01A 270.72–270.75 m).*

Sample: KFM01A 396.6–396.7 m
Rock type: Amphibolite
Fracture: Open fissure surface with a thin, banded fracture filling.
Orientation: N72E/86S
Minerals: Laumontite, hematite, calcite.

Sequence of mineralisations:

1. Calcite
2. Laumontite + hematite

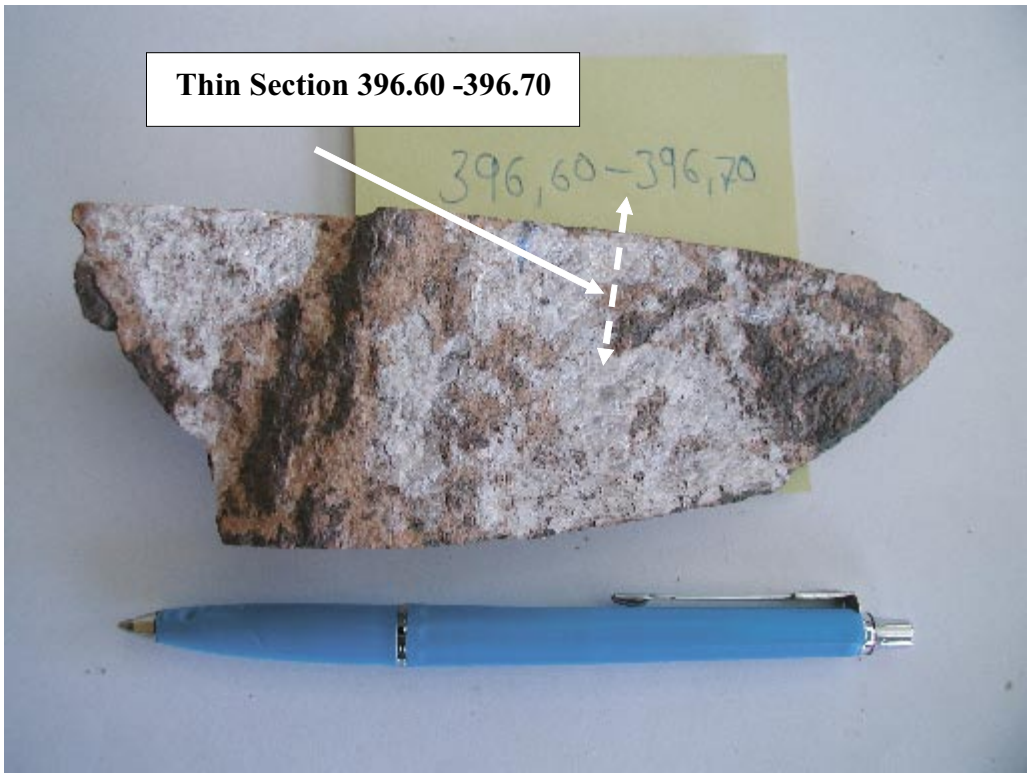


***Figure A-22.*** *Open fracture with a thin mineral coating (KFM01A 396.6–396.7 m).*

Sample: KFM01A 481.1–481.2 m
Rock type: Metagranitoid
Fissure description: Open fracture with thick mineral coating.
Orientation: Data missing
Minerals: Quartz, K-feldspar, albite, anorthite, epidote, titanite, chlorite, adularia.

Sequence of mineralisations:

1. Highly altered pegmatite (quartz + k-feldspar + albite + anorthite + chlorite + titanite)
2. Epidote + recrystallized quartz
3. Adularia

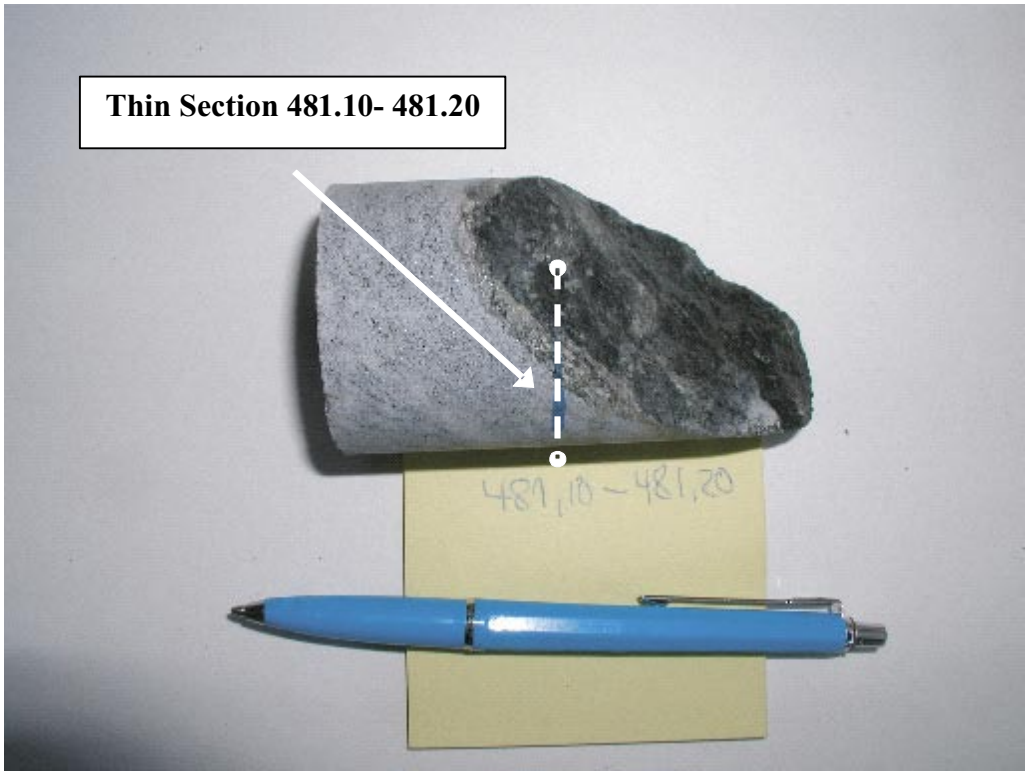


***Figure A-23.*** *Open fracture with thick mineral coating (KFM01A 481.1–481.2 m).*

Sample: KFM01A 652.0 m (A)
Rock type: Metagranite
Fracture: An open, rough, fracture surface in a banded segment of the host rock. Fracture parallel to the foliation in the wall rock.
Orientation: N47E/79SE
Minerals: Epidote, titanite, calcite, chlorite, K-feldspar, quartz, anorthite.

Sequence of mineralisations:

1. (Inner band) quartz + anorthite
2. (Outer band) epidote, titanite, calcite, chlorite, K-feldspar, quartz

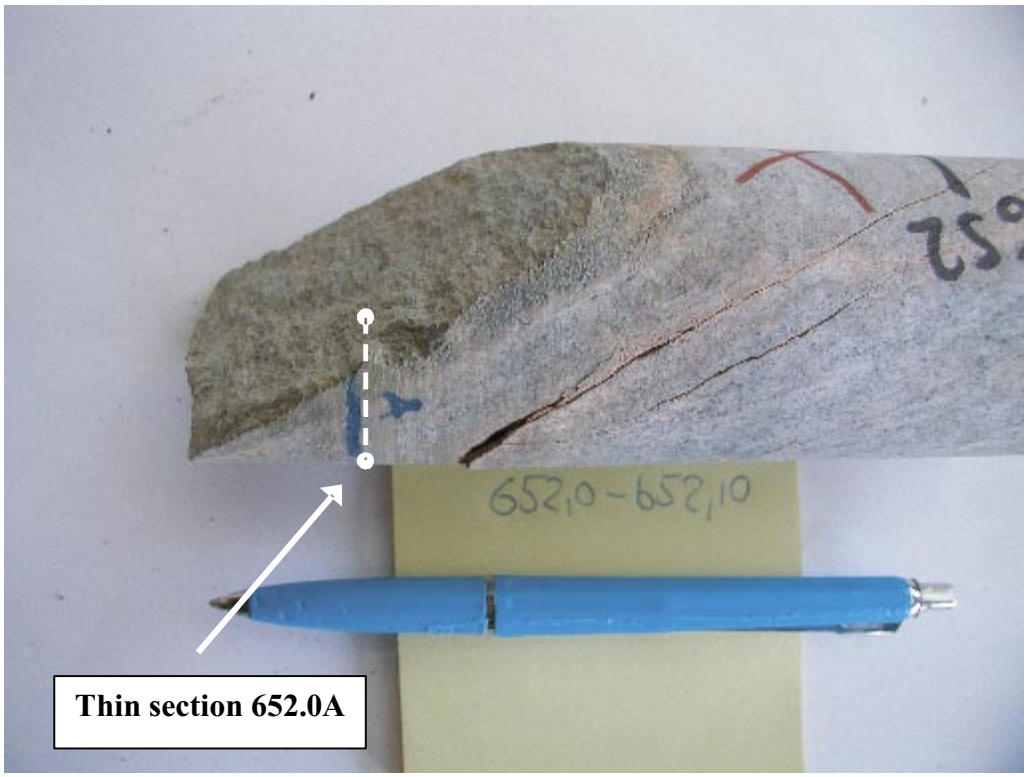


***Figure A-24.*** *Open fracture (KFM01A 652.0 m (A)).*

Sample: KFM01A 652.0 m (B)
Rock type: Metagranite
Fracture: A mostly, sealed, straight, thin fissure. A larger cavity can be seen in the fissure.
Orientation: N47E/79SE
Minerals: Laumontite, hematite, quartz.

Sequence of mineralisations:

1. Laumontite + hematite
2. Quartz

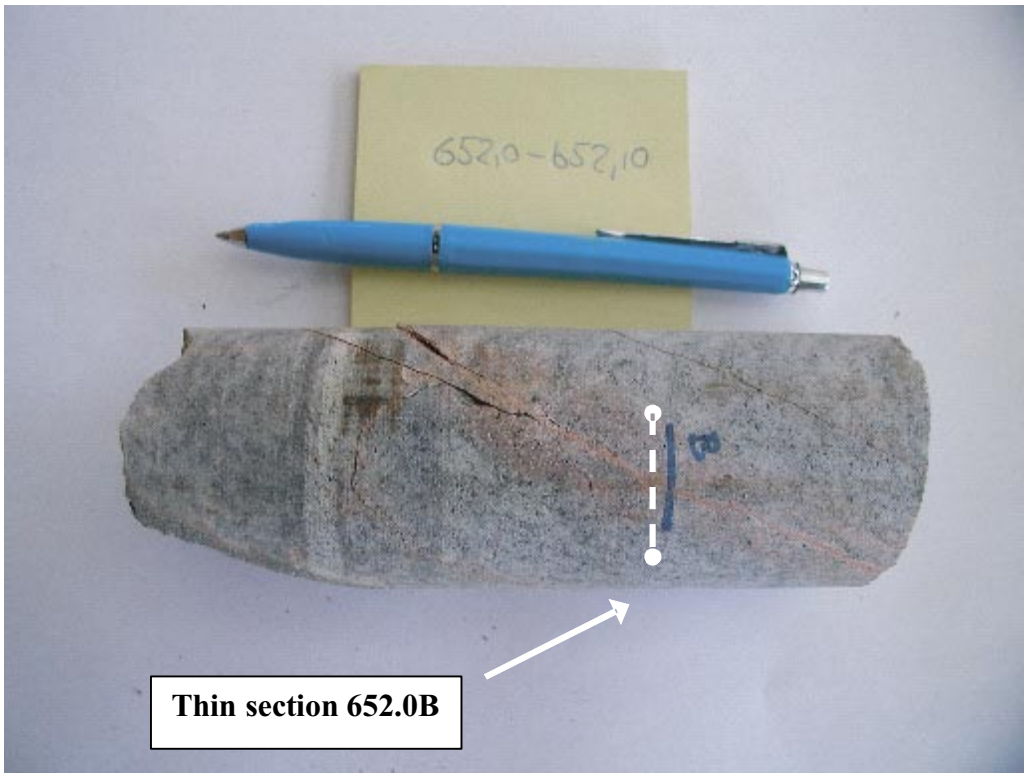


***Figure A-25.*** *Laumontite sealed thin fracture with hematite and later quartz (KFM01A 652.0 m (B)).*

Sample: KFM01A 671.4–671.55 m
Rock type: Metagranitoid
Fracture: An open, rough, fracture with small covering of an unknown black mineral.
Orientation: Data missing
Minerals: Unknown black mineral.

Sequence of mineralisations: None

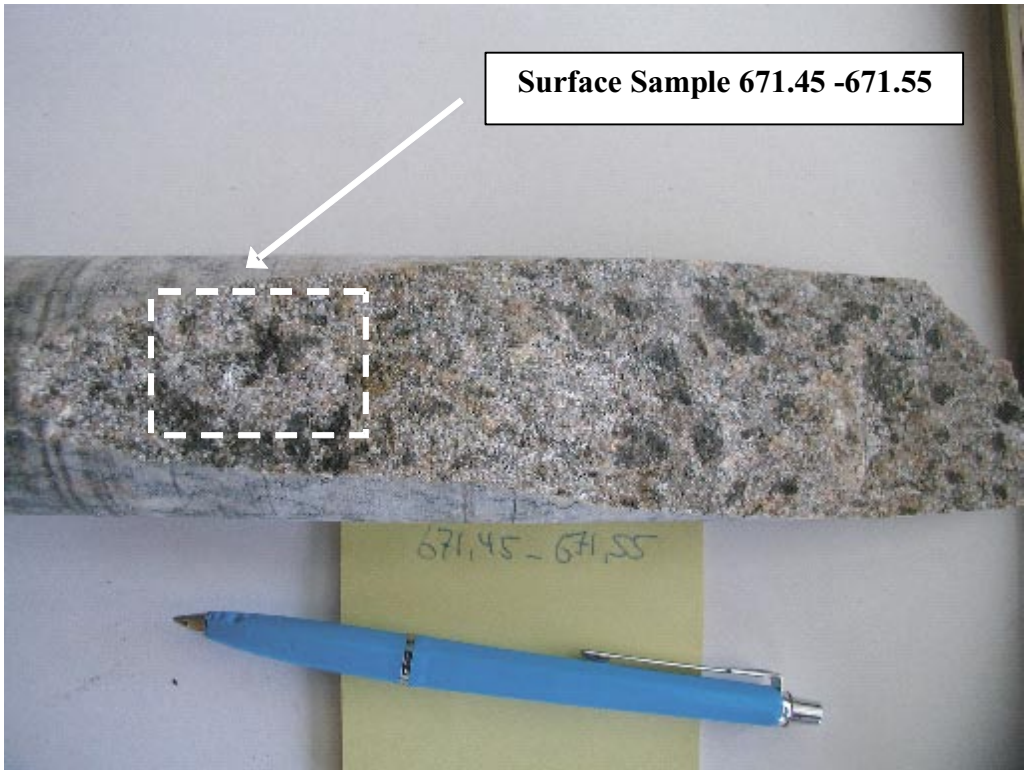


***Figure A-26.*** *Open fracture (KFM01A 671.4–671.55 m).*

Sample: KFM01A 671.9–672.0 m
Rock type: Metagranitoid
Fissure description: A network of parallel, thin sealed fissures.
Orientation: N37E/77SE
Minerals: Laumontite, hematite, (quartz, K-feldspar, albite).

Sequence of mineralisations:

1. Laumontite + hematite + wall rock fragments (quartz + K-feldspar + albite)

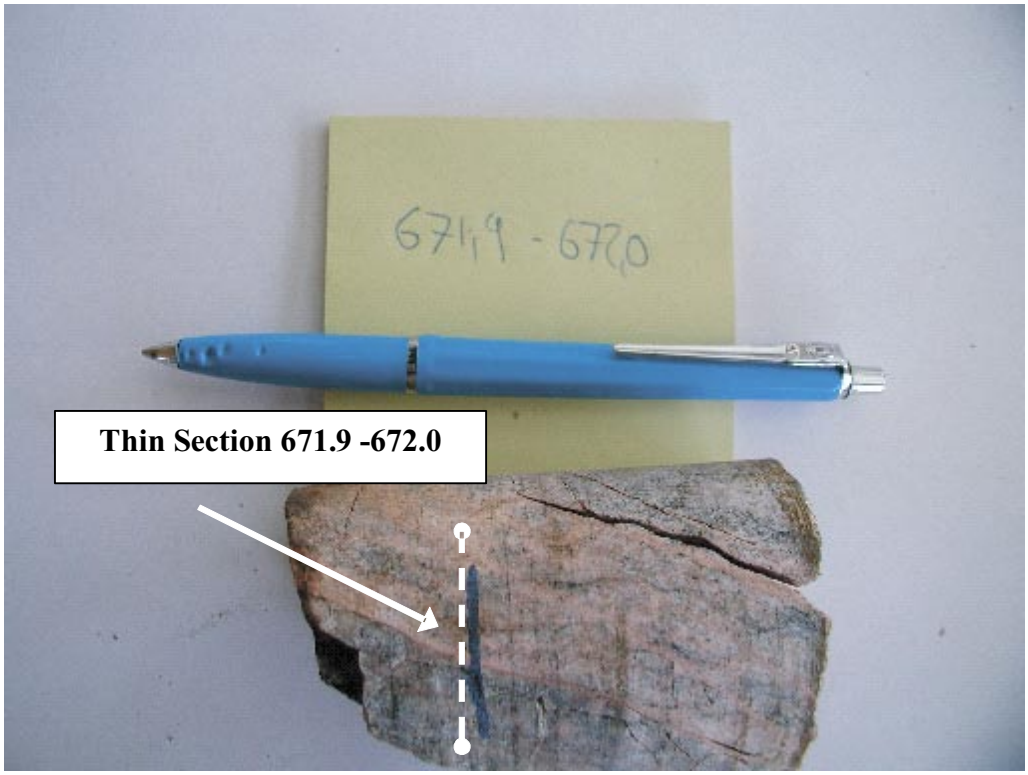


***Figure A-27.*** *Laumontite sealed fractures (KFM01A 671.9–672.0 m).*

Sample: KFM01A 712.54–712.57 m
Rock type: Tonalite
Fracture: This is a rough, open, fracture surface in some places covered by a thin fracture coating.
Orientation: No data available
Minerals: Epidote.

Sequence of mineralisations:

1. Epidote.


***Figure A-28.*** *Epidote coated open fracture (KFM01A 712.54–712.57 m).*

Sample: KFM01A 828.7–828.8 m
Rock type: Tonalite
Fracture: This is a steep, open, tectonically reactivated fracture covered by a thick fracture filling.
Orientation: N32W/78SW
Minerals: Biotite, quartz, anorthite, albite, calcite.

Sequence of mineralisations:

1. Biotite + recrystallized quartz + wall rock fragments (quartz + K-feldspar + anorthite + albite)
2. Calcite


***Figure A-29.*** *Open fracture (KFM01A 828.7–828.8 m).*

Sample: KFM02A 111.0–111.15 m
Rock type: Tonalite/amphibolite
Fracture: Closed fracture, 0.5–1 cm wide.
Orientation: N16W/33E
Minerals: Prehnite, adularia, albite, chlorite, illite, hematite, mixed layer clays.

Sequence of mineralizations:

1. Prehnite
2. The prehnite has been partly altered and replaced by chlorite, illite, mixed layer clays and hematite

Wall rock alteration: Extensive alteration and contains chlorite, epidote and apatite.

***Figure A-30.*** *Fracture filled with altered prehnite. The diameter of the drill-core is c 5 cm (KFM02A 111.0–111.15 m).*

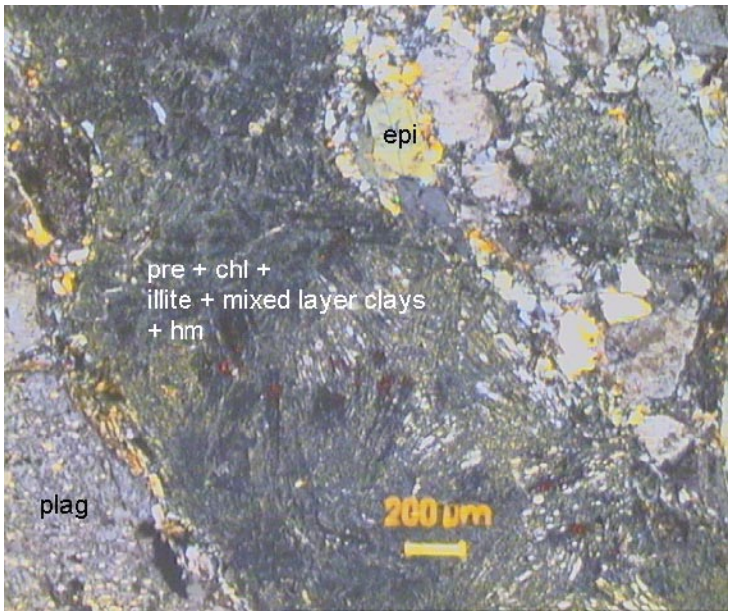


***Figure A-31.*** *The epidote in the wall rock is cut by the altered prehnite. (pre = prehnite, chl = chlorite, hm = hematite). Fotomicrograph (KFM02A 111.0–111.15 m).*

Sample: KFM02A 118,28 m
Rock type: Metagranite
Fracture: Open fracture with thick mineral coating.
Orientation: N77E/22S
Minerals: Calcite, adularia, quartz, fluorite, hematite, illite, pyrite.

Sequence of mineralizations:

1. Calcite
2. Fine-grained adularia
2. Idiomorphic quartz, adularia, fluorite, illite and hematite
3. Pyrite

Wall rock alteration: Saussuritized plagioclase

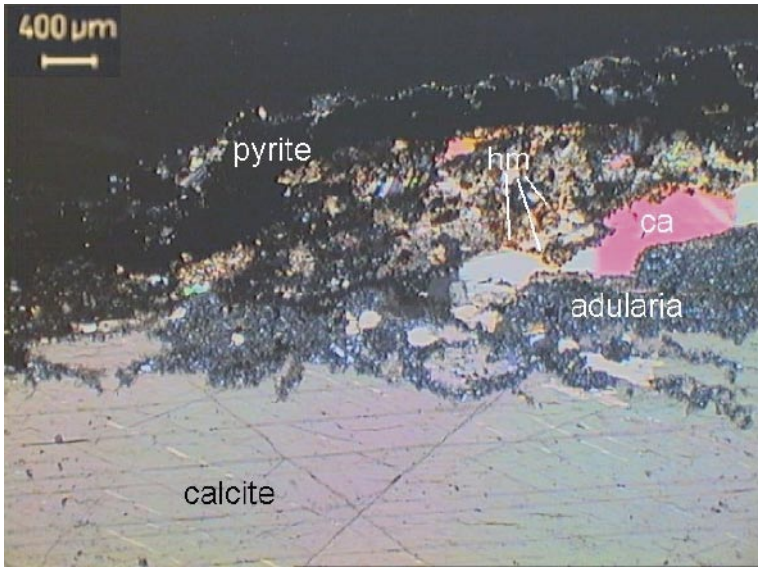


***Figure A-32.*** *Calcite over-grown by adularia and hematite, pyrite on the fracture surface. Microphotograph (KFM02A 118,28 m).*

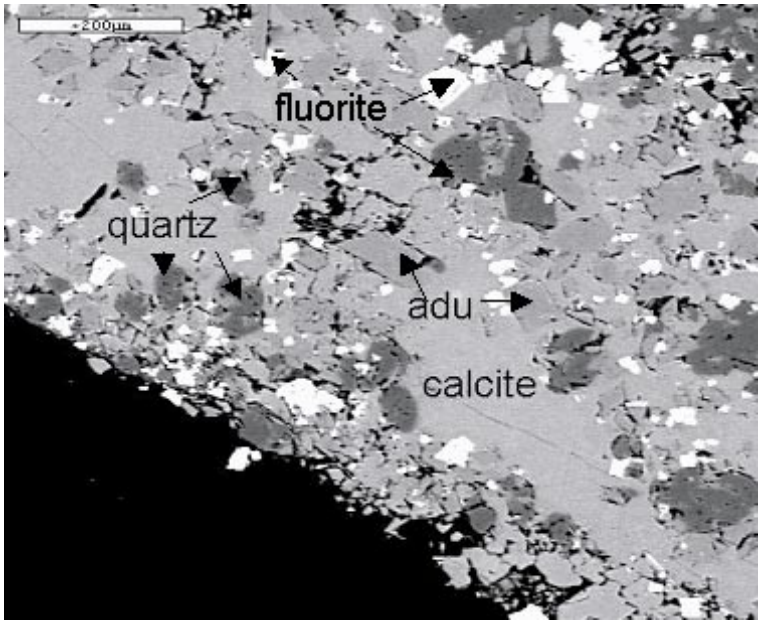


***Figure A-33.*** *Calcite with later idiomorphic quartz, fluorite and adularia. (adu = adularia). Back-scattered electron image (KFM02A 118,28 m).*

Sample: KFM02A 171.40 m
Rock type: Pegmatite
Fracture: Open fracture.
Orientation: N87W/28S
Minerals: Quartz, pyrite.

Sequence of mineralizations

1. Idiomorphic quartz
2. Idiomorphic pyrite

***Figure A-34.*** *Open fracture coated with small idiomorphic quartz crystals under larger idiomorphic pyrite crystals. The diameter of the drill-core is c 5 cm (KFM02A 171.40 m).*

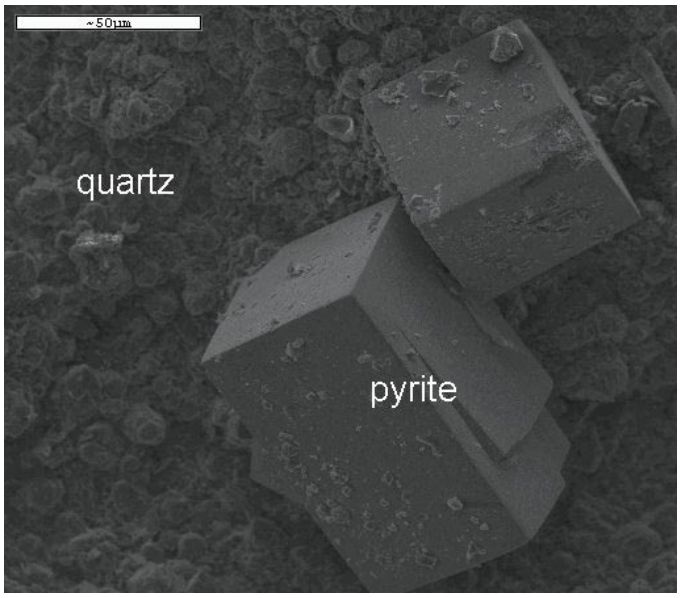


***Figure A-35.*** *Cubic pyrite crystals over small quartz crystals. Electron image (KFM02A 171.40 m).*

Sample: KFM02A 179.39–179.44 m
Rock type: Metagranite
Fracture: Open fracture.
Orientation: N11E/5W
Minerals: Quartz, chlorite, asphaltite.

Sequence of mineralizations

1. Small quartz crystals cover the fracture surface
2. Asphaltite

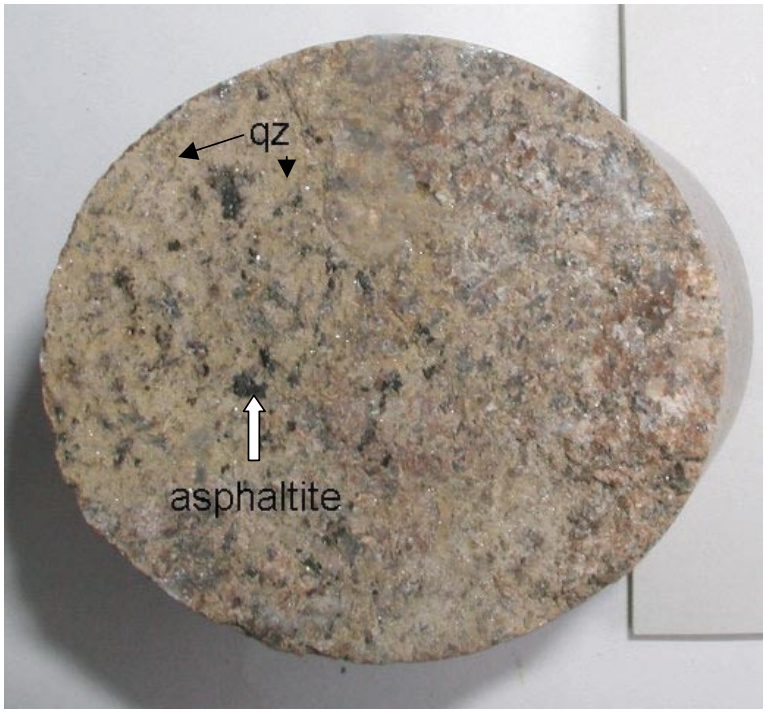


***Figure A-36.*** *Beige coating of small idiomorphic quartz crystals with small asphaltite crystals. The diameter of the drill-core is c 5 cm (KFM02A 179.39–179.44 m).*

Sample: KFM02A 403.13 m
Rock type: Metagranite
Fracture: Open fracture.
Orientation: N24E/5E
Minerals: Calcite, small grains of ilmenite and feldspar.

***Figure A-37.*** *The white mineral is calcite and the small green-coloured minerals are feldspar. The illite is not visible in this scale. The base of the figure is c 2 cm (KFM02A 403.13 m).*

Sample: KFM02A 422.30–422.40 m
Rock type: Metagranite
Fracture: Cataclasite with open fracture.
Orientation: N79W/79N
Minerals: Calcite, adularia, quartz, pyrite, chlorite/corrensite.

Sequence of mineralizations

1. Cataclasite with K-feldspar and quartz
2. Calcite
3. Chlorite/corrensite and pyrite

Wall rock alteration: The plagioclase in the wall rock has been saussuritized and contains e.g. epidote. The biotite has been partly chloritized and contains titanite.

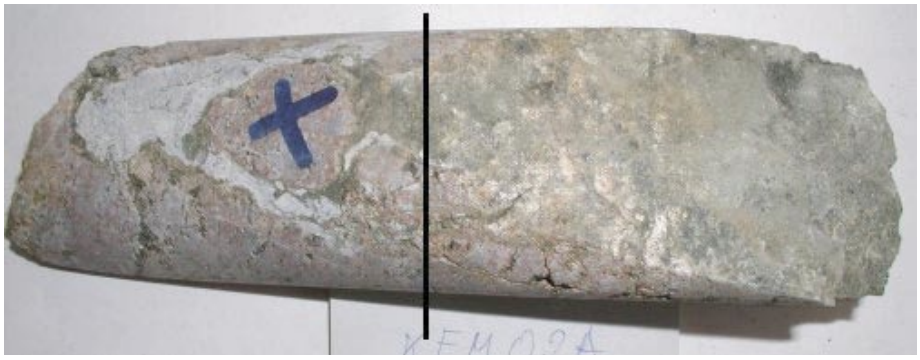

***Figure A-38.*** *The wall rock is cut by a white, mainly calcite-sealed fracture. The drill-core is 5 cm in diameter (KFM02A 422.30–422.40 m).*

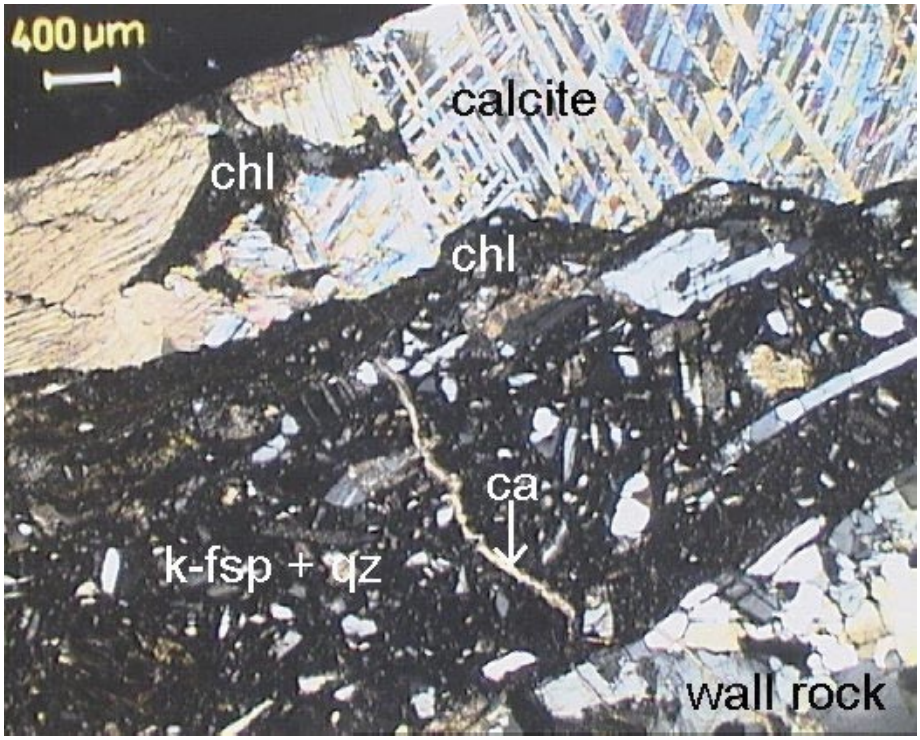


***Figure A-39.*** *K-feldspar and quartz cataclasite cut by calcite that later has been cut by chlorite. Photomicrograph (KFM02A 422.30–422.40 m).*

Sample: KFM02A 423.13–423.23 m
Rock type: Metagranite
Fracture: Thin red vein cut by open fracture.
Orientation: N74E/50S
Minerals: Adularia, calcite, hematite, chlorite, fluorite.

Sequence of mineralizations

1. Adularia, hematite and fluorite in the thin vein
2. The vein is cut by an open fracture with calcite and chlorite

Wall rock alteration: The rock contains chlorite and epidote and the plagioclase is highly saussuritized.

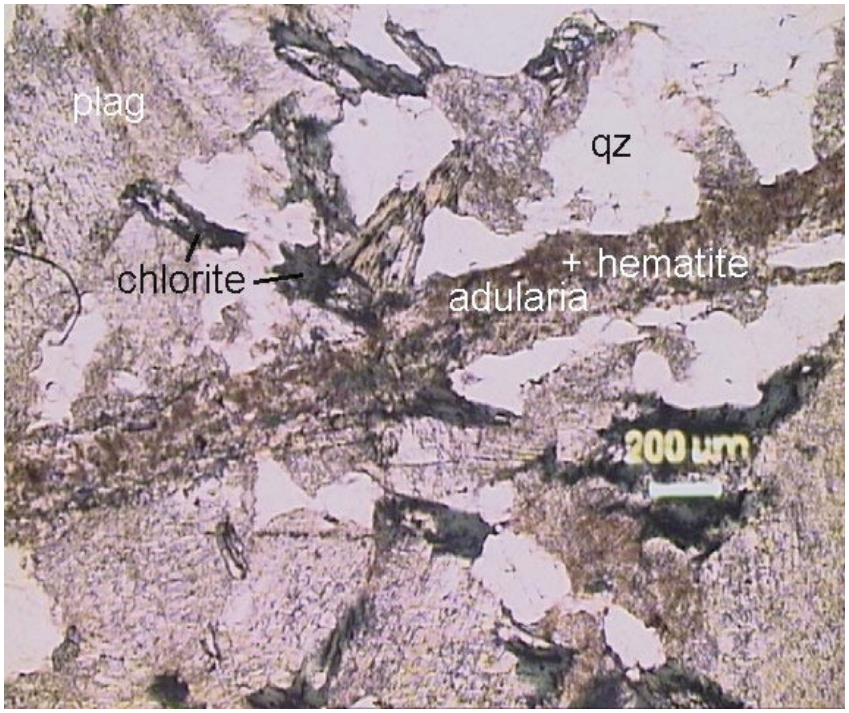


***Figure A-40.*** *Small vein with adularia and micro-grains of hematite. Photomicrograph (KFM02A 423.13–423.23 m).*

Sample: KFM02A 423.65–423.70 m
Rock type: Metagranite/pegmatite
Fracture: Mylonite with open fracture.
Orientation: N20E/49E
Minerals: Quartz, albite, K-feldspar, chlorite/corrensite, calcite.
Minerals in the mylonite: Chlorite, quartz, plagioclase, epidote, adularia, titanite, apatite.

Sequence of mineralizations

1. Mylonite with chlorite, quartz, plagioclase, epidote, adularia, titanite, apatite
2. Crystallization of quartz, albite, K-feldspar, chlorite/corrensite and calcite on the open fracture

Wall rock alteration: seritized K-feldspar, saussuritized plagioclase

***Figure A-41.*** *Open fracture with a mixture of quartz, albite, K-feldspar, chlorite/corrensite and calcite. The diameter of the drill-core is c 5 cm (KFM02A 423.65–423.70 m).*

Sample: KFM02A 513.55–513.70 m
Rock type: Fine-grained metagranite
Fracture: Cataclasite with open fracture.
Orientation: N51E/27SE
Minerals: Chlorite, epidote, quartz, hematite.

Sequence of mineralizations

1. Cataclasite with quartz, k-feldspar, albite, epidote, Mg/Fe-chlorite and hematite
2. Open fracture with Mg-chlorite, hematite and idiomorphic quartz

Wall rock alteration: The wall rock is a cataclasite

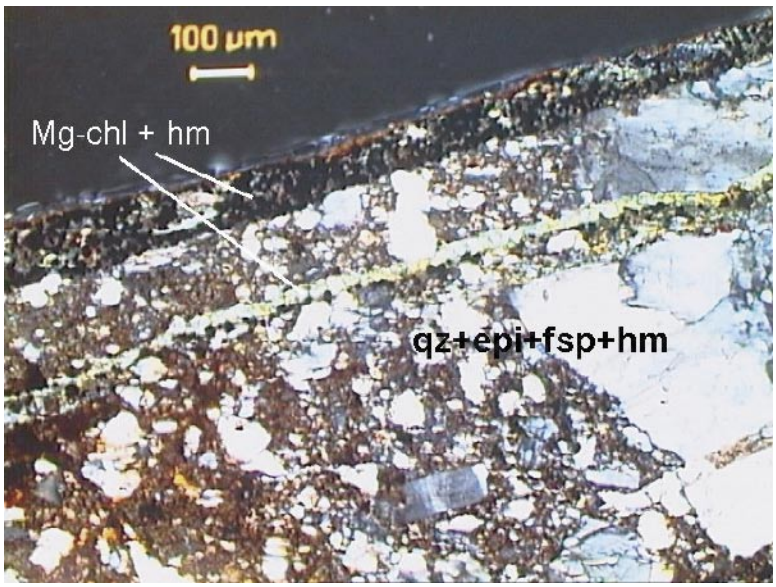


***Figure A-42.*** *Cataclasite cut by Mg-chlorite with micro-grains of hematite. Micro Photograph (KFM02A 513.55–513.70 m).*

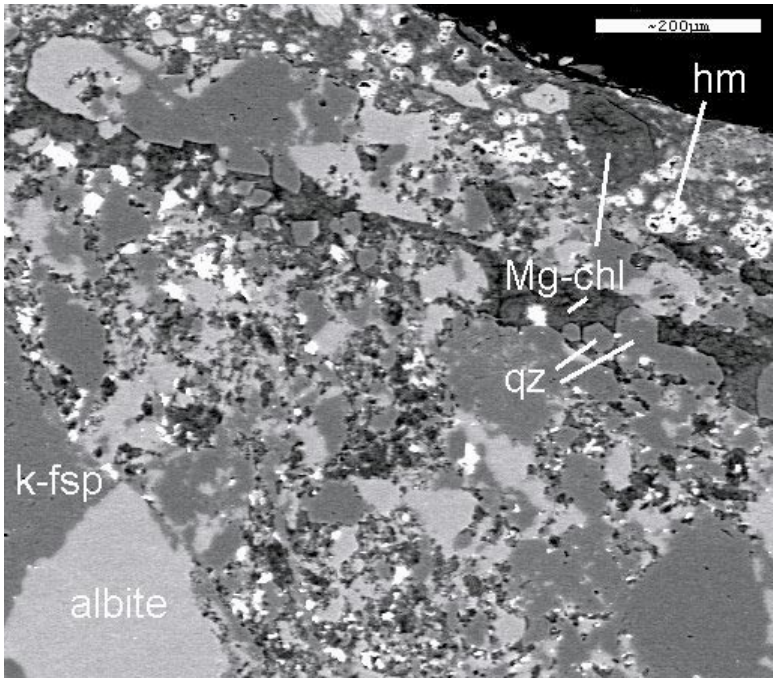


***Figure A-43.*** *Back-scattered electron image of the same area as above. Small idiomorphic quartz crystals are visible in the chlorite (KFM02A 513.55–513.70 m).*

Sample: KFM02A 516.60–516.65 m
Rock type: Metagranite
Fracture: Closed fracture, c 1 cm wide cut by open fracture.
Orientation: N84E/20S
Minerals: Epidote, quartz, K-feldspar, chlorite, calcite, hematite.

Sequence of mineralizations

1. Epidote with some fragments of quartz and K-feldspar
2. The epidote has been partly mylonitized
3. The mylonite is cut by an open surface with chlorite, calcite and hematite

Wall rock alteration:

***Figure A-44.*** *Epidote filled fracture, partly mylonitized, cut by open fracture. The diameter of the drill-core is c 5 cm (KFM02A 516.60–516.65 m).*

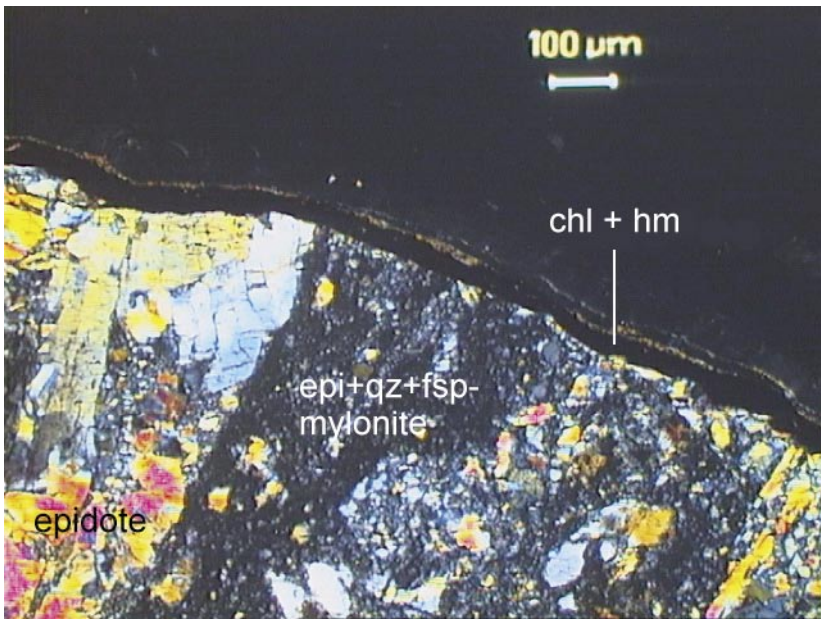


***Figure A-45.*** *Epidote mylonite cut by chlorite and hematite. Photomicrograph (KFM02A 516.60–516.65 m).*

Sample: KFM02A 893.45–893.65 m
Rock type: Metagranite
Fracture: Open fracture.
Orientation: N32W/79SW
Minerals: Apophyllite, calcite, corrensite.

Sequence of mineralizations

1. Calcite
2. Apophyllite, calcite and chlorite/corrensite

Wall rock alteration: The plagioclase in the wall rock is saussuritized while the K-feldspar is more unaltered. Most of the biotite is unaltered

***Figure A-46.*** *Open fracture with apophyllite (the shiny mineral) and corrensite (the black mineral). The diameter of the drill-core is c 5 cm (KFM02A 893.45–893.65 m).*

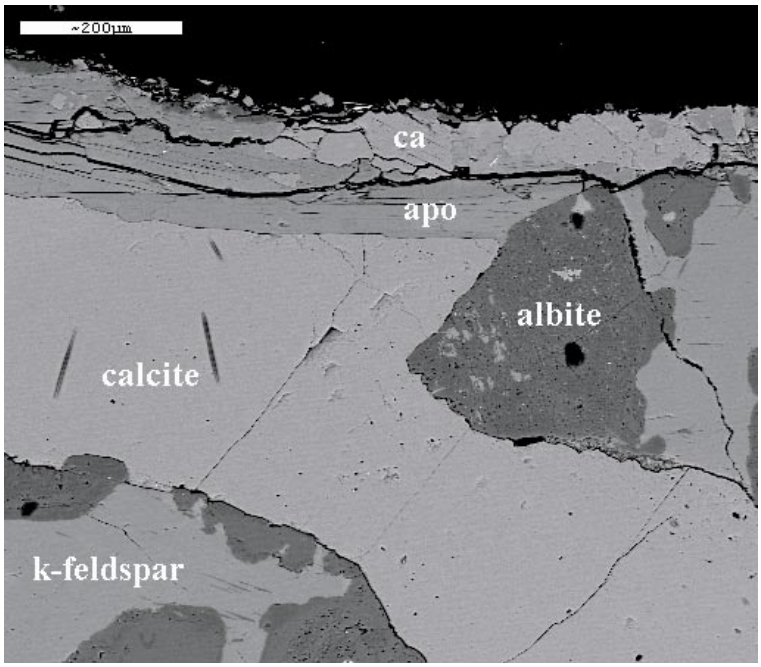


***Figure A-47.*** *Calcite vein cut by apophyllite. Backscattered electron image (KFM02A 893.45–893.65 m).*

Sample: KFM03A 184.34–184.50 m
Rock type: Metagranite
Fracture: Closed fracture.
Orientation: N33E/64SE
Minerals: Adularia, calcite, hematite, quartz.

Sequence of mineralizations

1. The adularia, calcite, hematite and quartz have crystallized at approximately the same time.

Wall rock alteration: The plagioclase has been saussuritized and replaced by pure albite, K-feldspar, epidote and sericite.

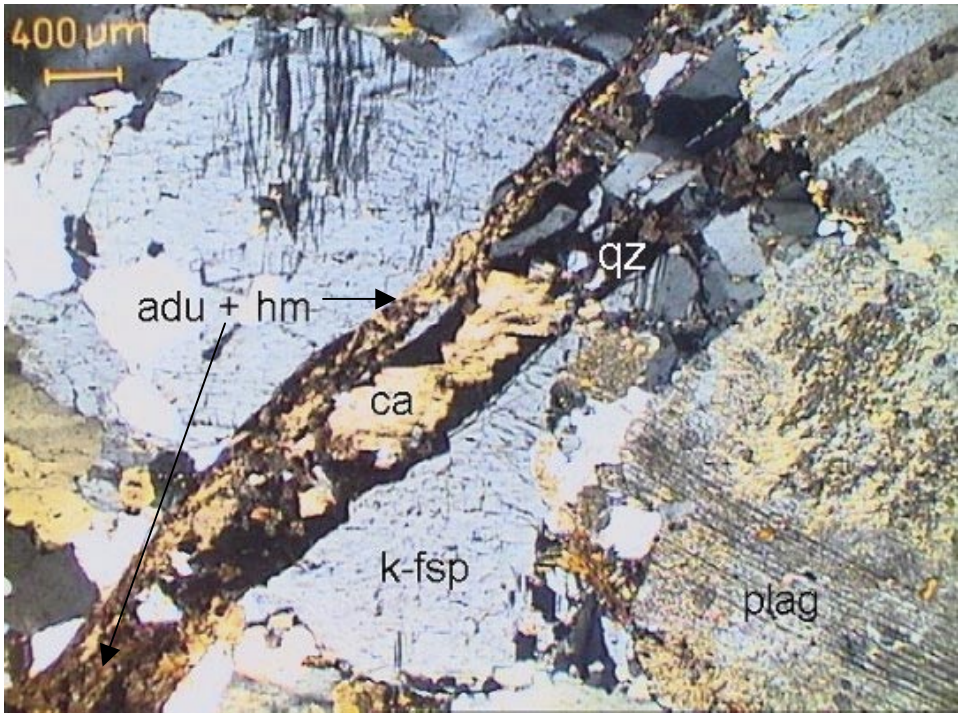


***Figure A-48.*** *Small fracture filled with adularia, hematite and calcite. Photomicrograph (KFM03A 184.34–184.50 m).*

Sample: KFM03A 316.93–317.15 m
Rock type: Metabasite
Fracture: Closed fracture, c 0.5–1.5 cm wide.
Orientation: N66E/74S
Minerals: Calcite, adularia, chlorite, titanite.

Sequence of mineralizations

1. Calcite
2. Fine-grained adularia
3. Small micro fractures with adularia that cut both the calcite and the older adularia.

Wall rock alteration: The plagioclase in the rock is highly saussuritized. Near the fracture, the amphibole has been partly replaced by chlorite and epidote.

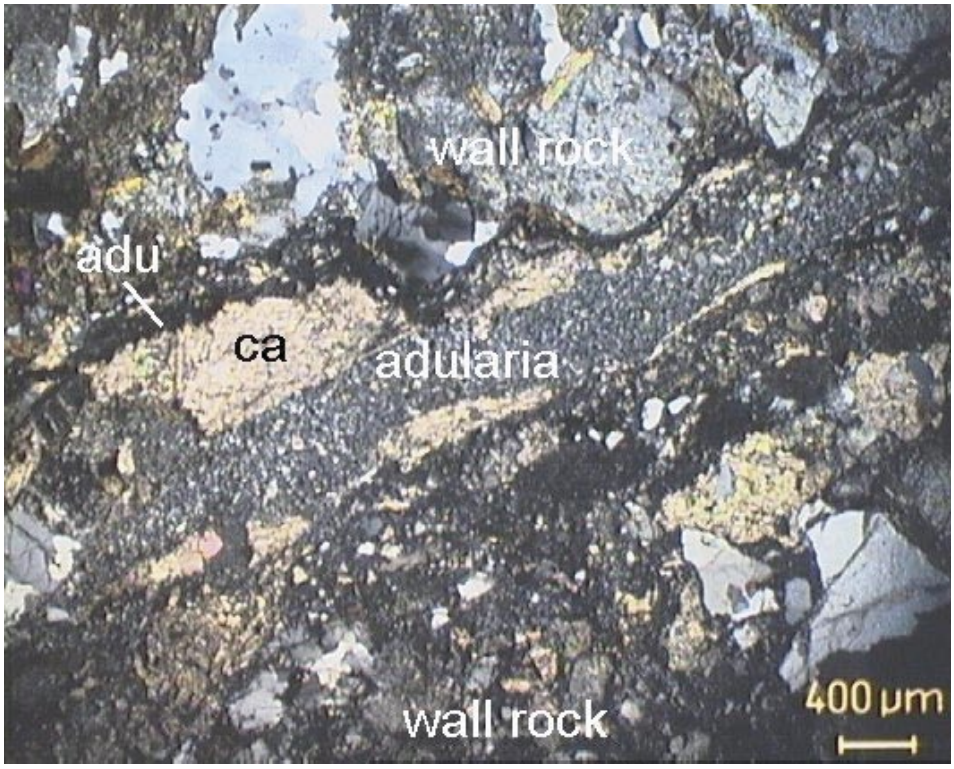


***Figure A-49.*** *Older calcite filling cut by fine-grained adularia. Microphotograph (KFM03A 316.93–317.15 m).*

Sample: KFM03A 332.72–333.00 m
Rock type: Metabasite
Fracture: Open fracture
Orientation: N66E/82S
Minerals: Laumontite

Wall rock alteration: The unaltered rock consists of mainly plagioclase ($Ab_{\sim 58-65}$), amphibole, biotite and quartz. In the altered rock near the laumontite-bearing fracture, the plagioclase has been replaced by an almost pure albite ($Ab_{95}$) with small inclusions of pure K-feldspar and prehnite. The biotite has partly been replaced by Fe-chlorite (FeO ~33%, MgO ~8%) and prehnite. The FeO content in the prehnite is ~5 %. The prehnite is quite abundant closest to the fracture.

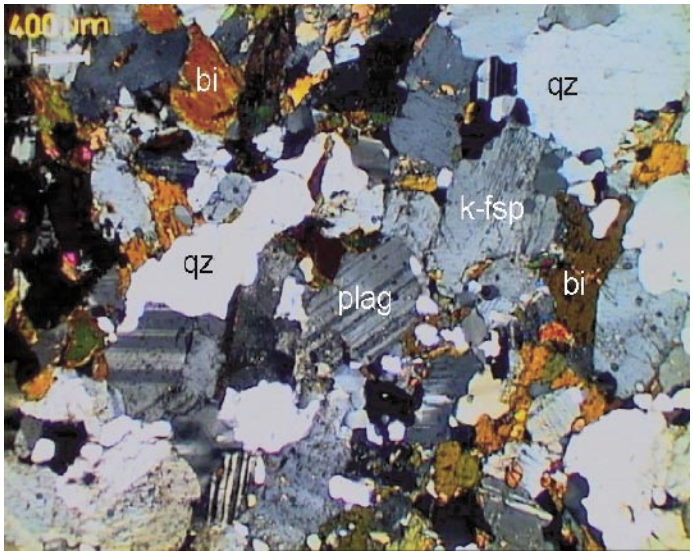


***Figure A-50.*** *Unaltered wall rock Microphotograph (KFM03A 332.72–333.00 m).*

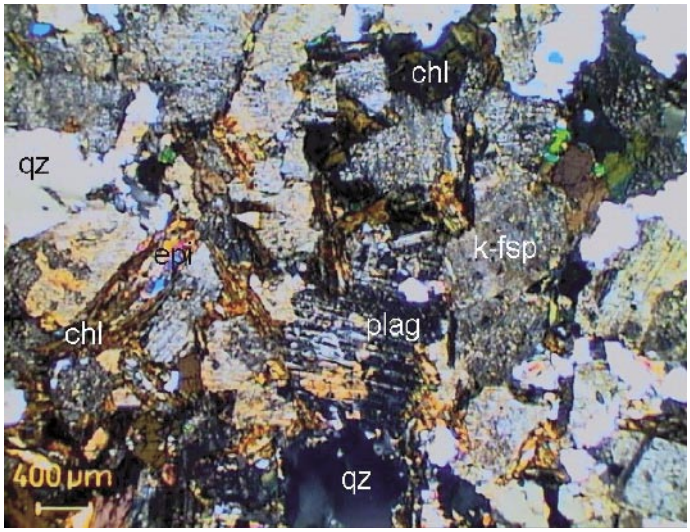


***Figure A-51.*** *Altered wall rock. Microphotograph (KFM03A 332.72–333.00 m).*

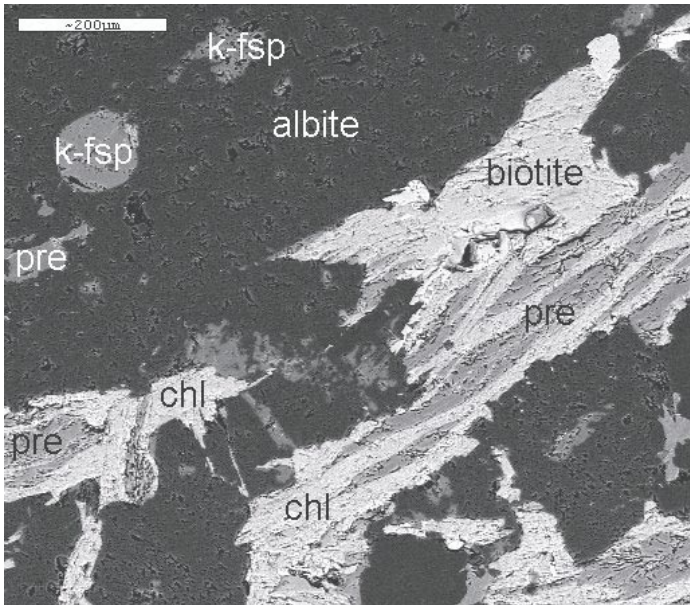


***Figure A-52.*** *Altered wall rock. Backscattered electron image (KFM03A 332.72–333.00 m).*

Sample: KFM03A 334.41–334.56 m
Rock type: Metabasite
Fracture: Three parallel closed fractures.
Orientation: N59E/75SE
Minerals: Calcite, laumontite, adularia, quartz.

Sequence of mineralizations

1. Laumontite
2. Adularia-quartz cataclasite and laumontite
3. Idiomorphic quartz
4. Calcite
5. Pure adularia and a younger calcite.

Wall rock alteration: The biotite in the wall rock has been almost completely altered into chlorite and has in some places begun to alter into clay minerals. The plagioclase is saussuritized and red-coloured due to micro-grains of hematite.

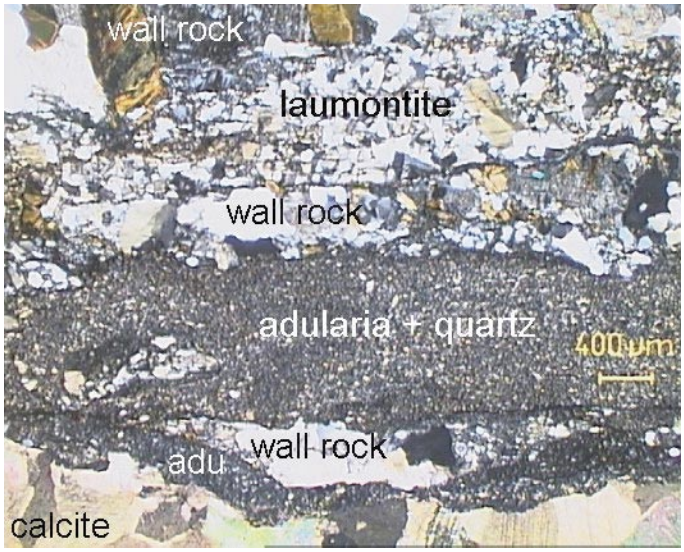


***Figure A-53.*** *Parallel fracture fillings with adularia + quartz, laumontite, calcite and pure adularia. Photomicrograph ( KFM03A 334.41–334.56 m).*

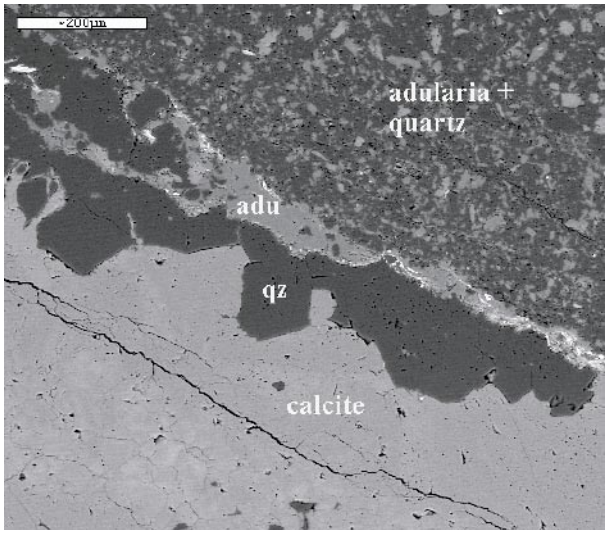


***Figure A-54.*** *Cataclasite, idiomorphic quartz and calcite cut by adularia. Backscattered electron image.*

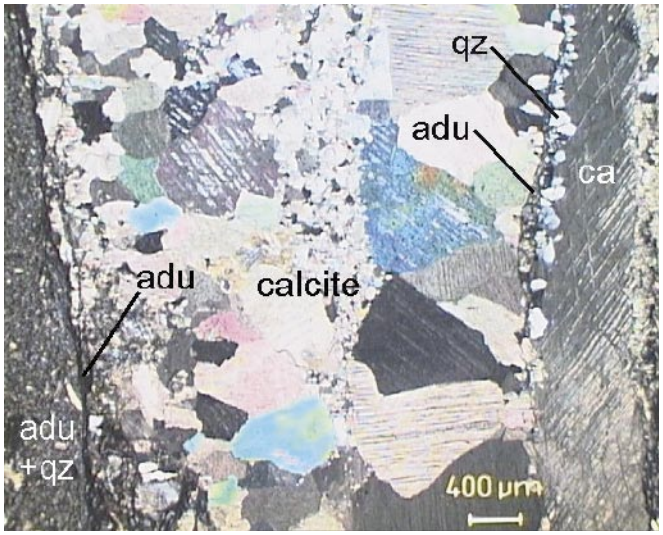


***Figure A-55.*** *Two generations of calcite.*

Sample: KFM03A 424.85–424.95 m
Rock type: Metagranite
Fracture: Open fracture.
Orientation: N23E/88W
Minerals: Chlorite, calcite, adularia, albite.

Sequence of mineralizations

1. Chlorite
2. Calcite with small grains of adularia and albite


***Figure A-56.*** *Surface sample with chlorite covered with calcite together with adularia and albite (KFM03A 424.85–424.95 m).*

Sample: KFM03A 451.85–451.90 m
Rock type: Pegmatite
Fracture: Open fracture.
Orientation: N54W/43SW
Minerals: Fe-chlorite, epidote, titanite, apatite, quartz, albite, prehnite, calcite.

Sequence of mineralizations

1. The pegmatite has been cut by a mylonite with epidote (FeO ~6.5–9%), Fe-chlorite (FeO ~20–24%, MgO ~12–15%), and small grains of quartz. Titanite occurs both inside the chlorite and together with the epidote. Under crossed polarizing sheets, the chlorite has a blue-black colour. A few apatite crystals are also present.
2. Idiomorphic prehnite crystals have crystallized in thin layers near the open fracture and cut the epidote mylonite. The FeO content in the prehnite is ~ 2–4 %.
3. Nearest the open fracture, bands with quartz, adularia and Fe-chlorite are present.
4. Calcite has crystallized on the open fracture.

Wall rock alteration: The plagioclase in the pegmatite is saussuritized and red-coloured by micro-grains of hematite.

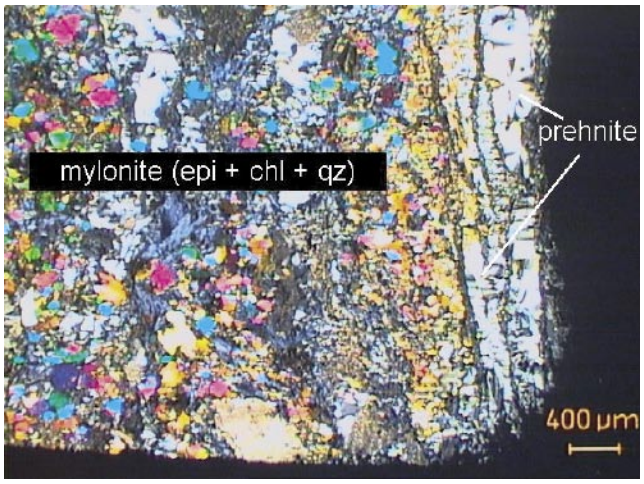


***Figure A-57.*** *Mylonite with epidote, chlorite and quartz on which prehnite has crystallized. (epi = epidote). Microphotograph (KFM03A 451.85–451.90 m).*

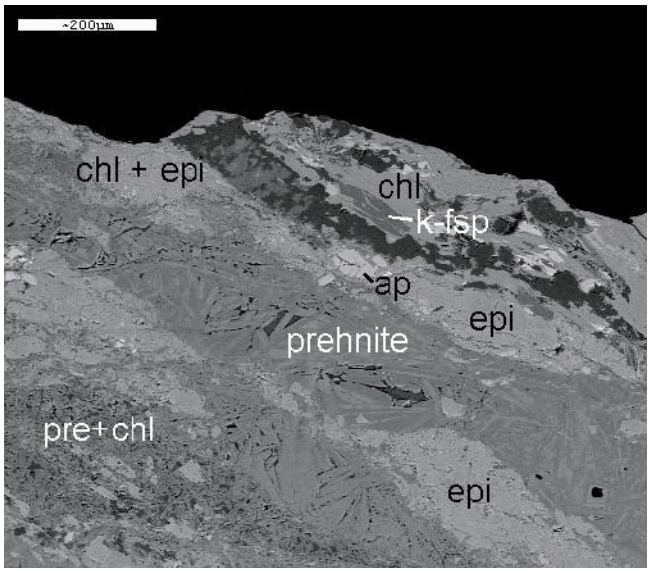


***Figure A-58.*** *Epidote and apatite cut by prehnite together with K-feldspar and chlorite. (ap = apatite). Backscattered electron image (KFM03A 451.85–451.90 m).*

Sample: KFM03A 813.88–813.97 m
Rock type: Metagranite
Fracture: Open fracture.
Orientation: N55E/24NW
Minerals: Apophyllite, adularia, quartz, corrensite.

Sequence of mineralizations

1. Adularia and quartz
2. Apophyllite and corrensite

Wall rock alteration: The plagioclase in the wall rock is highly saussuritized and red-coloured by micro-grains of hematite while the K-feldspar and biotite are relatively unaltered.

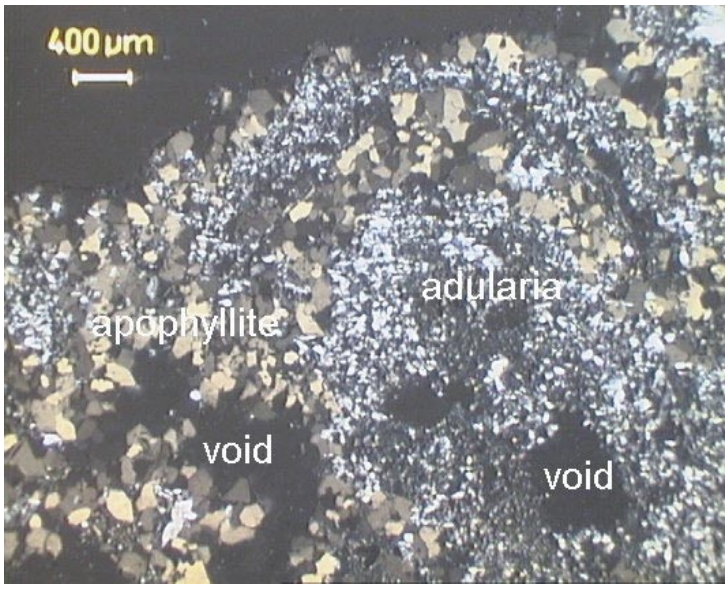


***Figure A-59.*** *Adularia surrounded by apophyllite. Microphotograph (KFM03A 813.88–813.97 m).*

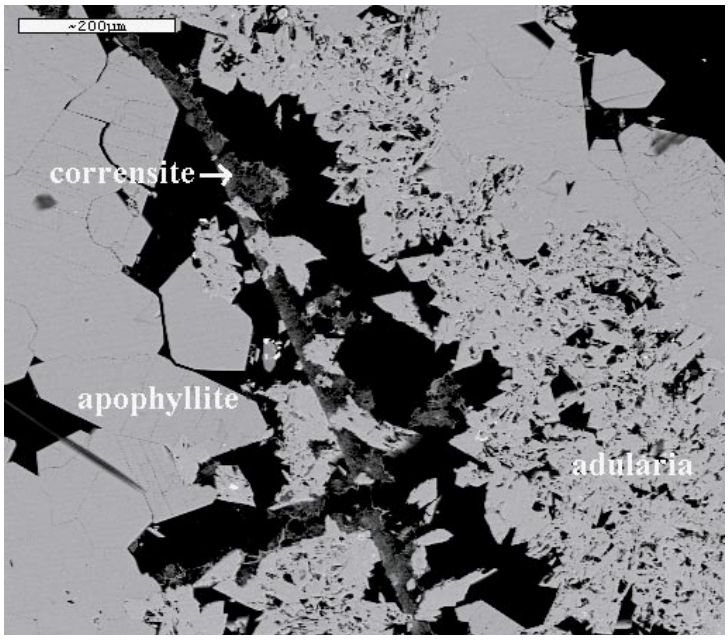


***Figure A-60.*** *Partly dissolved adularia together with idiomorphic apophyllite and corrensite. Backscattered electron image (KFM03A 813.88–813.97 m).*

# Appendix II

## SEM-EDS analyses

| Sample | | Na2O | MgO | Al2O3 | SiO2 | K2O | CaO | TiO2 | MnO | FeO | Total | Comment |
|---|---|---|---|---|---|---|---|---|---|---|---|---|
| KFM01A 110.9 | Plagioclase | 8.7 | * | 22.3 | 65.6 | * | 2.6 | * | * | * | 100.3 | |
| KFM01A 128.4a | Albite | 10.9 | * | 19.6 | 67.8 | * | * | * | * | * | 98.7 | |
| KFM01A 128.4b | Albite | 11.1 | * | 19.7 | 68.9 | * | * | * | * | * | 99.7 | |
| KFM02A 118.28 3 | Albite | 10.7 | * | 21.2 | 66.1 | 0.3 | 0.7 | * | * | 0.4 | 99.2 | |
| KFM03A 332.72–333.00 | Albite | 11.3 | * | 20.2 | 67.6 | * | * | * | * | * | 99.3 | |
| KFM02A 893.45 | Apophyllite | * | * | * | 50.3 | 6.0 | 23.9 | * | * | * | 79.4 | |
| KFM03A 813.45 | Apophyllite | * | * | 0.3 | 50.4 | 5.9 | 23.4 | * | * | * | 79.2 | |
| KFM01A 110.9 | Chlorite | 0.5 | 7.6 | 17.0 | 29.4 | 1.3 | 0.5 | 1.4 | 0.7 | 31.7 | 90.1 | |
| KFM01A 112.88 | Chlorite | * | 8.5 | 10.8 | 34.2 | 0.4 | 1.8 | * | * | 25.0 | 83.6 | |
| KFM01A 127.4 | Chlorite | 0.4 | 3.4 | 11.8 | 28.3 | 0.1 | 1.7 | * | * | 32.3 | 81.6 | |
| KFM01A 128.4a | Chlorite | 0.2 | 12.5 | 18.3 | 26.5 | * | 0.2 | * | 0.7 | 29.0 | 87.5 | |
| KFM01A 128.4b | Chlorite | * | 17.6 | 14.6 | 34.4 | * | 0.9 | * | 0.3 | 18.4 | 86.4 | |
| KFM01A 128.4b | Chlorite | * | 19.3 | 12.3 | 33.5 | 0.1 | 0.5 | * | 0.3 | 21.6 | 87.8 | |
| KFM01A 128.4b | Chlorite | * | 13.7 | 17.4 | 33.2 | 0.2 | 0.8 | * | 0.3 | 19.5 | 85.3 | |
| KFM01A 159.4 | Chlorite-cor-rensite? | 0.4 | 22.2 | 12.7 | 34.5 | 0.1 | 0.6 | * | 0.2 | 9.7 | 81.6 | |
| KFM01A 170.45a | Chlorite | * | 13.0 | 18.3 | 27.4 | * | 0.2 | * | 0.9 | 28.6 | 88.8 | |
| KFM01A 170.45a | Chlorite | * | 13.4 | 17.4 | 26.9 | * | 0.2 | * | 0.8 | 28.2 | 87.1 | |
| KFM01A 221.9 | Chlorite | * | 6.7 | 10.3 | 30.6 | 0.5 | 1.0 | * | 0.4 | 40.6 | 90.2 | |
| KFM01A 221.9 | Chlorite | * | 24.2 | 12.6 | 34.6 | * | 0.3 | * | * | 13.0 | 85.0 | |
| KFM01A 269.85 | Chlorite-cor-rensite? | * | 18.3 | 15.0 | 33.2 | * | 0.9 | * | 0.4 | 17.5 | 85.5 | |
| KFM20A 111.0 B3 | Chlorite | * | 17.0 | 14.9 | 35.3 | 0.4 | 0.5 | * | 0.2 | 20.8 | 89.3 | |
| KFM02A 111.0 A4 | Chlorite | 0.4 | 18.0 | 13.3 | 34.1 | 0.1 | 0.5 | * | 0.3 | 21.5 | 88.1 | |
| KFM02A 179.39 A1 | Chlorite | 0.3 | 12.0 | 19.5 | 35.2 | 0.5 | 0.7 | * | 0.4 | 22.0 | 90.7 | |
| KFM02A 513.55 C1 | Chlorite | * | 18.1 | 25.0 | 42.6 | 0.2 | 0.9 | * | * | 3.5 | 90.4 | |
| KFM02A 423.13 1 | Chlorite | 0.3 | 11.6 | 16.9 | 27.2 | * | * | * | * | 33.8 | 90.5 | |
| KFM03A 332.72–333.00 | Chlorite | * | 8.2 | 16.2 | 27.1 | 1.2 | * | 1.4 | 0.4 | 32.9 | 88.6 | |

| Sample | | Na2O | MgO | Al2O3 | SiO2 | K2O | CaO | TiO2 | MnO | FeO | Total | Comment |
|---|---|---|---|---|---|---|---|---|---|---|---|---|
| KFM03A 451.85 C | Chlorite? | * | 14.4 | 17.0 | 27.1 | * | * | * | 0.4 | 24.3 | 83.5 | |
| KFM01A 110.9 | Epidote | * | * | 22.1 | 37.8 | * | 23.0 | * | 0.4 | 12.5 | 95.9 | |
| KFM01A 137.8 | Epidote | * | * | 26.1 | 37.3 | * | 22.1 | * | 0.5 | 8.2 | 95.3 | |
| KFM01A 170.45b | Epidote | * | * | 21.4 | 37.0 | * | 22.1 | * | 0.2 | 14.0 | 95.2 | |
| KFM01A 219 | Epidote | * | * | 23.1 | 37.1 | * | 23.3 | 0.3 | 0.1 | 11.0 | 95.0 | |
| KFM02A 111.0,B.1 | Epidote | * | * | 24.4 | 37.2 | * | 23.6 | * | 0.2 | 11.6 | 96.6 | |
| KFM02A 516.60,A.1 | Epidote | * | * | 27.5 | 37.3 | * | 23.6 | * | * | 7.7 | 96.3 | |
| KFM02A 516.60,A.2 | Epidote | * | * | 25.9 | 37.2 | * | 23.0 | * | 0.3 | 9.6 | 96.0 | |
| KFM02A 516.60,C.2 | Epidote | * | * | 25.1 | 37.0 | * | 22.8 | * | 0.3 | 10.4 | 95.7 | |
| KFM02A 516.60,E1 | Epidote | * | * | 25.0 | 37.8 | * | 23.2 | 0.2 | 0.8 | 11.8 | 99.1 | |
| KFM02A 516.60 E2 | Epidote | * | * | 25.7 | 37.0 | * | 23.4 | * | 0.3 | 10.3 | 96.5 | |
| KFM02A 516.60 E3 | Epidote | * | * | 22.5 | 35.9 | * | 22.9 | * | 0.2 | 12.9 | 94.4 | |
| KFM02A 516.60 A1 | Epidote | * | * | 27.5 | 37.3 | * | 23.6 | * | * | 7.7 | 96.3 | |
| KFM02A 516.60 A2 | Epidote | * | * | 25.9 | 37.2 | * | 23.0 | * | 0.3 | 9.6 | 96.0 | |
| KFM02A 516.60 A3 | Epidote | * | * | 24.1 | 37.6 | * | 24.5 | * | 0.3 | 12.9 | 99.2 | |
| KFM02A 516.60 C2 | Epidote | * | * | 25.1 | 37.0 | * | 22.8 | * | 0.3 | 10.4 | 95.7 | |
| KFM02A 516.60 E2 | Epidote | * | * | 25.7 | 37.0 | * | 23.4 | * | 0.3 | 10.3 | 96.5 | |
| KFM02A 516.60 E3 | Epidote | * | * | 22.5 | 35.9 | * | 22.9 | * | 0.2 | 12.9 | 94.4 | |
| KFM01A 110.9 | K-feldspar | 0.6 | * | 18.8 | 65.5 | 16.3 | * | 0.4 | * | * | 101.4 | |
| KFM01A 128 | K-feldspar | * | * | 17.7 | 66.6 | 14.3 | 0.1 | * | * | 0.3 | 99.4 | |
| KFM01A 128.4a | K-feldspar | * | * | 19.0 | 65.0 | 16.2 | * | * | * | * | 100.6 | |
| KFM02A 111.0 A3 | K-feldspar | * | * | 19.1 | 63.9 | 16.7 | * | 0.1 | * | 0.3 | 100.1 | |
| KFM02A 111.0 B2 | Adularia | * | * | 19.2 | 63.8 | 16.3 | * | * | * | 0.2 | 99.2 | |
| KFM02A 118.24 1 | Adularia | * | * | 19.2 | 64.2 | 16.2 | * | * | * | * | 99.6 | |
| KFM02A 118.28 6 | Adularia | * | * | 19.3 | 64.8 | 16.2 | * | * | * | 0.1 | 100.6 | |
| KFM01A 110.9 | Calcite | * | * | 0.3 | 0.2 | * | 50.9 | * | * | * | 51.6 | |
| KFM01A 137.8 | Calcite | * | * | * | * | * | 51.5 | * | * | * | 51.9 | |
| KFM01A 159.4 | Calcite | * | * | 0.2 | * | * | 51.6 | * | * | * | 52.1 | |
| KFM01A 185.45 | Calcite | * | * | 0.2 | * | * | 47.0 | * | 1.2 | * | 48.9 | |
| KFM01A 219 | Calcite | * | * | * | * | * | 51.1 | * | * | * | 51.2 | |
| KFM01A 396.6 | Calcite | * | * | 0.7 | * | * | 53.9 | * | * | * | 54.6 | |
| KFM02A 118.28a | Calcite | * | * | 0.2 | * | 0.1 | 62.8 | * | * | * | 63.2 | |
| KFM02A 118.28b | Calcite | * | * | 0.2 | * | * | 49.0 | * | 0.2 | * | 49.4 | |

| Sample | | Na2O | MgO | Al2O3 | SiO2 | K2O | CaO | TiO2 | MnO | FeO | Total | Comment |
|---|---|---|---|---|---|---|---|---|---|---|---|---|
| KFM03A 334.41a | Calcite | * | 0.3 | 0.8 | * | * | 43.6 | * | 0.7 | 1.1 | 46.6 | |
| KFM03A 334.41b | Calcite | * | * | 0.5 | * | * | 43.2 | * | 0.8 | 1.1 | 45.7 | |
| KFM03A 334.41c | Calcite | * | * | 0.7 | * | * | 46.4 | * | * | * | 47.4 | |
| KFM01A 112.88 | Laumontite | * | * | 23.5 | 56.2 | * | 12.5 | * | * | * | 92.6 | |
| KFM01A 159.4 | Laumontite | * | * | 21.9 | 52.4 | 0.2 | 11.8 | * | * | * | 86.5 | |
| KFM01A 170.45b | Laumontite | 0.3 | * | 21.8 | 52.2 | 0.2 | 10.8 | * | * | 0.5 | 85.9 | |
| KFM01A 179.7 | Laumontite | * | * | 22.0 | 51.5 | 0.2 | 11.6 | * | * | 0.9 | 86.3 | |
| KFM01A 219 | Laumontite | * | * | 21.2 | 51.5 | * | 12.2 | * | * | * | 85.0 | |
| KFM01A 396.6 | Laumontite | * | * | 21.3 | 51.5 | 0.2 | 11.0 | * | * | * | 84.2 | |
| KFM01A 652.0b | Laumontite | * | * | 21.2 | 50.8 | * | 11.3 | * | * | * | 83.6 | |
| KFM03A 334.41c | Laumontite | * | * | 19.3 | 45.1 | 0.4 | 9.9 | * | * | 0.5 | 75.1 | |
| KFM01A 127.4 | Analcime | 9.7 | * | 22.5 | 58.0 | * | * | * | * | * | 90.2 | |
| KFM01A 148.9 | Analcime | 11.2 | * | 20.0 | 53.2 | * | * | * | * | * | 84.6 | |
| KFM01A 269.85 | Analcime | 12.1 | * | 21.8 | 56.7 | * | * | * | * | 0.3 | 91.7 | |
| KFM03A 334.41d | Analcime | 7.9 | * | 18.8 | 47.3 | * | * | * | * | * | 74.0 | |
| KFM03A 334.41e | Analcime | 7.4 | * | 19.4 | 47.0 | * | 0.1 | * | * | * | 75.1 | |
| KFM01A 128.4b | Prehnite | * | 0.1 | 21.5 | 43.6 | * | 26.8 | * | * | 4.7 | 96.7 | |
| KFM01A 128.4b | Prehnite | * | * | 23.7 | 42.6 | * | 26.3 | * | 0.1 | 1.0 | 93.7 | |
| KFM01A 128.4b | Prehnite | * | * | 20.7 | 41.7 | * | 26.0 | 0.2 | * | 4.4 | 92.9 | |
| KFM01A 148.9 | Prehnite | * | * | 22.4 | 40.9 | * | 25.1 | * | * | 1.6 | 90.1 | |
| KFM01A 185.45 | Prehnite | * | * | 24.3 | 44.0 | * | 27.1 | * | * | 1.1 | 96.4 | |
| KFM01A 221.9 | Prehnite | * | * | 23.3 | 43.0 | * | 27.1 | * | * | 1.0 | 94.6 | |
| KFM01A 221.9 | Prehnite | * | * | 21.6 | 42.2 | * | 26.6 | * | * | 3.2 | 93.7 | |
| KFM01A 269.85 | Prehnite | * | * | 20.2 | 42.7 | * | 26.0 | * | * | 6.8 | 95.9 | |
| KFM02A 111.0 D2 | Prehnite | * | * | 18.8 | 42.0 | * | 27.1 | * | * | 7.8 | 95.6 | partly altered |
| KFM02A 111.0 C1 | Prehnite | * | 1.0 | 20.9 | 44.5 | 0.4 | 24.1 | * | * | 7.1 | 97.8 | partly altered |
| KFM02A 111.0 D3 | Prehnite | * | * | 18.8 | 42.9 | * | 27.1 | * | * | 8.4 | 97.2 | partly altered |
| KFM03A 332.72–333.00 | Prehnite | * | * | 21.6 | 42.6 | * | 25.5 | * | * | 4.9 | 94.2 | |
| KFM03A 451.85 G | Prehnite | * | 1.4 | 20.5 | 40.8 | * | 21.8 | * | * | 3.6 | 88.8 | |
| KFM01A 219 | Hematit | 0.4 | 0.6 | 3.2 | 5.7 | 0.5 | 0.8 | 1.4 | 0.2 | 69.9 | 82.7 | |
| KFM01A 652.0b | Hematit | * | 0.2 | 16.5 | 27.6 | * | 4.8 | * | * | 45.4 | 94.5 | |
| KFM01A 396.6 | Hematit | * | 4.9 | 6.2 | 11.7 | 0.1 | 0.6 | 1.4 | 0.6 | 61.9 | 87.7 | |

# Appendix III

## XRD

| Sample | Ep | Qz | Pr | Ana | Lau | Hm | Chl | Kfsp | Alb | Apo | Ca | Py | Fl | Clay | X |
|---|---|---|---|---|---|---|---|---|---|---|---|---|---|---|---|
| KFM01A | | | | | | | | | | | | | | | |
| 110.90 | 1 | 1 | | | | | 1Fe | 1 | 1 | | 2 | | | | |
| 112.88 | | | | | 1 | 2 | 3Fe | | | | | | | | |
| 127.4 | | 2 | | 3 | | 2 | 4Fe | 1,2 | | | | | | | |
| 128.0 | | 1 | | | | | | 1 | | | | | | | |
| 128.4 | | 1 | 2 | | | | 1 | 1,3,4 | 1 | | | | | | |
| 137.8 | 1 | | | | 4 | 4 | | | | | 2Mn,3 | | | | |
| 146.77 | 1 | 1,3 | | | | | 1 | 1,2 | | | 4 | | | | |
| 148.9 | | 7 | 1 | 5 | | | 4,7 | 3,7 | | | | 2,6 | | | |
| 159.4 | | 1 | | | 2 | 2 | 3Mg | 1 | | | 2 | | | | |
| 170,45 | 1 | 1,5 | | | 4 | 4 | 1 | 2 | | | 4,5 | | | | |
| 179.7 | | | | | 1 | 1 | | | | | 2 | | 3 | | |
| 185.25 | | | 1 | | | 4 | | 2 | | | 3 | | | 4 | |
| 219.0 | 1 | 1 | | | 3 | 1 | 1,2Fe | 1 | | | 2 | | | | |
| 221.9 | 1 | | 2 | | | | 4Fe | 5 | | | 3 | | 1 | | |
| 267.0 | 1 | 1,3,4 | | | 2 | | | 1,3 | | | | | | | |
| 268.8 | | 1 | | | | | | 1 | | | | 2 | | 4 | 3’ |
| 270.72 | | 2 | | | 1 | 1 | | | | | 3 | 4 | | 5 | |
| 396,6 | | | | | 2 | 2 | | | | | 1 | | | | |
| 481.1 | 1 | 1 | | | | | | 2 | | | | | | | |
| 652.0b | | 2 | | | 1 | 1 | | | | | | | | | |
| 671.9 | | | | | 1 | 1 | | | | | | | | | |
| 712.54 | 1 | | | | | | | | | | | | | | |
| 828.7 | | 1 | | | | | | | | | 2 | | | | 1’’ |
| KFM02A | | | | | | | | | | | | | | | |
| 111.0 | | | 1 | | | 2 | 2 | | | | | | | 2 | |
| 118.28 | | 3 | | | | 3 | | 2,3 | | | 1 | 4 | | 3 | |
| 171.4 | | 1 | | | | | | | | | | 2 | | | |
| 422.3 | | 1 | | | | | | 1,3 | | | 2 | 3 | | 3 | |
| 423.13 | | | | | | 1 | 2 | 1 | | | 2 | | 1 | | |
| 423.65 | 1 | 1,2 | | | | | 1,2 | 1,2 | 2 | | 2 | | | 2 | |
| 513.55 | 1 | 1,2 | | | | 1,2 | 1,2Mg | 1 | 1 | | | | | | |
| 516.6 | 1 | 1 | | | | 2 | 2 | 1 | | | 2 | | | | |
| 893.45 | | | | | | | 2 | | | 2 | 1,2 | | | | |
| KFM03A | | | | | | | | | | | | | | | |
| 184.34 | | 1 | | | | 1 | | 1 | | | 1 | | | | |
| 316.93 | | | | | | | | 2,3 | | | 1 | | | | |
| 332.7 | | | | | 1 | 1 | | | | | | | | | |
| 334.41 | | 2,4 | | 6 | 1 | | 5 | 4,5 | | | 3,7 | | | | |
| 424.85 | | | | | | | 1 | 2 | 2 | | 2 | | | | |
| 451.85 | 1 | 1,3 | 2 | | | | 1,3Fe | 3 | | | 4 | | | | |
| 813.88 | | 1 | | | | | | 1 | | 2 | | | | 2 | |

’ = Baryte
’’= Biotite

# Appendix IV

## Calcite analyses, stable isotopes

| Borehole | Depth (m) | $\delta^{13}$C o/oo PDB | $\delta^{18}$O o/oo PDB | $^{87}$Sr/$^{86}$Sr | Comment | Chem. analysis |
|---|---|---|---|---|---|---|
| KFM01A | 103 | –21.3 | –12 | 0.717800 | | |
| KFM01A | 103 | –24.6 | –12.4 | | | |
| KFM01A | 128 | –9.1 | –13.8 | | | |
| KFM01A | 137.8 | –2.4 | –9.8 | 0.707377 | A | |
| KFM01A | 137.8 | –5.4 | –14.2 | | B | |
| KFM01A | 146.7 | –34.2 | –12 | | older | |
| KFM01A | 146.7 | –34.6 | –11.7 | 0.715122 | older | X |
| KFM01A | 146.77 | –18.2 | –10.4 | 0.714936 | equant | |
| KFM01A | 148.4 | –15.9 | –9.9 | 0.715849 | short C-axis | |
| KFM01A | 148.4 | –24.6 | –12 | 0.715498 | older | |
| KFM01A | 148.9 | –20.6 | –12.9 | 0.715991 | sealed older | X |
| KFM01A | 148.9 | –15.9 | –11 | 0.714613 | short C-axis | |
| KFM01A | 159.4 | –5.4 | –16.5 | 0.710725 | | |
| KFM01A | 170.45 | –5.4 | –17.4 | 0.710434 | older | X |
| KFM01A | 170.45 | –5.4 | –17 | | older | |
| KFM01A | 170.45 | –13.4 | –12.3 | 0.716582 | open younger | |
| KFM01A | 179.85 | –4.8 | –15 | 0.708560 | sealed breccia | X |
| KFM01A | 192.55 | –12.4 | –11 | 0.716790 | | |
| KFM01A | 267 | –17.1 | –12.2 | 0.715326 | older | X |
| KFM01A | 267 | –18.774 | –11.079 | | short C-axis | |
| KFM01A | 269.85 | –5.1 | –17.1 | 0.709327 | | X |
| KFM01A | 396.6 | –2.3 | –11.1 | 0.709775 | | X |
| KFM01A | 396.6 | –2.4 | –11.7 | | | |
| KFM02A | 110.6 | 8.12 | –8.259 | | | |
| KFM02A | 111 | –2.849 | –17.771 | | older | |
| KFM02A | 111 | 5.194 | –9.144 | | Scalenoedral | |
| KFM02A | 116.8 | 6.642 | –8.621 | | | |
| KFM02A | 118.28 | –6.842 | –7.369 | | Massive | |
| KFM02A | 118.28 | 6.402 | –9.351 | | Scalenohedral | |
| KFM02A | 182.71 | –14.952 | –12.086 | | | |
| KFM02A | 422 | 6.66 | –10.64 | | fracture surface | |
| KFM02A | 422.3 | 0.025 | –8.961 | | sealed fracture | |
| KFM02A | 423.13 | –16.192 | –12.005 | | yngre | |
| KFM02A | 423.65 | –4.509 | –10.701 | | | |
| KFM02A | 486 | –6.688 | –11.788 | | Eq | |
| KFM02A | 513.55 | –3.578 | –11.782 | | | |
| KFM02A | 513.55 | –10.456 | –11.917 | | Short C-axis | |
| FsmkBP5:4 A | 0 | –7.588 | –9.339 | | | |
| FsmkBP5:4 B | 0 | –7.829 | –9.399 | | | |
| KFM03B | 0.9 | –5.83 | –11.57 | | | |

| Borehole | Depth (m) | $\delta^{13}$C o/oo PDB | $\delta^{18}$O o/oo PDB | $^{87}$Sr/$^{86}$Sr | Comment | Chem. analysis |
|---|---|---|---|---|---|---|
| KFM03B | 0.5 | –1.29 | –10.41 | | | |
| KFM03B | 0.5 | –7.37 | –12.36 | | | |
| KFM03B | 92.7 | –4.84 | –15.87 | | | |
| KFM03A | 334.41 | –2.05 | –8.17 | | | |
| KFM03A | 389.4 | –4.49 | –15.19 | | | |
| KFM03A | 389.43 | –6.35 | –9.37 | | | |
| KFM03A | 451.25 | –5.25 | –14.03 | | | |
| KFM03A | 451.85 | –4.79 | –8.82 | | | |
| KFM03A | 451.85 | –4.06 | –9.057 | | | |
| KFM03A | 497.78 | –10.11 | –12.66 | | | |
| KFM03A | 643.80 | –7.43 | –12.49 | | | |
| KFM03A | 986.60 | –8.03 | –11.57 | | | |
| KFM03A | 944.3 | –8 | –13.95 | | A | |
| KFM03A | 944.3 | –5.86 | –11.49 | | B | |

# Appendix V

## Calcite chemistry

| 2003-nov Sample: weight | mg | KFM01A 146.77–1 12.87 | KFM01A 146.77–2 12.93 | KFM01A 148.9 12.66 dissol.rest | KFM01A 170.45–1 12.35 | KFM01A 170.45–2 10.71 | KFM01A 179.70 10.67 | KFM01A 267.0 13.34 | KFM01A 269.85 12.12 | KFM01A 396.60 12.47 |
|---|---|---|---|---|---|---|---|---|---|---|
| Na/23 | ppm | 94 | 97 | 399 | 26 | 21 | 36 | < 20 | 88 | 113 |
| Mg/24 | ppm | 12 | 7 | 16 | 143 | 154 | 349 | < 2 | 275 | 559 |
| Al/27 | ppm | 15 | 15 | 382 | 344 | 465 | 958 | 20 | 121 | 6196 |
| K/39 | ppm | < 50 | < 50 | 133 | < 50 | < 50 | < 50 | < 50 | < 50 | 106 |
| Ca/43 | ppm | 474083 | 484422 | 414088 | 485158 | 472701 | 466572 | 476392 | 462142 | 450221 |
| Sc/45 | ppm | 0.52 | 0.51 | 0.43 | 0.66 | 0.56 | 0.43 | 0.49 | 0.56 | 1.92 |
| Mn/55 | ppm | 613 | 634 | 348 | 4414 | 5395 | 74 | 335 | 486 | 25 |
| Fe/57 | ppm | 984 | 976 | 1045 | 917 | 937 | 962 | 959 | 1150 | 842 |
| Rb/85 | ppm | 0.05 | 0.04 | 0.39 | 0.01 | 0.01 | 0.33 | 0.02 | 0.04 | 1.58 |
| Sr/88 | ppm | 39 | 41 | 38 | 172 | 168 | 238 | 31 | 173 | 103 |
| Y/89 | ppm | 9.72 | 10.17 | 9.39 | 7.12 | 7.18 | 10.36 | 4.03 | 2.43 | 6.83 |
| Ba/137 | ppm | 3 | 2 | 3 | 0.2 | 2 | 4 | < 0.1 | < 0.1 | 3 |
| La/139 | ppm | 23.15 | 23.94 | 13.84 | 1.83 | 1.86 | 0.95 | 33.02 | 2.49 | 0.50 |
| Ce/140 | ppm | 62.42 | 65.54 | 34.76 | 0.47 | 0.40 | 0.27 | 65.90 | 3.31 | 0.40 |
| Pr/141 | ppm | 7.49 | 7.80 | 4.30 | 0.46 | 0.47 | 0.37 | 6.17 | 0.43 | 0.15 |
| Nd/146 | ppm | 32.13 | 33.12 | 21.41 | 2.58 | 2.85 | 1.99 | 24.06 | 2.09 | 0.98 |
| Sm/147 | ppm | 4.19 | 4.59 | 4.39 | 0.56 | 0.64 | 0.55 | 2.96 | 0.37 | 0.30 |
| Eu/153 | ppm | 0.44 | 0.45 | 0.30 | 0.10 | 0.10 | 0.10 | 0.21 | 0.05 | 0.12 |
| Gd/157 | ppm | 4.61 | 4.59 | 3.81 | 0.69 | 0.77 | 0.77 | 2.28 | 0.31 | 0.56 |
| Tb/159 | ppm | 0.36 | 0.37 | 0.39 | 0.08 | 0.10 | 0.13 | 0.20 | 0.03 | 0.08 |
| Dy/163 | ppm | 1.53 | 1.56 | 1.50 | 0.62 | 0.63 | 0.85 | 0.82 | 0.17 | 0.37 |
| Ho/165 | ppm | 0.23 | 0.21 | 0.27 | 0.12 | 0.13 | 0.22 | 0.12 | 0.03 | 0.11 |
| Er/166 | ppm | 0.63 | 0.62 | 0.67 | 0.48 | 0.41 | 0.82 | 0.26 | 0.21 | 0.38 |
| Tm/169 | ppm | 0.07 | 0.07 | 0.08 | 0.05 | 0.06 | 0.12 | 0.05 | 0.03 | 0.04 |
| Yb/172 | ppm | 0.33 | 0.34 | 0.53 | 0.52 | 0.57 | 1.07 | 0.22 | 0.17 | 0.28 |
| Lu/175 | ppm | 0.06 | 0.05 | 0.10 | 0.06 | 0.09 | 0.18 | 0.04 | 0.03 | 0.07 |
| Th/232 | ppm | 0.04 | 0.04 | 0.04 | 0.02 | < 0.01 | < 0.02 | < 0.03 | < 0.04 | < 0.05 |
| U/238 | ppm | 0.04 | 0.04 | 0.05 | 0.06 | 0.06 | 0.82 | 0.04 | 0.12 | 0.13 |

# Appendix VI

## $\delta^{34}$S ‰ (CDT) values for pyrites

| Sample | $\delta^{34}$S ‰ CDT |
|---|---|
| KFM01A:103.0–103.05 | 31.5 |
| KFM01A:146.77 | 15.3 |
| KFM01A:148.4–148.7 | 8.4 |
| KFM01A:148.9–149.1 | 5.4 |
| KFM01A:267.0 | 15.7 |
| KFM01A:269.85–269.90 | 15.4 |